NON LINEAR OPTICS

LECTURE NOTES

2007

Prof. dr. W. UBACHS
LASER CENTRE VRIJE UNIVERSITEIT AMSTERDAM
DEPARTMENT OF PHYSICS AND ASTRONOMY

Contents

Ch 5: Coherent Raman Scattering in Gases

Ch 6: The production of vacuum ultraviolet radiation by FWM

Chapter 1

Non-linear optics: Introduction

1.1 *THE FIRST OBSERVATION OF A NON-LINEAR OPTICAL PROCESS*

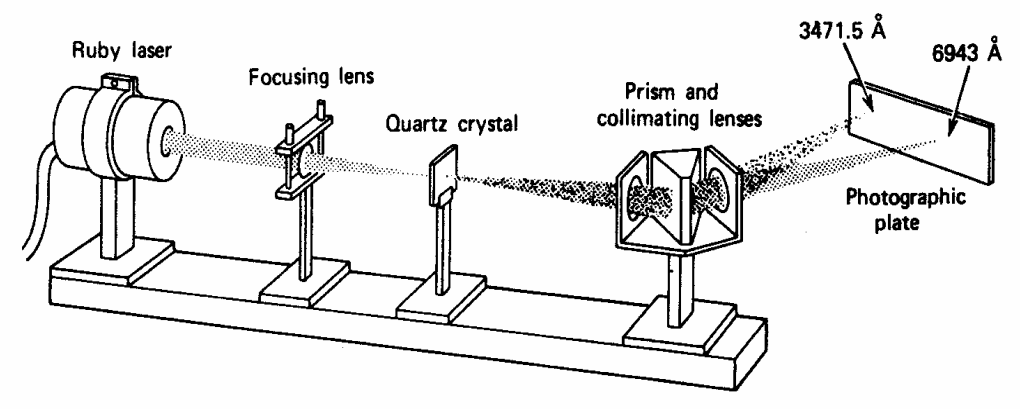

Fig: Frequency doubling of a Ruby laser: $\lambda = 694.3$ nm $\rightarrow$ $\lambda = 347.1$ nm as shown by Franken et al.[13]

1.2 *THE NONLINEAR SUSCEPTIBILITY*

The polarization **P** induced in a medium when electric field **E** is applied may be expanded as a power series in the electric field vector:

$$\mathbf{P} = \chi^{(1)}\,\mathbf{E} + \chi^{(2)}\,\mathbf{E}\,\mathbf{E} + \chi^{(3)}\,\mathbf{E}\,\mathbf{E}\,\mathbf{E} + \chi^{(4)}\,\mathbf{E}\,\mathbf{E}\,\mathbf{E}\,\mathbf{E} + \text{etc} \qquad [1.1]$$

where the $\chi^{(i)}$ are tensors, even for the first order contribution:

$$P_i = \chi_{ij}^{(1)}\,E_j \qquad [1.2]$$

As a consequence the orientation of the induced polarization may be different from the applied field. In a *centro-symmetric* medium, that is a medium with inversion symmetry, one may derive (use the inversion symmetry operator I_{op}):

$$I_{op}\,\mathbf{P} = -\mathbf{P} = -\chi^{(1)}\,\mathbf{E} - \chi^{(2)}\,\mathbf{E}\,\mathbf{E} - \chi^{(3)}\,\mathbf{E}\,\mathbf{E}\,\mathbf{E} - \chi^{(4)}\,\mathbf{E}\,\mathbf{E}\,\mathbf{E}\,\mathbf{E} + \text{etc} \qquad [1.3]$$
$$I_{op}\,\mathbf{E} = -\mathbf{E}$$

because of the last relation we find

$$I_{op}\,\mathbf{P} = -\chi^{(1)}\,\mathbf{E} + \chi^{(2)}\,\mathbf{E}\,\mathbf{E} - \chi^{(3)}\,\mathbf{E}\,\mathbf{E}\,\mathbf{E} + \chi^{(4)}\,\mathbf{E}\,\mathbf{E}\,\mathbf{E}\,\mathbf{E} + \text{etc} \qquad [1.4]$$

Thus we find the important relation for (inversion)-symmetric media: $\chi^{(2n)} = 0$ [1.5]
All even powers in the susceptibility expansion are zero.

[13] P.A. Franken, A.E. Hill, C.W. Peters and G. Weinreich, Phys. Rev. Lett. **7** (1961) 118

1.3 *GRAPHICAL REPRESENTATION OF NONLINEAR OPTICS*

LINEAR RESPONSE	NONLINEAR RESPONSE
$\mathbf{P} = \chi^{(1)}\,\mathbf{E}$	$\mathbf{P} = \chi^{(1)}\,\mathbf{E} + \chi^{(2)}\,\mathbf{E}\,\mathbf{E}$

in the steady state

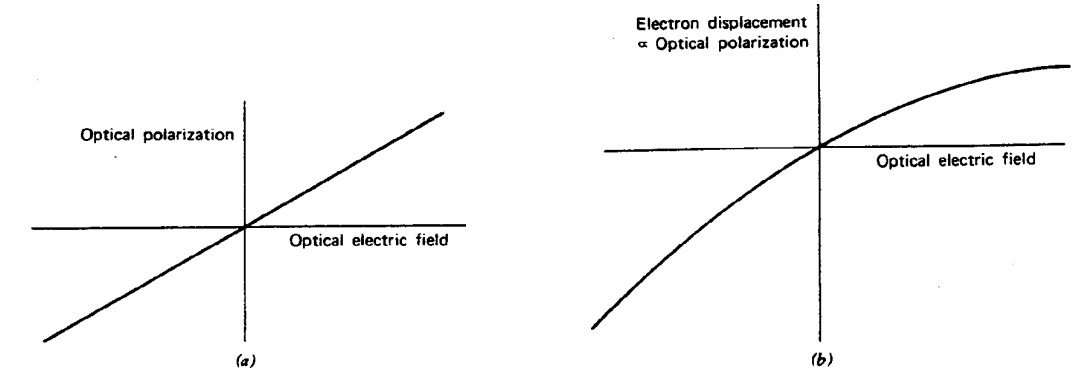

and for oscillatory E.M.-waves

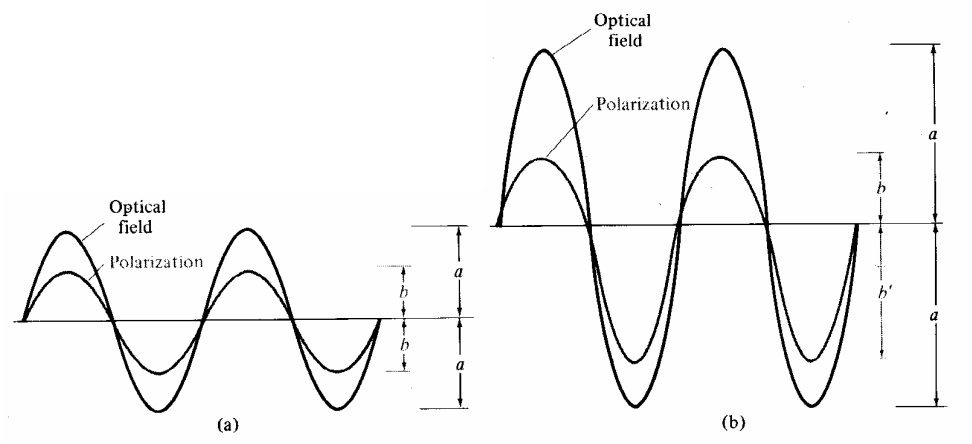

The nonlinear response, e.g. in the case of an electromagnetic wave (a periodic function), may be evaluated in terms of a Fourier series expansion:

$$P = \sum a_n \sin(n\omega t + \phi_n) \qquad [1.6]$$

Graphically the Fourier series expansion may be shown as follows. The nonlinear polarization induced can be represented as:

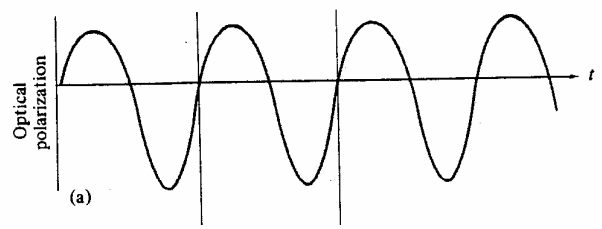

This function can be Fourier analyzed:

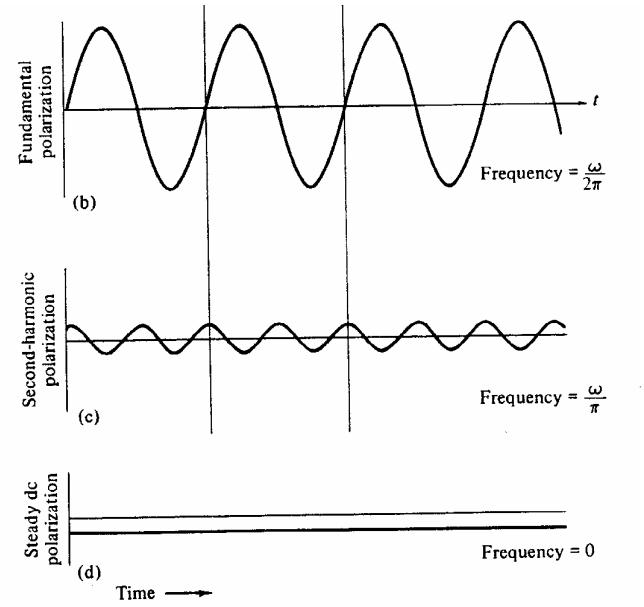

Fig.: Fourier analysis of the non-linear polarization in (b): Sin ωt; (c): Sin 2ωt; and (d): Sin ϕ_C, the dc-component ("optical rectifying")

The nonlinear response of the medium produces higher harmonics in the polarization. The oscillating polarization $P^{(2\omega)}$ acts as a source term in the Maxwell equations (consider the nonlinear medium as an antenna):

$$\nabla^2\mathbf{E} - \left(\frac{n}{c}\right)^2 \frac{\partial^2}{\partial t^2}\mathbf{E} = \mu_0 \frac{\partial^2}{\partial t^2}\mathbf{P}^{(2\omega)} \qquad [1.7]$$

and thus produces a field $E^{(2\omega)}$.

1.4 *LORENTZ-MODEL OF THE SUSCEPTIBILITY*

In this model a medium is considered in which the electrons are affected by external electric forces that displace them. The motion of the electrons is restored by the binding force. As a result a harmonic motion of the electron in the combined field of the atom and the external Coulomb force is produced that may be described in terms of a damped harmonic oscillator.

1) In linear optics: the equation of motion for a damped (damping constant γ) electronic oscillator in one dimension:

$$\frac{d^2}{dt^2}\mathbf{r} + 2\gamma\frac{d}{dt}\mathbf{r} + \omega_0{}^2\mathbf{r} = -\frac{e}{m}\mathbf{E} \qquad [1.8]$$

with the electric field written as $\mathbf{E} = \mathrm{Re}\left[Ee^{i\omega t}\right]$ and for the position of the electron take the deviation from equilibrium: $\mathbf{r} = \mathrm{Re}\left[re^{i\omega t}\right]$ it follows that:

$$\left(\omega_0^2 - \omega^2\right)r + 2i\omega\gamma r = -\frac{e}{m}E \qquad [1.9]$$

So:

$$r = \frac{-eE}{m\left[\omega_0{}^2 - \omega^2 + i\omega\gamma\right]} \approx \frac{-eE}{2m\left[\omega_0(\omega_0 - \omega) + i\omega\gamma\right]} \qquad [1.10]$$

where the last part of the equation holds in the approximation of near resonance: $\omega = \omega_0$. The induced polarization in a medium is $P(\omega) = -Ner(\omega)$ and so:

$$r = \frac{Ne^2}{2m\left[\omega_0(\omega_0 - \omega) + i\omega\gamma\right]}E = \varepsilon_0\chi(\omega)E \qquad [1.11]$$

Thus we find a complex quantity representing the linear susceptibility $\chi(\omega) = \chi'(\omega) - i\chi''(\omega)$ of the medium with:

$$\chi'(\omega) = \frac{Ne^2}{2m\omega_0\gamma\varepsilon_0}\left[\frac{(\omega_0 - \omega)/\gamma}{1 + (\omega_0 - \omega)^2/\gamma^2}\right] \qquad [1.12]$$

and:

$$\chi''(\omega) = \frac{Ne^2}{2m\omega_0\gamma\varepsilon_0}\left[\frac{1}{1 + (\omega_0 - \omega)^2/\gamma^2}\right] \qquad [1.13]$$

The real part of the susceptibility $\chi'(\omega)$ is related to the index of refraction n of the medium, while the imaginary part $\chi''(\omega)$ is related to the absorption coefficient.

2) In nonlinear optics the motion of the electron is considered to have an anharmonic response to the applied electric fields. The equation of motion for the oscillator now becomes, with the anharmonic term ξr^2:

$$\frac{d^2}{dt^2}r + 2\gamma\frac{d}{dt}r + \omega_0{}^2 r - \xi r^2 = -\frac{e}{m}E \qquad [1.14]$$

Try a solution in power series $r = r_1 + r_2 + r_3 +$ etc, with $r_i = a_i E^i$, so $r_1 = a_1 E^1$ and $r_2 = a_2 E^2$. Now substitute $r = r_1 + r_2$ and collect terms in the same order of E:

first order: $$\frac{d^2}{dt^2}r_1 + 2\gamma\frac{d}{dt}r_1 + \omega_0{}^2 r_1 = -\frac{e}{m}E \qquad [1.15]$$

second order: $$\frac{d^2}{dt^2}r_2 + 2\gamma\frac{d}{dt}r_2 + \omega_0{}^2 r_2 = \xi r_1{}^2 \qquad [1.16]$$

A general form for the field:

$$E = \sum E(\omega_n) e^{-i\omega_n t} \qquad [1.17]$$

Calculate $\frac{d}{dt} r_1$ and $\frac{d^2}{dt^2} r_1$ with $r_1 = a_1 E^1$ and substitute in equation [1.15] and it is found that:

$$r_1 = -\frac{e}{m} \frac{\sum E(\omega_n) e^{-i\omega_n t}}{(\omega_0 - \omega_n)^2 - 2i\gamma\omega_n} \qquad [1.18]$$

Calculate r_1^2 and substitute in [1.16], while using that:

$$\left(\sum E(\omega_n) e^{i\omega_n t}\right)^2 = \sum\sum E(\omega_n) E(\omega_m) e^{-i(\omega_n + \omega_m)t} \qquad [1.19]$$

we find:

$$r_2 = -\frac{e\xi}{m^2} \frac{\sum\sum E(\omega_n) E(\omega_m) e^{-i(\omega_n + \omega_m)t}}{\left[\omega_0^2 - \omega_n^2 - 2i\gamma\omega_n\right]\left[\omega_0^2 - \omega_m^2 - 2i\gamma\omega_m\right]\left[\omega_0^2 - (\omega_n + \omega_m)^2 - 2i\gamma(\omega_n + \omega_m)\right]} \qquad [1.20]$$

As a result we have obtained a relation for the non-linear susceptibility from the simple model of the electron as an anharmonic oscillator. The polarization may be written as a series of higher nonlinear orders:

$$P = \sum P_k \qquad \text{with} \qquad P_k = -Ner_k$$

Then:

$$P_{linear} = \sum \chi^{(1)}(\omega_n) E(\omega_n) e^{-i\omega_n t} \qquad [1.21]$$

$$P_{second} = \sum\sum \chi^{(2)}(\omega_n, \omega_m) E(\omega_n) E(\omega_m) e^{-i(\omega_n + \omega_m)t} \qquad [1.22]$$

with the susceptibilities:

$$\chi^{(1)}(\omega_n) = \frac{Ne^2}{m} \frac{1}{(\omega_0 - \omega_n)^2 - 2i\gamma\omega_n} \qquad [1.23]$$

and:

$$\chi^{(2)}(\omega_n, \omega_m) = \frac{Ne^3\xi}{m^2} \frac{1}{\left[(\omega_0 - \omega_n)^2 - 2i\gamma\omega_n\right]\left[(\omega_0 - \omega_m)^2 - 2i\gamma\omega_m\right]} \frac{1}{\left[(\omega_0 - (\omega_n + \omega_m))^2 - 2i\gamma(\omega_n + \omega_m)\right]} \qquad [1.24]$$

The second order susceptibility can be written in terms of the first orders susceptibilities, and it depends on a product of three of these, the susceptibility at frequency ω_n, ω_m and the sum-frequency $\omega_n + \omega_m$:

$$\chi^{(2)}(\omega_n,\omega_m)=\frac{-m\xi}{N^2e^3}\chi^{(1)}(\omega_n)\chi^{(1)}(\omega_m)\chi^{(1)}(\omega_n+\omega_m) \qquad [1.25]$$

In these equations ω_0 represents the "eigenmodes" of the medium. These modes correspond to the eigenstates and should be calculated quantum mechanically. In case of $\omega_0 \approx \omega_n$ or $\omega_0 \approx \omega_m$ "resonance enhancement" will occur: an increase in the nonlinear susceptibility as a result of the resonance behavior of the medium. Even a resonance on the sum-frequency will aid to the susceptibility.

1.5 *MAXWELL'S EQUATIONS FOR NONLINEAR OPTICS*

Light propagating through a medium or through the vacuum may be described by a transverse wave, where the oscillating electric and magnetic field components are solutions to the Maxwell's equations. Also the nonlinear polarizations, induced in a medium, have to obey these equations:

$$\nabla \times \mathbf{E} = -(\partial/\partial t)\,\mathbf{B} \qquad [1.26]$$
$$\nabla \times \mathbf{H} = \mathbf{j} + (\partial/\partial t)\,\mathbf{D} \qquad [1.27]$$
$$\nabla \bullet \mathbf{D} = \rho \qquad [1.28]$$
$$\nabla \bullet \mathbf{B} = 0 \qquad [1.29]$$

with additional relations, and σ the conductivity:

$$\mathbf{D} = \varepsilon_0\mathbf{E} + \mathbf{P} \qquad [1.30]$$
$$\mathbf{j} = \sigma\mathbf{E} \qquad [1.31]$$

The induced polarization may be written in a linear and a nonlinear part:

$$\mathbf{P} = \varepsilon_0\chi\mathbf{E} + \mathbf{P}^{NL} \qquad [1.32]$$

Inserting this in the Maxwell equation for the curl of the magnetic field yields with $[\varepsilon=\varepsilon_0(1+\chi)]$:

$$\nabla \times \mathbf{H} = \sigma\mathbf{E} + \varepsilon\,(\partial/\partial t)\,\mathbf{E} + (\partial/\partial t)\,\mathbf{P}^{NL} \qquad [1.33]$$

Taking the curl of the curl of the electric field component, starting form the first equation gives:

$$\nabla \times \nabla \times \mathbf{E} = -(\partial/\partial t)\,\nabla \times \mathbf{B} = -\mu(\partial/\partial t)\,\nabla \times \mathbf{H} = -\mu(\partial/\partial t)\,[\sigma\mathbf{E} + \varepsilon(\partial/\partial t)\mathbf{E} + (\partial/\partial t)\mathbf{P}^{NL}] \qquad [1.34]$$

Also the general vector relation holds:

$$\nabla \times \nabla \times \mathbf{E} = \nabla(\nabla \bullet \mathbf{E}) - \nabla^2\mathbf{E} \qquad [1.35]$$

And by taking $\nabla \bullet \mathbf{E}=0$ (i.e. for a charge-free medium) we obtain:

$$\nabla^2\mathbf{E} = \mu\sigma\,(\partial/\partial t)\mathbf{E} + \mu\varepsilon(\partial^2/\partial t^2)\mathbf{E} + \mu(\partial^2/\partial t^2)\mathbf{P}^{NL} \qquad [1.36]$$

Above equations were derived in the SI or MKS units. In many handbooks (also at a few instances in this course) the fields are expressed in the esu units. Some simple substitution rules may be used for the transfer of SI to 'esu':

SI: $P^{(n)} = \varepsilon_0 \chi^{(n)} E^{(n)}$ in Cm^{-2}
esu: $P^{(n)} = \chi^{(n)} E^{(n)}$ in statvolt cm^{-1}

and:

$$\chi^{(n)}_{SI} / \chi^{(n)}_{esu} = 4\pi/(10^{-4}c)^{n-1} \quad \text{and} \quad P^{(n)}_{SI} / P^{(n)}_{esu} = 10^3/c$$

1.6 *THE COUPLED WAVE EQUATIONS*

Consider an input wave with electric field components at frequencies ω_1 and ω_2. In the approximation of *plane waves* the total field may then be written as:

$$\mathbf{E}(t) = \mathrm{Re}\,[\mathbf{E}(\omega_1)\exp(i\omega_1 t) + \mathbf{E}(\omega_2)\exp(i\omega_2 t)] \qquad [1.37]$$

In the medium a polarization at the sum frequency $\omega=\omega_1+\omega_2$ is generated. This polarization is now expressed in the vector components:

$$P_i(\omega_1+\omega_2) = \mathrm{Re}\,\{\chi_{ijk}(\omega=\omega_1+\omega_2)\,E_j(\omega_1)\,E_k(\omega_2)\exp[i(\omega_1+\omega_2)t]\} \qquad [1.38]$$

At the same time also a difference frequency component may be produced in the medium, however with a different nonlinear susceptibility tensor:

$$P_i(\omega_1-\omega_2) = \mathrm{Re}\,\{\chi_{ijk}(\omega=\omega_1-\omega_2)\,E_j(\omega_1)\,E_k^*(\omega_2)\exp[i(\omega_1-\omega_2)t]\} \qquad [1.39]$$

The notation of fields in terms of complex amplitudes has the consequence that whenever a negative frequency appears in the equations the complex conjugate of the field amplitude is to be taken, because:

$$E_k(-\omega_2) = E_k^*(\omega_2) \qquad [1.40]$$

The tensors $\chi_{ijk}(\omega=\omega_1+\omega_2)$ and $\chi_{ijk}(\omega=\omega_1-\omega_2)$ are material properties and have different values depending on the frequencies; this is related to the possibility of resonance enhancement and the energy level structure of the medium.
Now we will consider the above derived Maxwell equation:

$$\nabla^2\mathbf{E} - \mu\sigma\,(\partial/\partial t)\mathbf{E} - \mu\varepsilon(\partial^2/\partial t^2)\mathbf{E} = \mu(\partial^2/\partial t^2)\mathbf{P}^{NL} \qquad [1.41]$$

which is a vectorial expression that may be used in threefold for the three vector components. In the simple case of frequency mixing with two incoming plane waves propagating along the z-axis and the assumption of a linear polarization in a single transverse direction:

$$E_1(z,t) = E_1(z)\exp(i\omega_1 t - ik_1 z) \qquad [1.42]$$
$$E_2(z,t) = E_2(z)\exp(i\omega_2 t - ik_2 z)$$

These two incoming fields induce a nonlinear polarization at frequency $\omega=\omega_1+\omega_2$ that may be written as:

$$P_{NL}(z,t) = d\, E_1(z)\, E_2(z) \exp[i(\omega_1+\omega_2)t - i(k_1+k_2)z] \qquad [1.43]$$

And we assume that a new field is created at frequency $\omega_3=\omega_1+\omega_2$ with a field:

$$E_3(z,t) = E_3(z) \exp(i\omega_3 t - ik_3 z) \qquad [1.44]$$

Now substitute these fields into the wave equation. For plane waves traveling in the z-direction the field gradient may be written as:

$$\nabla^2 E_3(z,t) = \frac{\partial^2}{\partial z^2} E_3(z,t) \qquad [1.45]$$

The left side of Eq. [1.45] then yields:

$$\begin{aligned} &\frac{\partial^2}{\partial z^2} E_3(z,t) + \mu\sigma \frac{\partial}{\partial t} E_3(z,t) - \mu\varepsilon \frac{\partial^2}{\partial t^2} E_3(z,t) = \\ &= \frac{d^2}{dz^2} E_3(z,t) + 2ik_3 \frac{d}{dz} E_3(z,t) - k_3^2 E_3(z,t) + i\omega_3 \mu\sigma E_3(z,t) + \mu\varepsilon\omega_3^2 E_3(z,t) \end{aligned} \qquad [1.46]$$

The quantities $E_i(z,t)$ have the meaning of an amplitude and it will be a good assumption that the variation of the amplitude over the distance of one wavelength will be small; this assumption is called the *slowly varying amplitude approximation*:

$$\left| \frac{d^2}{dz^2} E_3(z,t) \right| << \left| 2ik_3 \frac{d}{dz} E_3(z,t) \right| \qquad [1.47]$$

As a consequence the second order spatial derivative may be dropped. Furthermore for plane waves propagating in a medium with dielectric constant ε and magnetic susceptibility μ the following relation holds:

$$\mu\varepsilon\omega_3^2 - k_3^2 = 0 \qquad [1.48]$$

So only two terms are left on the left side of the wave equation:

$$2ik_3 \frac{d}{dz} E_3(z) \exp(i\omega_3 t - ik_3 z) + i\omega_3 \mu\sigma E_3(z) \exp(i\omega_3 t - ik_3 z) \qquad [1.49]$$

The right side of the wave equation is evaluated as follows:

$$\begin{aligned} \mu \frac{\partial^2}{\partial t^2} P^{NL}(z,t) &= \mu \frac{\partial^2}{\partial t^2} dE_1(z) E_2(z) \exp\left[i(\omega_1+\omega_2)t - i(k_1+k_2)z\right] \\ &= -\mu(\omega_1+\omega_2)^2 dE_1(z) E_2(z) \exp\left[i(\omega_1+\omega_2)t - i(k_1+k_2)z\right] \end{aligned} \qquad [1.50]$$

Equating the two results yields:

$$\frac{d}{dz}E_3(z) = -\frac{\sigma}{2}\sqrt{\frac{\mu}{\varepsilon_3}}E_3(z) - \frac{i\omega_3}{2}\sqrt{\frac{\mu}{\varepsilon_3}}dE_1(z)E_2(z)\exp\left[-i(k_1 + k_2 - k_3)z\right] \qquad [1.51]$$

where use was made of energy conservation ($\omega_3=\omega_1+\omega_2$) and the above postulated relation between the frequency and the wave vector of a wave. The basic equation found implies that the amplitude of the newly produced wave is coupled through the nonlinear constant d to the incoming wave. There is an energy flow from the wave at frequencies ω_1 and ω_2 to the wave at frequency ω_1. At the same time inverse processes will take also place, i.e. processes where the newly generated frequency ω_3 mixes with one of the two incoming waves in a difference frequency mixing process like $\omega_3-\omega_2 \rightarrow \omega_1$. By inserting the fields in the Maxwell's wave equation in a similar fashion one can derive two more coupled amplitude equations:

$$\begin{aligned}\frac{d}{dz}E_1(z) &= -\frac{\sigma}{2}\sqrt{\frac{\mu}{\varepsilon_1}}E_1(z) - \frac{i\omega_1}{2}\sqrt{\frac{\mu}{\varepsilon_1}}dE_3(z)E_2(z)^*\exp\left[-i(k_3 - k_2 - k_1)z\right] \\ \frac{d}{dz}E_2(z)^* &= -\frac{\sigma}{2}\sqrt{\frac{\mu}{\varepsilon_2}}E_2(z)^* + \frac{i\omega_2}{2}\sqrt{\frac{\mu}{\varepsilon_2}}dE_1(z)E_3(z)^*\exp\left[-i(k_1 + k_2 - k_3)z\right]\end{aligned} \qquad [1.52]$$

Now we have derived three differential equations by which the three amplitudes of the waves are coupled.
NOTE: Even in the case where a wave at frequency $\omega_3=\omega_1+\omega_2$ is created the wave vectors do not cancel because of the dispersion in the medium (the frequency dependence of the index of refraction):

$$\omega_i = \frac{k_i}{\sqrt{\mu\varepsilon(\omega_i)}} = \frac{ck_i}{n(\omega_i)} \qquad [1.53]$$

Of course it should be realized that the k_i are vectors, with in the most general case a directionality, that may be different for the waves. We define the wave vector mismatch as:

$$\Delta\mathbf{k} = \mathbf{k}_3\text{-}\mathbf{k}_1\text{-}\mathbf{k}_2 \qquad [1.54]$$

1.8 *NONLINEAR OPTICS WITH FOCUSED GAUSSIAN BEAMS*

In previous sections the non-linear interactions are treated in the plane-wave approximation; the fields in Eq. [1.42-1.43] are expressed as plane waves propagating with a flat wave-front along the z-axis. This approximation is not valid in cases when the laser beams are focused. Focusing is often profitable in non-linear optics as the high peak intensities give high non-linear yields. We consider again the wave equation for a wave at frequency ω_n and neglecting absorptions:

$$\nabla^2\mathbf{E}_n - \left(\frac{n}{c}\right)^2\frac{\partial^2}{\partial t^2}\mathbf{E}_n = \frac{4\pi}{c^2}\frac{\partial^2}{\partial t^2}\mathbf{P}_n \qquad [1.55]$$

The electric field vector and the polarization are now defined different from Eq. [1.42-1.43] by explicitly taking a spatial dependence into account:

$$\mathbf{E}_n(\mathbf{r},t) = \mathrm{Re}\left[\mathbf{A}_n(\mathbf{r})e^{i(k_k z-\omega_n t)}\right]$$
$$\mathbf{P}_n(\mathbf{r},t) = \mathrm{Re}\left[\mathbf{p}_n(\mathbf{r})e^{i(k_k{}'z-\omega_n t)}\right] \qquad [1.56]$$

Here the complex amplitudes $\mathbf{A}_n$ and $\mathbf{p}_n$ are spatially varying. The Laplace operator of the wave function may now be expressed as:

$$\nabla^2 = \frac{\partial^2}{\partial z^2} + \nabla_{\mathrm{T}}^2 \qquad [1.57]$$

Similarly as in the plane wave case the slowly varying amplitude approximation may be applied and this then results in the *paraxial* wave equation:

$$2ik_n \frac{\partial \mathbf{A}_n}{\partial z} + \nabla_T{}^2 \mathbf{A}_n = -\frac{4\pi\omega_n{}^2}{c^2}\mathbf{p}_n e^{-i\Delta kz} \qquad [1.58]$$

This paraxial wave equation can first be considered in the case where the polarization p_n vanishes. From an analysis of *Gaussian* optics an amplitude distribution follows (see optics course):

$$\mathrm{A}(r,z) = \mathrm{A}\frac{w_0}{w(z)}\exp\left[-\frac{r^2}{w(z)^2}\right]\exp\left[\frac{ikr^2}{2R(z)}\right]\exp\left[i\Phi(z)\right] \qquad [1.59]$$

where *w(z)* represents the 1/e radius of the field distribution, *R(z)* the radius of curvature of the wave front and *Φ(z)* the spatial variation of the phase of the wave with respect to an infinite plane wave defined as:

$$w(z) = w_0\sqrt{1+\left(\frac{\lambda z}{\pi w_0^2}\right)^2} \qquad [1.60]$$

$$R(z) = z\left[1+\left(\frac{\pi w_0^2}{\lambda z}\right)^2\right] \qquad [1.61]$$

$$\Phi(z) = -\arctan\left(\frac{\lambda z}{\pi w_0^2}\right) \qquad [1.62]$$

It is convenient to express the Gaussian beam as:

$$\mathrm{A}(r,z) = \frac{\mathrm{A}}{1+i\frac{2z}{b}}\exp\left[-\frac{r^2}{w_0^2\left(1+i\frac{2z}{b}\right)}\right] \qquad [1.63]$$

where b is the so-called confocal parameter, a measure of the longitudinal extent of the focal region of the Gaussian beam:

$$b = \frac{2\pi w_0^2}{\lambda} = k w_0^2 \qquad [1.64]$$

In the Figure the characteristics of such a Gaussian beam is depicted.

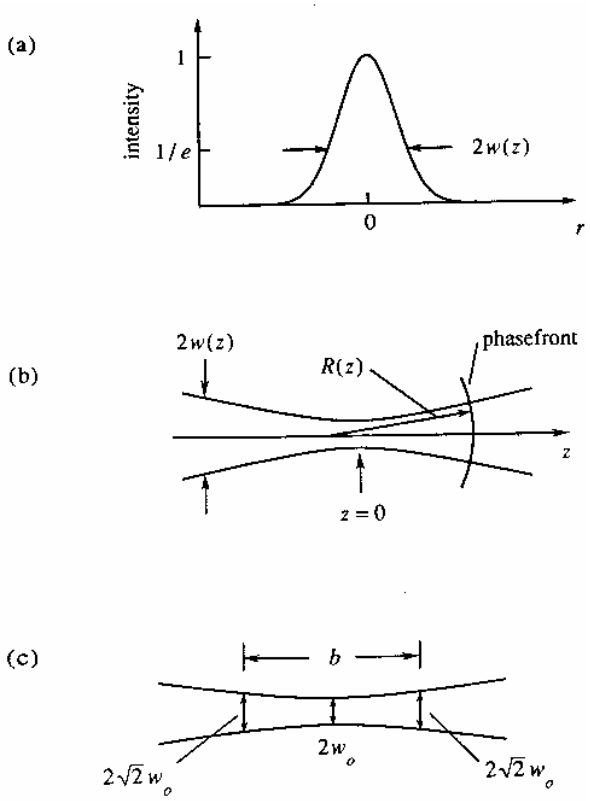

Fig.: (a) Intensity distribution of a Gaussian laser beam. (b) Variation of the beam radius w and wavefront radius of curvature R with position z. (c) Relation between the beam waist radius w_0 and the confocal parameter b.

In case of harmonic generation with Gaussian beams the above amplitude expressions may be used. If A_1 is the amplitude of the wave at the fundamental frequency then the q-th nonlinear polarization may be expressed as:

$$\mathbf{p}_q = \chi^{(q)} \mathbf{A}_1^{\,q} \qquad [1.65]$$

and the amplitude A_q of frequency $q\omega$ must obey the equation (use [1.65] and the paraxial wave equation [1.58]).

$$2ik_q \frac{\partial \mathbf{A}_q}{\partial z} + \nabla_T{}^2 \mathbf{A}_q = -\frac{4\pi\omega_q{}^2}{c^2} \chi^{(q)} \mathbf{A}_1{}^q e^{-i\Delta kz} \qquad [1.66]$$

where the phase-mismatch is defined as:

$$\Delta \mathrm{k} = \mathrm{k_q} - \mathrm{qk_1} \qquad [1.67]$$

For the amplitude of the fundamental we use [1.63] and for the harmonic we adopt the trial solution:

$$\mathrm{A}_q(r,z) = \frac{\mathrm{A}_q(z)}{1+i\frac{2z}{b}} \exp\left[-\frac{qr^2}{w_0^2\left(1+i\frac{2z}{b}\right)}\right] \qquad [1.68]$$

This is a function with a confocal parameter equal to that of the fundamental wave. After inserting the trial [1.67] into the wave equation [1.66] it follows that:

$$\frac{d}{dz}\mathrm{A}_q = \frac{2i\pi q\omega}{nc} \chi^{(q)} \mathrm{A}_1^q \frac{e^{i\Delta kz}}{\left(1+i\frac{2z}{b}\right)^{q-1}} \qquad [1.69]$$

The equation may be integrated:

$$\mathrm{A}_q(z) = \frac{2i\pi q\omega}{nc} \chi^{(q)} \mathrm{A}_1^q F_q(\Delta k, z_0, z) \qquad [1.70]$$

where the so-called phase-matching integral:

$$F_q(\Delta k, z_0, z) = \int_{z_0}^{z} \frac{e^{-i\Delta kz'}}{\left(1+\frac{2iz'}{b}\right)^{q-1}} dz' \qquad [1.71]$$

is over the length of the nonlinear medium, starting at z_0. The harmonic radiation is generated with a confocal parameter b, similar to that of the fundamental wave. The beam waist radius is therefore narrower by a factor of $\sqrt{q}$.

The integral can be evaluated numerically and in approximating cases also analytically. If $b>>z$ the result for a situation of plane waves should follow. In the limiting case $b<<z$ the fundamental wave is focused tightly. If the boundary conditions range over the complete focus, in the approximation $[-\infty,\infty]$, the integral can be evaluated via contour integration resulting in:

$$F_q(\Delta k, z_0, z) = \int_{-\infty}^{\infty} \frac{e^{-i\Delta kz'}}{\left(1+\frac{2iz'}{b}\right)^{q-1}} dz' \qquad [1.72]$$

which yields in two limiting cases:

$$F_q = 0 \qquad \text{for} \qquad \Delta k \geq 0 \qquad [1.73]$$

$$F_q = \frac{b}{2}\frac{2\pi}{(q-2)!}\left(\frac{b\Delta k}{2}\right)^{q-2} \exp\left(\frac{b\Delta k}{2}\right) \qquad \text{for} \qquad \Delta k \leq 0 \qquad [1.74]$$

So in the *tight-focusing limit* there is no yield of harmonics for $\Delta k>0$. Only in case of $\Delta k\leq 0$ harmonics are generated. This condition corresponds to media with *negative dispersion* at the frequency of the harmonic.

Chapter 2

Second Harmonic Generation

2.1 *SECOND HARMONIC GENERATION AND PHASE MATCHING*

Starting out from the coupled wave equations, assuming just a single input field, so $E_1(z) = E_2(z)$, a radiation field $E_3(z)$ may be generated:

$$\frac{d}{dz}E_3(z) = -\frac{\sigma}{2}\sqrt{\frac{\mu}{\varepsilon_3}}E_3(z) - \frac{i\omega_3}{2}\sqrt{\frac{\mu}{\varepsilon_3}}dE_1^2(z)e^{-i(2k_1-k_3)z} \qquad [2.1]$$

Under the assumptions:
- that there is a nonzero nonlinear coefficient d; this implies a certain symmetry of the medium;
- that there is no absorption in the medium, so the conductivity term may be neglected;
- there is only little production of the wave at ω_3, so that the field amplitudes are not affected by the conversion process;
- the wave vector mismatch is now:

$$\Delta k = k^{(2\omega)} - 2k^{(\omega)} \qquad [2.2]$$

the coupled wave equation can be integrated straightforwardly:

$$E^{(2\omega)}(z) = -i\omega\sqrt{\frac{\mu}{\varepsilon^{(2\omega)}}}dE^2(\omega)\int e^{i\Delta kz}dz \qquad [2.3]$$

where the integration is over the length of the medium (and the overlap of light beams) between 0 and L. The integration yields, assuming that $E^{(2\omega)}(0) = 0$:

$$E^{(2\omega)}(L) = -\omega\sqrt{\frac{\mu}{\varepsilon^{(2\omega)}}}dE^2(\omega)\frac{e^{i\Delta kL}-1}{\Delta k} \qquad [2.4]$$

The output intensity of the *second harmonic* is proportional to:

$$E^{(2\omega)}(L)E^{(2\omega)}(L)^* = \frac{\omega^2\mu}{n^2\varepsilon_0}d^2\left|E(\omega)\right|^4L^2\frac{\sin^2\left(\frac{\Delta kL}{2}\right)}{\left(\frac{\Delta kL}{2}\right)^2} \qquad [2.5]$$

If the beams are written in terms of beam intensities, so of power per unit area A, then it follows that the conversion efficiency for second harmonic generation is:

$$\eta_{SHG} = \frac{P^{(2\omega)}}{P^{(\omega)}} \propto \omega^2 d^2 L^2 \frac{\sin^2\left(\frac{\Delta kL}{2}\right)}{\left(\frac{\Delta kL}{2}\right)^2} \frac{P^{(\omega)}}{A} \qquad [2.6]$$

From this derivation we learn that:
- the conversion efficiency is proportional to the power density, so the total amount of generated light at the second harmonic is proportional to $[P^{(\omega)}]^2$. Thus second harmonic generation is a process that is *non-linear* in the power dependence.
- the efficiency is equal to the *square* of the nonlinear coefficient *d*, or in other terms proportional to $|\chi^{(2)}|^2$
- the efficiency is proportional with L^2 and a "sinc"-function involving *L*; it seems that longer crystals will produce more second harmonic; we will see that this effect will be restricted.
- the efficiency is optimal if $\Delta k=0$ and this is a condition that generally cannot be met in ordinary media; we will see that in birefringent media this condition, that can be written as $k^{(2\omega)}=2k^{(\omega)}$, and also the breakdown of inversion symmetry can be met at the same time.

The condition of $\Delta k=0$ is referred to as the *phase-matching condition*. With the use of $k=n\omega/c$ the phase matching relation is given by Eq. [2.2].
For ordinary waves in a medium there is always dispersion, with the consequence that:

$$n^{(2\omega)} > n^{(\omega)} \qquad [2.7]$$

so always $\Delta k \neq 0$. The *physical consequence* of the dispersion is that the two waves:

$$E_\omega(z,t) = E_\omega \exp\left[i\omega t - ik^{(\omega)}z\right] \qquad [2.8]$$
$$E_{2\omega}(z,t) = E_{2\omega} \exp\left[2i\omega t - ik^{(2\omega)}z\right]$$

will run out of phase and therefore the process of coherent generation of radiation at frequency 2ω will be stopped and even reversed if the phases differ by 180^0. Then destructive interference will take place and the original build up of the wave at 2ω will be destroyed. After a distance *l* for which holds:

$$\Delta k\, l = \pi \qquad [2.9]$$

the amplitude is at maximum. The particular length $L_C=2l$ is called *the coherence length*; it is the maximum crystal length useful in producing the second harmonic:

$$L_c = \frac{2\pi}{\Delta k} = \frac{2\pi}{k^{(2\omega)} - 2k^{(\omega)}} = \frac{\pi c}{2\omega\left(n^{(2\omega)} - n^{(\omega)}\right)} = \frac{\lambda}{4\left(n^{(2\omega)} - n^{(\omega)}\right)} \qquad [2.10]$$

For some typical values of a wavelength $\lambda = 1\mu m$ and a dispersion of $n^{(2\omega)} - n^{(\omega)} = 10^{-2}$ we find a coherence length of $L_C=50\ \mu m$. So in the equation derived above the dependence on the length L^2 is to be replaced by a dependence on L_C^2.
The proof of the coherence length effect was given in an experiment by Maker *et al.*[2] In a simple experimental setup with a rotating crystal and a transmission filter for the frequency 2ω

[2] P.D. Maker, R.W. Terhune, M. Nisenoff, and C. M. Savage, Phys. Rev. Lett. **8**, 19 (1962).

the variation of the produced second harmonic power was measured with variation of the angle of rotation of the crystal.

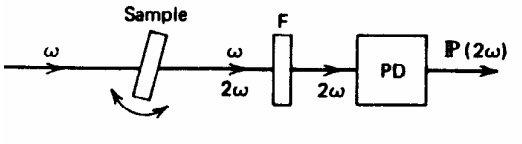

In a situation with $\Delta k \neq 0$ in the first coherence length L_C power at 2ω is produced. In the second coherence length also a field $E_{2\omega}$ is generated, but this is out of phase with the propagating field $E_{2\omega}$ that was generated in the first coherence length. In these parts the intensity at frequency 2ω will be coupled back into a wave at the fundamental frequency ω. As a net result the power will decrease.
So we find for a particular crystal length L:

$$L = 2n\,L_C \quad \rightarrow \quad P^{(2\omega)} = 0 \qquad [2.11]$$
$$L = (2n+1)\,L_C \quad \rightarrow \quad P^{(2\omega)} = \text{optimum}$$

As the crystal length we understand the path length of the light beam through the crystal, and this is dependent on the incident angle θ of the incoming beam onto the crystal surface:

$$L = d \cos\theta \qquad [2.12]$$

with d the thickness of the crystal. By varying the angle of rotation the effective length of the crystal will change and therewith the number of coherence lengths. This oscillatory effect of the second harmonic power was first observed by Maker *et al.*[2] and the oscillations are called *Maker fringes*.

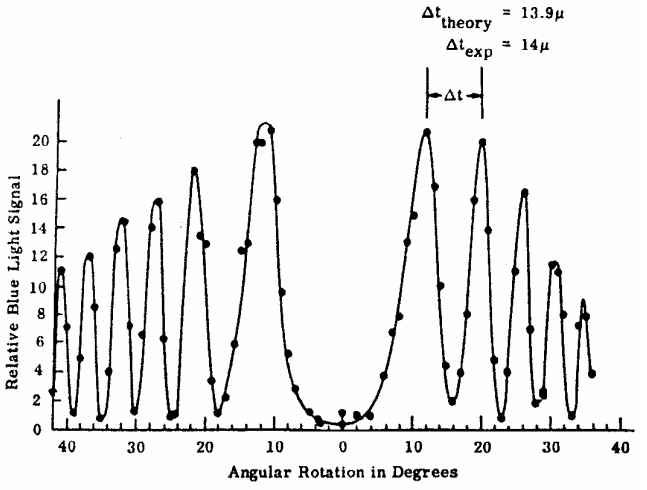

Fig.: adapted from ref [2].

If the *phase matching condition* could be fulfilled by some means then instead of the coherence length of L_C=50 μm the full length of a crystal of e.g. 2 cm could be used. This would lead to an increase of second harmonic power of a factor 1.6×10^5. This condition can be met in a

special class of crystals, the so-called *birefringent* crystals, that are known to have some peculiar and complicated properties, even in the realm of linear optics.

2.2 *WAVE PROPAGATION IN ANISOTROPIC MEDIA; INTERMEZZO*

In an anisotropic medium the induced polarization is not always parallel to the applied electric field. The susceptibility that governs the electromagnetic response of the medium is not just a scalar but a tensor of rank two. Physically this effect may be understood from the fact that the ordering of atoms in a crystal is not identical along different directions. The polarization is:

$$\mathbf{P} = \varepsilon_0 \chi \mathbf{E} \qquad [2.13]$$

or in components (in SI units):

$$\begin{aligned} P_1 &= \varepsilon_0 (\chi_{11} E_1 + \chi_{12} E_2 + \chi_{13} E_3) \\ P_2 &= \varepsilon_0 (\chi_{21} E_1 + \chi_{22} E_2 + \chi_{23} E_3) \\ P_3 &= \varepsilon_0 (\chi_{31} E_1 + \chi_{32} E_2 + \chi_{33} E_3) \end{aligned} \qquad [2.14]$$

The 9 elements of a second order tensor χ depend on the choice of a coordinate frame. From formal tensor theory it follows that there are *three invariants* in three dimensions for a second order tensor. As a consequence for a particular choice of axes x, y and z, the so-called principal dielectric axes of the crystal (that are not necessarily orthogonal) there will be only 3 non-zero elements left. The dielectric tensor can also be written in the form of Maxwell's displacement vector:

$$\mathbf{D} = \varepsilon_0 \mathbf{E} + \mathbf{P} = \varepsilon_0 (1+\chi_{ij}) \mathbf{E} = \varepsilon_{ij} \mathbf{E} \qquad [2.15]$$

where the susceptibility tensor χ_{ij} is replaced by the dielectric permittivity tensor ε_{ij}.
A monochromatic plane wave of angular frequency ω can be expressed with electric and magnetic field components, $\mathbf{E} \exp(i\omega t - i\mathbf{k}\cdot\mathbf{r})$ and $\mathbf{H} \exp(i\omega t - i\mathbf{k}\cdot\mathbf{r})$, where **k** is the wave vector, a vector in the direction of wave propagation. It is the vector that in Huygens theory is the normal to the wave front. It is equal to:

$$\mathbf{k} = n\omega/c\, \mathbf{s} \qquad [2.16]$$

with n the index of refraction and **s** a unit vector. In nonmagnetic media Maxwell's equations are:

$$\begin{aligned} \nabla \times \mathbf{E} &= -(\partial/\partial t)\, \mathbf{B} \\ \nabla \times \mathbf{H} &= (\partial/\partial t)\, \mathbf{D} \end{aligned} \qquad [2.17]$$

From these equations we will determine now the relative orientations of the vectors **k**, **H**, **E** and **D**. The derivatives, in case of plane waves may be written as:

$$\begin{aligned} \nabla \quad &\rightarrow \quad -i\mathbf{k} = -in\omega/c\, \mathbf{s} \\ (\partial/\partial t) \quad &\rightarrow \quad i\omega \end{aligned} \qquad [2.18]$$

and by insertion of the plane waves in the Maxwell equations we obtain:

$$\mathbf{k} \times \mathbf{E} = +\mu_0\omega\,\mathbf{H} \qquad [2.19]$$
$$\mathbf{k} \times \mathbf{H} = -\omega\,\mathbf{D}$$

From these equalities we learn that **H** and **D** are vectors perpendicular to the wave vector **k**. Also **H** and **D** are a pair of perpendicular vectors, because of the second relation. So we conclude that **H** and **D** constitute a proper transverse wave in an orthogonal frame with **k**. For the electric field vector **E** the following statements hold:
- **E** is perpendicular to **H**
- $\mathbf{D}=\varepsilon\mathbf{E}$; if ε is a scalar then **E** is along the direction of **D** and then **E** is perpendicular to the wave vector **k**. But in an anisotropic medium, where ε is a tensor, the vector **E** is no longer perpendicular to **k**.

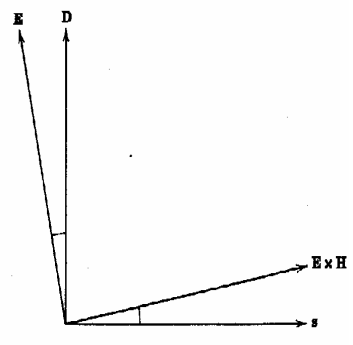

An important physical consequence for the wave propagation in anisotropic media follows from this. The Poynting vector:

$$\mathbf{S} = \mathbf{E} \times \mathbf{H} \qquad [2.20]$$

is not along **k**. So the direction of energy flow is different from the direction of the wave vector. In other words the *phase velocity* and the *group velocity* of the light beam are different, not only in size but also in direction.

By eliminating **H** from the above equations we find:

$$\mathbf{k} \times (\mathbf{k} \times \mathbf{E}) = -\mu_0\omega^2\,\mathbf{D}$$

Using the vector relation Ax(BxC)=B(A•C)-C(A•B) we obtain:

$$\mathbf{k} \times (\mathbf{k} \times \mathbf{E}) = \mathbf{k}(\mathbf{k}\bullet\mathbf{E})-\mathbf{E}(\mathbf{k}\bullet\mathbf{k}) = -\mu_0\omega^2\,\mathbf{D} \qquad [2.22]$$

so in terms of the unit vector **s**:

$$\mathbf{D} = n^2\varepsilon_0\,[\,\mathbf{E} - \mathbf{s}(\mathbf{s}\bullet\mathbf{E})] \qquad [2.23]$$

Now we choose a coordinate frame (x,y,z) corresponding to the principal dielectric axes of the medium. In this frame:

$$\begin{pmatrix} D_x \\ D_y \\ D_z \end{pmatrix} = \begin{pmatrix} \varepsilon_x & 0 & 0 \\ 0 & \varepsilon_y & 0 \\ 0 & 0 & \varepsilon_z \end{pmatrix} \begin{pmatrix} E_x \\ E_y \\ E_z \end{pmatrix} \qquad [2.24]$$

where of course the permittivities of the medium will be different along the various principal axes. Then it follows for i=x,y,z that :

$$D_i = n^2 \varepsilon_0 \left[\frac{D_i}{\varepsilon_i} - s_i (\mathbf{s} \cdot \mathbf{E}) \right] \qquad [2.25]$$

and by rearranging:

$$D_i = \frac{\varepsilon_0 (\mathbf{s} \cdot \mathbf{E})}{\frac{1}{n^2} - \frac{\varepsilon_0}{\varepsilon_i}} s_i \qquad [2.26]$$

Forming the scalar product $\mathbf{D} \bullet \mathbf{s} = D_x s_x + D_y s_y + D_z s_z = 0$, because **D** and **s** are perpendicular then gives:

$$\frac{s_x^2}{\frac{1}{n^2} - \frac{\varepsilon_0}{\varepsilon_x}} + \frac{s_y^2}{\frac{1}{n^2} - \frac{\varepsilon_0}{\varepsilon_y}} + \frac{s_z^2}{\frac{1}{n^2} - \frac{\varepsilon_0}{\varepsilon_z}} = 0 \qquad [2.27]$$

This equation is known as Fresnel's equation. This equation is quadratic in n and will therefore have two independent solutions n' and n''. So there are also two different waves $\mathbf{D}'(n')$ and $\mathbf{D}''(n'')$ that obey Fresnel's equation. A calculation of the dot product of the two solutions yields, by making use of Eq. [2.27]:

$$\mathbf{D}' \cdot \mathbf{D}'' = \varepsilon_0^{\,2} (\mathbf{s} \cdot \mathbf{E})^2 \left\langle \sum_{x,y,z} \frac{s_\alpha^2}{\left(\frac{1}{n'^2} - \frac{\varepsilon_0}{\varepsilon_\alpha} \right) \left(\frac{1}{n''^2} - \frac{\varepsilon_0}{\varepsilon_\alpha} \right)} \right\rangle$$

$$= \varepsilon_0^{\,2} (\mathbf{s} \cdot \mathbf{E})^2 \frac{(n' n'')^2}{(n'^2 - n''^2)} \left\langle \sum_{x,y,z} \left[\frac{s_\alpha^2}{\left(\frac{1}{n'^2} - \frac{\varepsilon_0}{\varepsilon_\alpha} \right)} + \frac{s_\alpha^2}{\left(\frac{1}{n''^2} - \frac{\varepsilon_0}{\varepsilon_\alpha} \right)} \right] \right\rangle \qquad [2.28]$$

where the summation index α is over coordinates x, y and z. So we find for the two solutions of the Fresnel equation:

$$\mathbf{D}' \bullet \mathbf{D}'' = 0 \qquad [2.29]$$

A general result is: an anisotropic crystal can transmit waves that are plane polarized in one of two mutually orthogonal directions. These two waves see different refractive indices n' and n''. Also the direction of energy flow is now perpendicular to the wave front. If an incoming light

beam is not polarized in one of the two allowed transmittance modes then the transmission may be calculated by first taking the projections of the polarizations of the incoming wave onto **D**' and **D**".

2.2.a *REFRACTION AT A BOUNDARY OF AN ANISOTROPIC MEDIUM*

Consider a plane wave incident on the surface of an anisotropic crystal. The polarization of the incoming beam is in general a mixture of the two different polarization eigenmodes, denoted with **D**' and **D**" in the above. So in general, except for the specific case where the polarization is exactly along one of the principal axes of the crystal, the polarization of the refracted beam is partly along **D**' and partly along **D**". These polarization waves are solutions to the Fresnel equation for *different indices of refraction*. So one wave with polarization **D**' undergoes refraction corresponding to n', while the second polarization component **D**" is refracted by an index n". Different indices of refraction at a boundary implies that the propagation direction of the two beams with **D**' and **D**" is different. In the figure it is graphically shown how to determine the direction of propagation at a boundary with n_0 at one side and n' and n" at the other side.

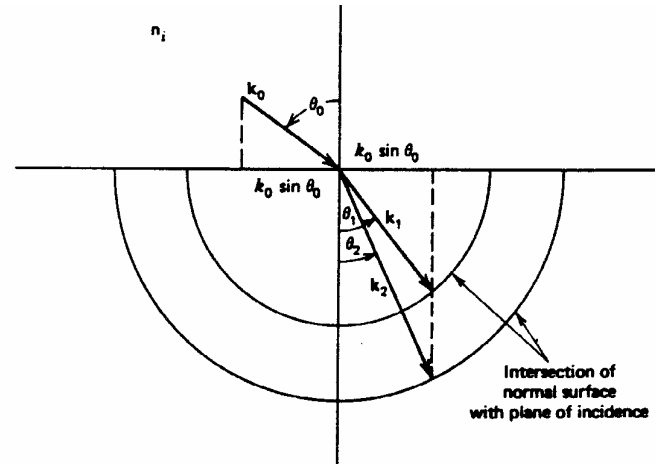

Fig.: Double refraction at a boundary of an anisotropic medium and the graphic method of determining θ_1 and θ_2.

A kinematic condition for refraction requires that:

$$k_0 \sin\theta_0 = k_1 \sin\theta_1 = k_2 \sin\theta_2 \qquad [2.30]$$

with the index 0 referring to the incoming wave and 1 and 2 referring to the refracted waves.

The physical effect of *double refraction* or *birefringence* is thus explained. An incoming wave with polarization $\mathbf{D}_0$ is split into two waves with orthogonal polarizations that transmit under different angles through a crystal.

2.2.b *THE INDEX ELLIPSOID*

The energy density of the stored electric field in a medium is known to be:

$$U_e = \frac{1}{2}(\mathbf{E}\cdot\mathbf{D}) \qquad [2.31]$$

With a coordinate frame of principal axes (x,y,z) and the relation $D_i = \varepsilon_i E_i$ for i=x,y,z a surface of constant energy in D-space is given by:

$$\frac{D_x^2}{\varepsilon_x} + \frac{D_y^2}{\varepsilon_y} + \frac{D_z^2}{\varepsilon_z} = 2U_e \qquad [2.32]$$

Now write $\mathbf{r} = \mathbf{D}\sqrt{2U_e}$ (so **r** relates to a normalized polarization vector) and $n_i^2=\varepsilon_i$ the equation reduces to a formula for a three dimensional ellipsoid:

$$\frac{x^2}{n_x^2} + \frac{y^2}{n_y^2} + \frac{z^2}{n_z^2} = 1 \qquad [2.33]$$

This ellipsoid can be used to find the two indices of refraction for the two polarizations of a wave with a wave vector in a specific direction **s**. For a certain direction of the wave vector the plane normal to **s** intersecting the ellipsoid forms a two-dimensional ellipse. The two axes of this ellipse then determine the two indices of refraction. These axes are parallel to the direction of the vectors $\mathbf{D}_{1,2}$ of the two allowed solutions of the Fresnel equation.

Consideration of a so-called *uniaxial crystal* simplifies the geometry somewhat. A uniaxial crystal, in contrast to a bi-axial crystal, has a single *optical axis*. In terms of the index ellipsoid this becomes a three-dimensional body with cylindrical symmetry. Two indices of refraction are identical, so the plane intersecting perpendicular to the one optical axis forms a *circl*e. If *z* is taken as the axis of cylindrical symmetry (the optical axis of a uniaxial crystal) then the principal indices of refraction are:

$$n_0^2 = \frac{\varepsilon_x}{\varepsilon_0} = \frac{\varepsilon_y}{\varepsilon_0} \quad \text{and} \quad n_e^2 = \frac{\varepsilon_z}{\varepsilon_0}$$

and the equation for the index ellipsoid becomes:

$$\frac{x^2}{n_0^2} + \frac{y^2}{n_0^2} + \frac{z^2}{n_e^2} = 1 \qquad [2.34]$$

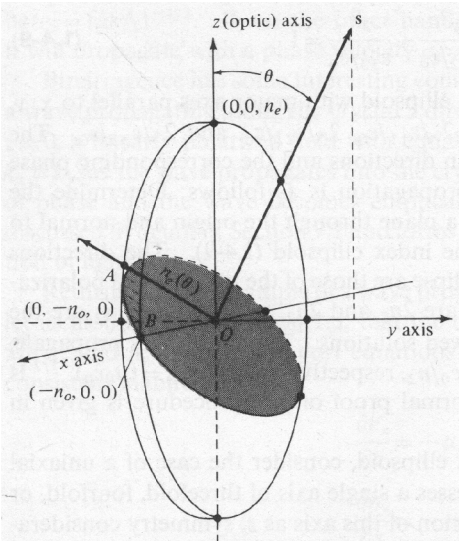

If the direction of the wave vector **s** now makes a certain angle θ to the optic z-axis then the indices of refraction for both the polarization components can be found from the intersecting plane of the ellipsoid perpendicular to the vector **s**. The coordinate frame is chosen such that the vector **s** is in the y-z-plane; because of the cylindrical symmetry around the z-axis this may be done without loss of generality.

The dark plane of intersection forms a two-dimensional ellipse with two principal axes. The two allowed polarization directions are parallel to the axes of the ellipse:
- one polarized along the x-axis; this wave has the polarization vector perpendicular to the optic axis and is defined as the *ordinary wave*; it transmits with index n_O.
- one polarized in the x-y plane but perpendicular to s; this wave , with the polarization vector in the plane with the optic axis is called the *extraordinary wave*.

For clarity the projection of the ellipsoid onto the y-z plane is shown separately. The polarization of the ordinary wave now points perpendicular to the paper.

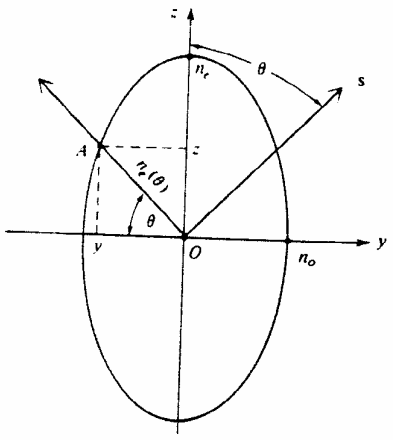

The polarization of the extraordinary wave is along the vector OA and the index of refraction is $n_e(\theta)$. From the figure it follows that that for an arbitrary angle θ the relations hold:

$$z = n_e(\theta) \sin\theta \qquad [2.35]$$

$$y = n_e(\theta)\cos\theta$$

The equation of the ellipse (projection of the ellipsoid with x=0) is:

$$\frac{y^2}{n_o^2} + \frac{z^2}{n_e^2} = 1 \qquad [2.36]$$

Combining these results yields an equation for the index of refraction experienced by the extraordinary wave in a birefringent crystal:

$$\frac{1}{n_e^2(\theta)} = \frac{\cos^2\theta}{n_o^2} + \frac{\sin^2\theta}{n_e^2} \qquad [2.37]$$

So *the index is dependent on the direction of propagation of the wave vector*. In the special case of θ=0, when the wave vector is along the optical axis, there is no birefringence; both polarizations experience an index n_O. If the wave vector s is perpendicular to the optic axis two waves will travel through the medium with indices n_O and n_e. The index of the extraordinary wave then reaches a maximum (for positive birefringence $n_e > n_O$) or a minimum (for negative birefringence $n_e < n_O$).

Usually the refractive indices are represented with a Sellmeier equation of the form:

$$n^2 = A + \frac{B}{1-\nu^2/C} + \frac{D}{E-\nu^2} \qquad [2.38]$$

Where *A, B, C, D,* and *E* are parameters to be derived from experiment. For the important crystals ADP and KDP the Sellmeier constants are:

	ADP		KDP	
	n_e	n_o	n_e	n_o
A	2.133831	2.260476	2.164692	2.304082
B	8.653247×10^{-11}	1.011279×10^{-10}	9.633312×10^{-11}	1.114773×10^{-10}
C	8.134538×10^{9}	7.726552×10^{9}	7.691000×10^{9}	7.542305×10^{9}
D	8.069838×10^{6}	3.249268×10^{6}	1.479865×10^{6}	3.774363×10^{6}
E	2.500000×10^{5}	2.500000×10^{5}	2.500000×10^{5}	2.500000×10^{5}

Table : adapted from ref [3]

2.3 *THE NONLINEAR COEFFICIENT*

In the framework of Maxwell's equations usually a factor $\chi^{(2)}_{ijk}(\omega_1,\omega_2,\omega_3)$ is used as the second order non-linear susceptibility. Here $\chi^{(2)}$ obeys the general rules for a 2nd rank tensor and it can be shown, that as a result of the free permutation of ω_i there are 27 independent components. From the experimentalists view usually a non-linear coefficient *d* is used, that may be defined as:

[3] Zernike, J. Opt. Soc. Am. **54**, 1215 (1964).

$$d_{ijk} = \frac{1}{2}\chi^{(2)}_{ijk} \qquad [2.39]$$

But is usually written in a contracted form to represent the nonlinear polarization as:

$$\begin{pmatrix} P_x \\ P_y \\ P_z \end{pmatrix} = \begin{pmatrix} d_{11} & d_{12} & d_{13} & d_{14} & d_{15} & d_{16} \\ d_{21} & d_{22} & d_{23} & d_{24} & d_{25} & d_{26} \\ d_{31} & d_{32} & d_{33} & d_{34} & d_{35} & d_{36} \end{pmatrix} \begin{pmatrix} E_x^2 \\ E_y^2 \\ E_z^2 \\ 2E_yE_x \\ 2E_xE_z \\ 2E_xE_y \end{pmatrix} \qquad [2.40]$$

Note that sometimes the factors 2 are included in the d_{ij} coefficients, leading to some confusion.

It can be shown (beyond the scope of these lectures; for further reading see ref.[4])

- Only 18 of the tensor elements in d_{ij} are independent;
- In crystals with a center of symmetry all d_{ij} =0, consistent with Eq. [1.5];
- Of the 32 existing crystal classes, 21 are non-centro-symmetric;
- There is one crystal class (Class 1: triclinic system) with the lowest symmetry and 18 independent elements; in the figure shown the connected elements have the same value;

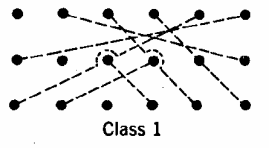

- Additional symmetry is imposed by Kleinman's conjecture: if the nonlinear polarization is of purely electronic origin and if the crystal is lossless in the spectral range of interest the i,j and k can be freely permuted and this gives rise to additional symmetry;
- For quartz (belonging to crystal class 32) the *d*-matrix reads as (if Kleinman's symmetry is imposed):

$$\begin{pmatrix} d_{11} & -d_{11} & 0 & d_{14} & 0 & 0 \\ 0 & 0 & 0 & 0 & -d_{14} & -d_{11} \\ 0 & 0 & 0 & 0 & 0 & 0 \end{pmatrix} \qquad [2.41]$$

- For each symmetry class the effective nonlinear polarization can be derived for each type of phase-matching; a few examples are listed below (adapted from ref. [5]). The important crystals ADP and KDP and their analogues belong to the point group $\underline{4}$2m, and hence have tetragonal symmetry.

[4] J.F. Nye, *Physical Properties of Crystals*, Oxford, 1960
[5] Zernike and Midwinter, *Applied Nonlinear Optics*, J. Wiley & Sons, 1973

Effective nonlinear coefficient d_{eff}:

Class *32*	with Kleinman symmetry	without Kleinman symmetry
Type I (e+e→o)	$d_{11}\cos^2\theta\sin 3\phi$	$d_{11}\cos^2\theta\sin 3\phi - d_{14}\sin 2\theta$
Type II (e+o→e)	-same-	$d_{11}\cos^2\theta\sin 3\phi + d_{14}\sin\theta\cos\theta$
Type I (o+o→e)	$d_{11}\cos\theta\sin 3\phi$	$d_{11}\cos\theta\sin 3\phi$
Type II (e+o→o)	-same-	$d_{11}\cos\theta\sin 3\phi$

Class *$\bar{4}$2m*	with Kleinman symmetry	without Kleinman symmetry
Type I (e+e→o)	$d_{14}\cos 2\theta\sin 2\phi$	$d_{14}\cos 2\theta\sin 2\phi$
Type II (e+o→e)	-same-	$(d_{14}+d_{36})\sin\theta\cos\theta\cos 2\phi$
Type I (o+o→e)	$-d_{41}\sin\theta\sin 2\phi$	$-d_{36}\sin\theta\sin 2\phi$
Type II (e+o→o)	-same-	$-d_{14}\sin\theta\sin 2\phi$

Note that not all processes indicated yield effective second harmonic power under all conditions. Of course phase-matching is required for a specific combination of wavelengths, and therewith the angles θ and ϕ become fixed at these values. Note also that the d_{ij} are material properties of the specific crystals.

2.4 *PHASE MATCHING IN BIREFRINGENT MEDIA*

In section 2.1 we have found that in isotropic media the phase matching condition $\Delta k=0$ cannot be obtained, because of the phenomenon of dispersion. In anisotropic media the *ordinary* and *extraordinary* waves can be mixed and phase matching can be obtained, because it is possible to "tune" the index of refraction of the transmitted extraordinary wave by varying the angle θ between the k-vector and the optical axis of the medium:

$$n_e(\theta) = \frac{n_e n_o}{\sqrt{n_o^2 \sin^2\theta + n_e^2 \cos^2\theta}} \qquad [2.42]$$

In anisotropic media the effect of *dispersion*, i.e. the wavelength dependence of the index of refraction, is of course also present. As a result the indices n_o and n_e and therewith $n_e(\theta)$ are a function of frequency of the incoming light.

KDP is obviously a crystal with negative birefringence ($n_e<n_o$). The dispersion curves for this material are also plotted in the following figure:

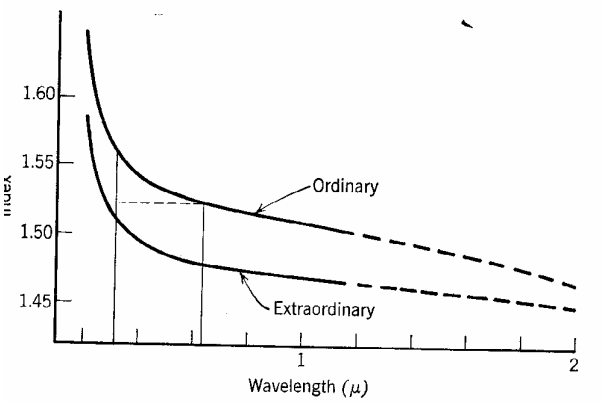

The figure should be understood as follows. The two curves for n_O and n_e represent the maximum and the minimum attainable index of refraction in the crystal, and the whole range in between the two curves covers the possible indices of refraction.

Considering this wide range of possible indices, and particularly the tunability of the index by the setting of the optic axis, the phase matching relation Δk=0 for second harmonic generation may be fulfilled in a crystal. This condition is met when:

$$n^{\omega} = n^{2\omega} \qquad [2.43]$$

Because of dispersion it will still not be possible to meet the conditions $n_o^{\omega} = n_o^{2\omega}$ or $n_e^{2\omega}(\theta) = n_e^{\omega}(\theta)$, but in the case of a negatively birefringent crystal ($n_e < n_O$) there will exist an angle θ_m for which the following condition can be met:

$$n_e^{2\omega}(\theta_m) = n_o^{\omega} \qquad [2.44]$$

Before solving in an algebraic way the equations in order to find the particular angle for which the phase matching condition is fulfilled, the so-called *phase matching angle*, we will first adopt a geometrical procedure to clarify the problem. The problem is that of a crystal that is *birefringent* and *dispersive* at the same time. The *index surfaces* for ordinary and extra-ordinary rays can be drawn at both the frequencies ω and 2ω. So we have four different index surfaces as shown in the figure (for a negative birefringent crystal):

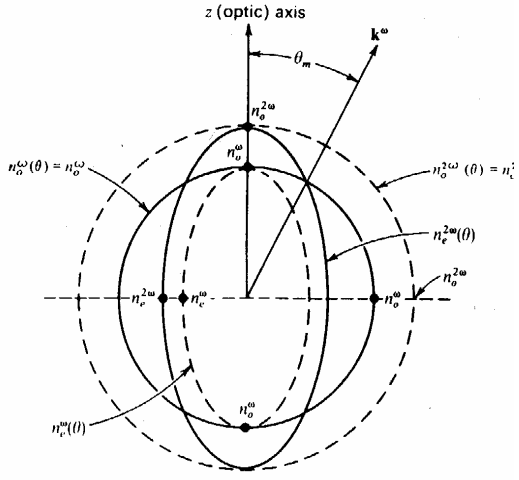

Note the interpretation of *index surfaces*: they are drawn such that the indices n_o and $n_e(\theta)$ are found at the crossings of the ellipsoids with the k-vector.
The index surfaces for n_o at frequency 2ω (outward circle) and for n_e at frequency ω (inner ellipse) are shown as dotted curves, because they are not important for the phase matching problem in negatively birefringent media. The curves for n_o at frequency ω and for n_e at frequency 2ω determine the phase matching angle. At the point where the circle of n_o^{ω} crosses the ellipse of $n_e^{2\omega}$ the phase matching condition is met. The relation then holds for the particular angle θ_m between the optical axis and the k-vector as shown in the figure.

Algebraically the problem of finding the phase matching angle can also be solved. At frequency 2ω the equation for the index ellipsoid is:

$$n_e^{2\omega}(\theta_m) = \frac{n_e^{2\omega} n_o^{2\omega}}{\sqrt{\left(n_o^{2\omega}\right)^2 \sin^2\theta_m + \left(n_e^{2\omega}\right)^2 \cos^2\theta_m}} \qquad [2.45]$$

In order to obtain phase matching this needs to equal n_o^{ω}. Thus we obtain an equation with an unknown variable θ_m and involving a $\sin^2\theta_m$ and a $\cos^2\theta_m$ function which may be solved for $\sin^2\theta_m$:

$$\sin^2\theta_m = \frac{\left(n_o^{\omega}\right)^{-2} - \left(n_o^{2\omega}\right)^{-2}}{\left(n_e^{2\omega}\right)^{-2} - \left(n_o^{2\omega}\right)^{-2}} \qquad [2.46]$$

Let us now consider some of the physics behind the mathematical equations. Phase matching, so efficient frequency doubling, is achieved when a beam travels through a crystal under a particular angle θ_m between the k-vector and the optical axis. It should be noted that the angle θ_m is defined for propagation within the crystal; for all calculations (or experiments on finding the phase matching angle) starting from a ray impinging under a certain angle on a crystal surface refraction at the boundary has to be taken into account. Because of the dispersive effect on all three parameters in the above equation (n_o^{ω}, $n_o^{2\omega}$, and $n_e^{2\omega}$) the phase matching angle will be different for frequency doubling of different frequencies ω. It was assumed that the ray at frequency ω was an ordinary ray (so polarized perpendicular to the optical axis) while the second harmonic is an extra-ordinary ray (polarized in the plane of the optical axis). Thus we find that in this process the *polarization of the second harmonic is perpendicular to the polarization of the fundamental*. In this example we assumed that the crystal was negatively birefringent; the phase matching condition was found for an *ordinary fundamental* and an *extraordinary second harmonic*. Considering index surfaces of positively birefringent media will show that the phase matching condition is fulfilled for an *extraordinary fundamental* and an *ordinary second harmonic*.

The phase matching condition for sum-frequency mixing was originally written as:

$$\Delta\mathbf{k} = \mathbf{k}_3 - \mathbf{k}_1 - \mathbf{k}_2 \qquad [2.47]$$

The process of frequency doubling or second harmonic generation can also be understood as a process of sum-frequency mixing of an ordinary and an extraordinary wave at the same frequency within a crystal. In that case the phase matching relation $\Delta k=0$ reduces to:

$$n_e^{2\omega}(\theta) = \frac{1}{2}\left[n_o^{\omega} + n_e^{\omega}(\theta)\right] \qquad [2.48]$$

This relation may be fulfilled, for certain angles θ_m in negatively birefringent crystals. In positively birefringent crystals another condition holds:

$$n_o^{2\omega} = \frac{1}{2}\left[n_o^{\omega} + n_e^{\omega}(\theta)\right] \qquad [2.49]$$

In both cases $n_e^{\omega}(\theta)$ and/or $n_e^{2\omega}(\theta)$ may be expressed in terms of the four parameters $n_e^{\omega}(\theta)$, n_o^{ω}, $n_e^{2\omega}$, and $n_o^{2\omega}$, and the equation may be solved to find the particular phase matching angle θ_m. It is obvious that the thus found phase-matching angle θ_m in the two different cases is different, although in both the processes the frequency is doubled.

Commonly a distinction is made between these different Types of Phase-matching:

TYPE I phase matching	$E_o\omega + E_o\omega \rightarrow E_e2\omega$	negative birefringence
and	$E_e\omega + E_e\omega \rightarrow E_o2\omega$	positive birefringence
TYPE II phase matching	$E_o\omega + E_e\omega \rightarrow E_e2\omega$	negative birefringence
and	$E_o\omega + E_e\omega \rightarrow E_o2\omega$	positive birefringence

2.5 *OPENING ANGLE*

Consider Type I phase-matching and a negatively birefringent crystal. The phase-matching relation is:

$$\Delta k = \frac{2\omega}{c}\left[n_e^{2\omega}(\theta) - n_o^{\omega}\right] = 0 \qquad [2.50]$$

which is satisfied for a certain angle θ_m. In order to evaluate a Taylor expansion around the optimum phase matching angle $(\theta\text{-}\theta_m)$ the first derivative of Δk with respect to θ is calculated:

$$\begin{aligned}\frac{dk}{d\theta} &= \frac{2\omega}{c}\frac{d}{d\theta}\left[n_e^{2\omega}(\theta) - n_o^{\omega}\right] = \frac{2\omega}{c}\frac{d}{d\theta}\frac{n_e n_o}{\sqrt{n_o^2\sin^2\theta + n_e^2\cos^2\theta}} \\ &= -\frac{\omega}{c}\frac{n_e n_o}{\left\{n_o^2\sin^2\theta + n_e^2\cos^2\theta\right\}^{3/2}}\left(n_o^2 - n_e^2\right)\sin 2\theta \\ &= -\frac{\omega}{c}\frac{\left\{n_e^{2\omega}(\theta)\right\}^3}{n_e^2 n_o^2}\left(n_o^2 - n_e^2\right)\sin 2\theta\end{aligned} \qquad [2.51]$$

so:

$$\left|\frac{dk}{d\theta}\right|_{\theta m} = -\frac{\omega}{c}n_o^3\left(n_e^{-2} - n_o^{-2}\right)\sin 2\theta_m \qquad [2.52]$$

where in the last step it was used that $n_e^{(2\omega)}(\theta)=n_o$ and the value of the angle was set at $\theta=\theta_m$.

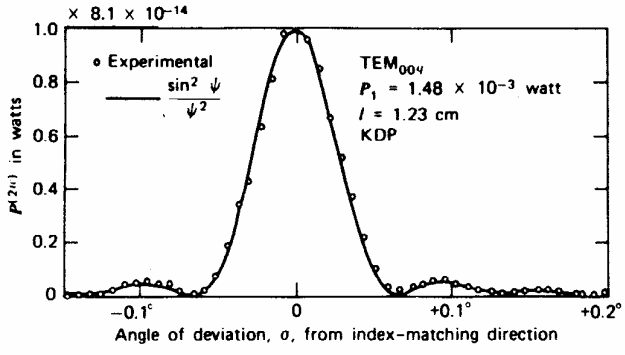

So the spread in allowed k-values is proportional to the spread in angles around the phase matching angle θ_m:

$$\Delta k = \frac{2\beta}{L}\Delta\theta \qquad [2.53]$$

with:

$$\beta \propto \sin 2\theta_m \qquad [2.54]$$

The power of the second harmonic generated thus becomes:

$$P^{(2\omega)}(\theta) \propto \frac{\sin^2\left[\frac{\Delta kL}{2}\right]}{\left[\frac{\Delta kL}{2}\right]^2} \propto \frac{\sin^2\left[\beta(\theta-\theta_m)\right]}{\left[\beta(\theta-\theta_m)\right]^2} \qquad [2.55]$$

This relation was verified in an experiment on frequency doubling in a KDP-crystal:
For the particular example of a KDP crystal, with a certain thickness *L*=1.23 cm and index parameters it is found that the full spread in angles that allow for phase matching is 0.1º of angular variation. The concept of *opening angle* may be understood in different ways:
- for a fixed wavelength λ, in a focused light beam the angular convergence angle should not exceed this 0.1º, otherwise the efficiency of the process will be reduced.
- in case of a co-linear light beam, the wavelength spread Δλ around a center wavelength λ is related to a spread in wave-vectors:

$$\frac{\Delta k}{k} = -\frac{\Delta\lambda}{\lambda} \qquad [2.56]$$

As a result only a limited bandwidth around the center wavelength is efficiently frequency doubled because of the opening angle.

The experiment again (as in the experiment on the Maker fringes) proofs that phase matching plays a role in second harmonic generation. It is important to note that at θ_m=90º the first term in the Taylor expansion is zero. Then the second order term in the expansion has to be taken, and then:

$$\Delta k \propto (\Delta\theta)^2 \qquad [2.57]$$

So a small spread in angle $\Delta\theta$ will allow for a large spread in the wave-vector domain. Also the bandwidth that may be efficiently frequency doubled is larger. This effect at $\theta_m=90^o$ is dubbed *non-critical phase-matching*.
Note that the concept of angle tuning is particularly important for the frequency doubling of large bandwidth short pulse lasers.

2.6 *PHASE MATCHING BY ANGLE TUNING*

In the above we have seen that under certain conditions of polarization of incoming waves, vs the birefringence of the material phase matching can be achieved for second harmonic generation at specific wavelengths. The indices of refraction for ordinary and extraordinary rays for the $LiIO_3$ crystal are given in the Table (from ref [6])

A	n_o	n_e
4000	1.948	1.780
4360	1.931	1.766
5000	1.908	1.754
5300	1.901	1.750
5780	1.888	1.742
6900	1.875	1.731
8000	1.868	1.724
10600	1.860	1.719

With the method described in the preceding paragraphs the phase-matching angle for second harmonic generation is as a function of the fundamental wavelength (for type I phase matching).

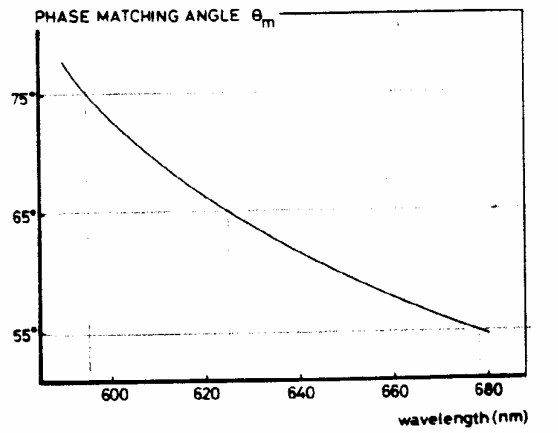

Fig.: Calculated phase matching angles for type I for SHG in $LiIO_3$; obtained from ref[7]

When using this crystal for frequency doubling of a scanning tunable laser, the angle θ_m has to be tuned, while scanning the fundamental. In general phase matching in a particular crystal can be achieved down to wavelengths $\lambda(90^o)$, where the angle reaches a value of $\theta_m=90^o$. In $LiIO_3$ the situation is different: it starts *absorbing* at 295 nm, and therefore SHG is not possible beyond fundamental wavelengths of 590 nm.

[6] Nath and Haussuhl, Appl. Phys.Lett **12**, 186 (1968)

[7] W. Ubachs, PhD Thesis, Nijmegen University 1986

2.7 *PHASE MATCHING BY TEMPERATURE TUNING*

Before this point it was assumed that the indices of refraction are just dependent on the angles of k-vector and polarization of the transmitted wave in the crystal. In reality the indices will depend on all external influences that will influence the lattice spacings in the three dimensions of the crystal. In principle all four parameters n_e^{ω}, n_o^{ω}, $n_e^{2\omega}$, and $n_o^{2\omega}$ are dependent of the *temperature*. Qualitatively it may be understood that the phase-matching condition $\Delta k=0$ can be achieved by merely changing the temperature of the crystal. Of course the angle setting of θ_m will remain important. There is a class of crystals, similar to KDP, that is particularly suited for temperature tuning; moreover phase matching may be achieved at θ_m=90º.
By changing the temperature both the conditions of:

$\Delta k = 0$ and $\theta_m=90^o$

are fulfilled at different wavelengths. The figure shows the *temperature tuning curves* for two crystals: ADP and KDP.

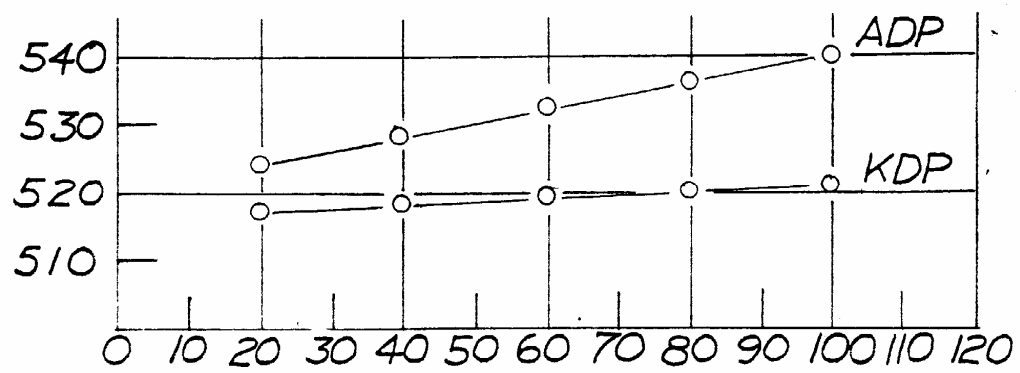

Temperature tuning has several advantages:
a) The properties of walk-off are unimportant if phase matching is obtained at an angle of θ_m=90º. This situation is called *non-critical phase matching*.
b) At this angle the ray travels along the optical axis and there is *no* effect of *double refraction* and optical activity in the medium. This makes temperature tuning very suitable for use in intra-cavity phase-matching of SHG, because these side effects would additional losses to the lasing process.
c) At θ_m=90º the first order expansion term in the Taylor series for the derivation of the opening angle, containing a factor $\sin 2\theta_m$, disappears and we find that for non-critical phase matching:

$$\Delta k \propto (\Delta\theta)^2 \qquad [2.58]$$

So at non-critical phase matching larger opening angles are allowed.
d) At θ_m=90º the nonlinear coefficient d_{eff} is largest.

2.8 QUASI PHASE-MATCHING BY PERIODIC POLING

In angle phase-matching some angles of propagation are not possible; hence some elements of the d_{ij} tensor element cannot be accessed. The underlying problem is that the phase of the second harmonic changes with respect to the fundamental, due to the different light speeds in the crystal: dispersion. In each coherence length, defined in [2.10], the nonlinear polarization wave is shifted in phase by π radians, and the relative phase slips by $\pi/2$. After the first coherence length, the phase has slipped into a regime where energy is lost from the field. The idea behind an alternative way of phase-matching is to adjust the phase of the non-linear polarization appropriately after each coherence length. Under those circumstances the non-linear intensity will grow (monotonically), although less rapid as in case of perfect phase-matching. This condition of quasi phase-matching (QPM) can be achieved in a so-called periodically poled crystal.

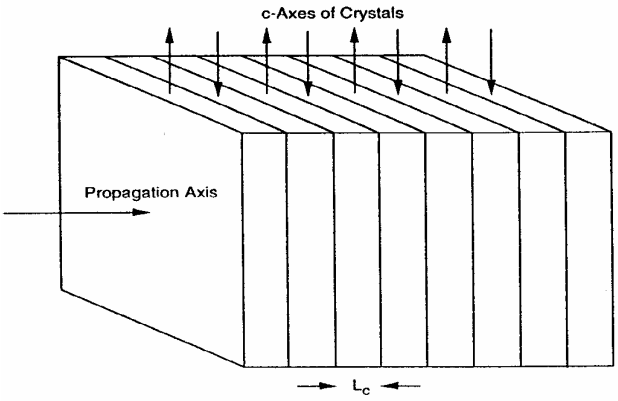

Material segments with the optical axis alternating in reverse directions are stacked together. From the perspective of the propagating wave the segments are rotated by 180^o to the effect that the phase shift built up in the first L_c is decreased again in the next L_c. The phase relation between the generated optical field and the time derivative of the driving nonlinear polarization for SHG are sketched in the figure.

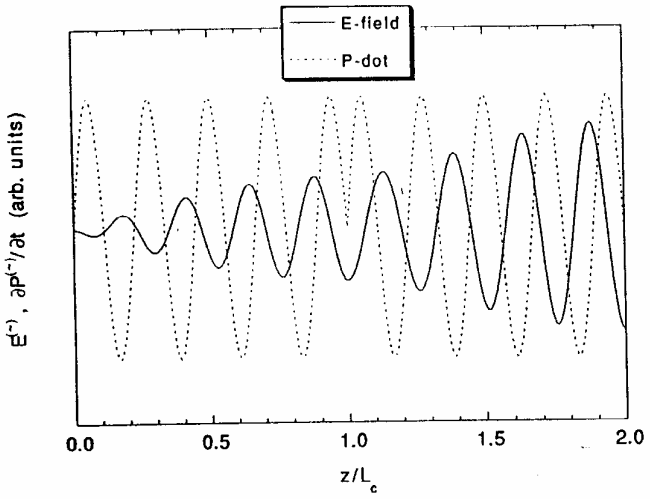

Although this idea of QPM was conceived by Bloembergen, already in the early days of non-linear optics, it is only through recent progress in crystal technology that such periodically poled materials can be grown. The period Λ of the crystal modulation is in most applications on the order of 10 μm. Technologically the growth of such materials does not proceed forming a stack of thin wafers. A more practical approach is to use ferro-electric crystals ($LiNbO_3$ is an important one) forming regions of periodically reversed polarization domains by applying electric fields; these domains remain intact when the applied field is switched off.

The most rapid growth of the second harmonic is obtained by changing the sign of the polarization (and thus the sign of the non-linear coefficient) every coherence length. This situation is illustrated in part (a) of the figure obtained from ref [8]:

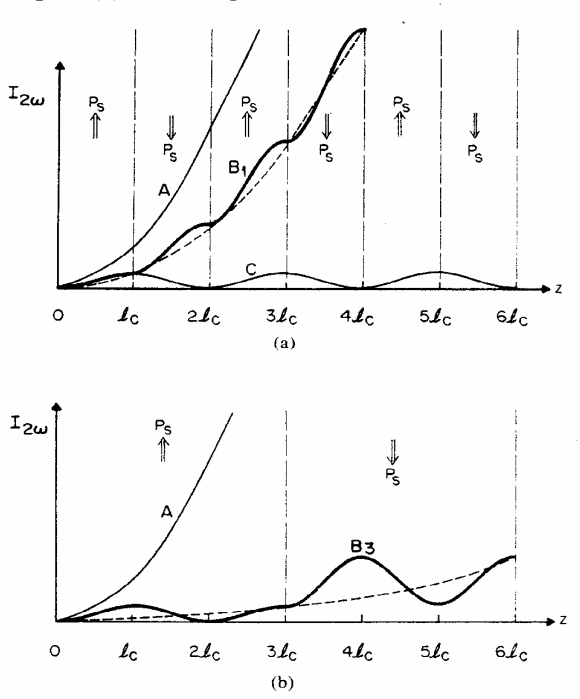

Curve A represents the condition of perfect phase-matching over the length of the entire crystal. Curve C represents the case of phase-mismatch with a coherence length of phase-match of l_c. Curve B_1 represents the case where the polarization is flipped after every coherence length. In the lower part of the figure curve B_3 represents third order QPM: every three coherence lengths the nonlinear coefficient is flipped. The harmonic yield is less in third order QPM, but the technological requirements are less strict in view of the larger domain structures, so it is useful in some conditions. It can be shown by using Fourier analysis, that a full polarization switch is not necessary: even a period modulation of the nonlinear coefficient already enhances the SHG output.

The coupled wave equation can be written again as:

$$\frac{d}{dz}E_2 = \Gamma d(z)\exp[-i\Delta k' z] \qquad [2.59]$$

[8] M.M. Fejer, G.A. Magel, D.H. Jundt, and R.L. Byer, IEEE J. Quant. Electr. **28**, 2631 (1992)

where Γ represent the usual factor $\Gamma = i\omega E_1^2 / n_2 c$. The second harmonic at the end of the sample *L* is then:

$$E_2(L) = \Gamma \int_0^L d(z) \exp[-i\Delta k' z] dz \qquad [2.60]$$

In the trivial case that $d(z) = d_{eff}$ and $\Delta k' = 0$ the second harmonic field is:

$$E_2(L) = \Gamma d_{eff} L \qquad [2.61]$$

In the real space description the function *d(z)* can be assumed to consist of domains with $\pm d_{eff}$ with sign changes at positions z_j. Let g_k the sign and l_k the length of the k^{th} domain, then [2.60] can be integrated to:

$$E_2 = \frac{i\Gamma d_{eff}}{\Delta k'} \sum_{k=1}^{N} g_k \left[\exp(-i\Delta k' z_k) - \exp(-i\Delta k' z_{k-1})\right] \qquad [2.62]$$

with *N* the number of domains. The sign changes in a perfect structure occur at positions:

$$e^{-i\Delta k_0' z_{k,0}} = (-1)^k \qquad [2.63]$$

where $\Delta k_0'$ is the wave vector mismatch at the design wavelength, and for m^{th} order QPM:

$$z_{k,0} = mkl_c \qquad [2.63]$$

For a perfect structure, without phase errors at the boundaries the generated field yields:

$$E_{2,ideal} \approx i\Gamma g_1 d_{eff} \frac{2}{m\pi} L \qquad [2.64]$$

We see that in an interaction with perfect m^{th} order QPM, the effective non-linearity is reduced by a factor of $2/m\pi$ with respect to a conventional phase-matched interaction.

Since the crystals have to be grown at specific poling periodicity Λ they match only a single wavelength. SHG at any other wavelength gives rise to a mismatch and reduced SHG output. Additionally the domain structure is never perfect, also giving rise to boundary mismatches.

2.9 *PUMP DEPLETION IN SECOND HARMONIC GENERATION*

The conversion efficiency for second harmonic generation was calculated in the approximation that the efficiency η_{SHG} <<1. In case of large conversion efficiencies other processes have to be taken into consideration also. In a generalized picture apart from the sum-frequency process, in which a new frequency ω_3 is generated, also reverse processes take place when the intensity at ω_3 becomes large:

$$\begin{aligned} \omega_1 + \omega_2 &\rightarrow \omega_3 \\ \omega_3 - \omega_2 &\rightarrow \omega_1 \\ \omega_3 - \omega_1 &\rightarrow \omega_2 \end{aligned} \qquad [2.65]$$

We go back to the coupled wave equations and we define amplitudes A_i and coefficients α_i:

$$A_i = \frac{\sqrt{n_i}}{\omega_i} E_i \qquad \text{and} \qquad \alpha_i = \frac{\sigma_i}{\sqrt{\mu_0/\varepsilon_i}} \qquad [2.66]$$

Then the coupled wave equations become the **coupled amplitude equations**:

$$\begin{aligned} \frac{d}{dz} A_1 &= -\frac{1}{2}\alpha_1 A_1 - i\kappa A_3 A_2^* e^{-i\Delta kz} \\ \frac{d}{dz} A_2 &= -\frac{1}{2}\alpha_2 A_2^* + i\kappa A_1 A_3^* e^{i\Delta kz} \\ \frac{d}{dz} A_3 &= -\frac{1}{2}\alpha_3 A_3 - i\kappa A_1 A_2 e^{i\Delta kz} \end{aligned} \qquad [2.67]$$

where κ was defined as:

$$\kappa = d\,\frac{1}{2}\sqrt{\frac{\mu_0}{\varepsilon_0}}\sqrt{\frac{\omega_1\omega_2\omega_3}{n_1 n_2 n_3}} \qquad [2.68]$$

The terms proportional with the α_i coefficients represent linear polarization effects, such as absorptions in the media. Some assumptions are made now:

$\alpha_i = 0$	so no absorptions
$\omega_1 = \omega_2$	for frequency doubling
$\Delta k = 0$	a phase matched combination of waves (holds for all processes)

Then:

$$\begin{aligned} \frac{d}{dz} A_1 &= -i\kappa A_3 A_1^* \\ \frac{d}{dz} A_3 &= -i\kappa \frac{1}{2} A_1^2 \end{aligned} \qquad [2.69]$$

In fact there is no field with amplitude A_2, because of the degeneracy $\omega_1 = \omega_2$ the factor 1/2 comes in the second equation. Now we choose $A_1(0)$ to be a real amplitude and we rewrite $A_3' = -iA_3$, then we obtain:

$$\begin{aligned} \frac{d}{dz} A_1 &= -\kappa A_3' A_1 \\ \frac{d}{dz} A_3' &= \frac{1}{2}\kappa A_1^2 \end{aligned} \qquad [2.70]$$

We calculate:

$$\frac{d}{dz}\left[A_1^2 + 2\left(A_3'(z)\right)^2\right] = 2A_1\frac{d}{dz}A_1 + 4A_3'\frac{d}{dz}A_3' = 0 \qquad [2.71]$$

so in the crystal (assuming no input at ω_3):

$$\left[A_1^2 + 2(A_3'(z))^2\right] = const = A_1^2(0) \qquad [2.72]$$

If we consider:

$$I_i = \frac{1}{2}\sqrt{\frac{\mu_0}{\varepsilon_0}} n_i |E_i|^2 = \frac{1}{2}\sqrt{\frac{\mu_0}{\varepsilon_0}} \omega_i |A_i|^2 \qquad [2.73]$$

and also that:

$$I_i \propto N_i h_{bar} \omega_i \qquad [2.74]$$

We find that $|A_i|^2$ is proportional to the *number of photons* in the beam. So the fact that $\left[A_1^2(z) + 2A_3'(z)^2\right]$ = constant has the physical meaning that for every 2 photons taken away at the fundamental, there is one generated in the second harmonic beam. Energy is thus conserved because $\omega 3 = 2\omega 1$.
The differential equation in A_3' is:

$$\frac{d}{dz} A_3' = -\frac{1}{2}\kappa\left[A_1^2(0) - 2(A_3')^2\right] = 0 \qquad [2.75]$$

with a solution:

$$A_3'(z) = \frac{A_1(0)}{\sqrt{1/2}} \tanh\left[\frac{A_1(0)\kappa z}{\sqrt{1/2}}\right] \qquad [2.76]$$

So for the conversion efficiency we find:

$$\eta_{SHG} = \frac{P^{(2\omega)}}{P^{(\omega)}} = \frac{|A_3(z)|^2}{\frac{1}{2}|A_1(0)|^2} = \tanh^2\left[\frac{A_1(0)\kappa z}{\sqrt{1/2}}\right] \qquad [2.77]$$

If $A_1(0)\kappa z \to \infty$, then $A_3'(z) \to A_1(0)/\sqrt{1/2}$ and hence $|A_3'(z)|^2 \to (1/2)|A_1(0)|^2$, so the number of input photons will be converted into half the number of frequency doubled photons. The figure shows the deviation at high input powers from the quadratic behavior.
Note that from this analysis it follows that *conversion efficiencies larger than 50% are possible*.

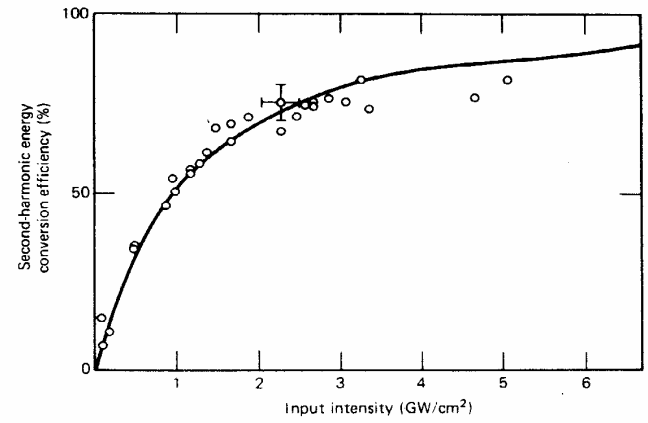

Chapter 3

The optical parametric oscillator

3.1 *PARAMETRIC AMPLIFICATION*

Now we consider a non-linear medium with two co-linear incoming light beams; one high power at frequency ω_3 (*the pump beam*), and a low power beam at frequency ω_3 (*the signal beam*). The intense pump beam will amplify the signal beam under conditions of phase-matching for the non-linear process:

$$\omega_3 \rightarrow \omega_1 + \omega_2. \qquad [3.1]$$

With the amplification of the signal beam a third beam at frequency ω_2 is generated, the so-called *idler beam*. Again we start from the coupled wave equations, derived above with some assumptions:

- no losses, $\alpha_i = 0$,
- $\Delta k = 0$, a phase-matched combination of waves
- similar definition of κ

$$\frac{dA_1}{dz} = -\frac{1}{2} i\kappa A_3 A_2^* e^{-i\Delta kz} \qquad [3.2]$$

$$\frac{dA_2^*}{dz} = \frac{1}{2} i\kappa A_1 A_3^* e^{i\Delta kz} \qquad [3.3]$$

Also we assume that the pump intensity will not be depleted, so $A_3(z) = A_3(0)$ and we define:

$$g = \kappa A_3(0) \qquad [3.4]$$

The coupled amplitude equations reduce to:

$$\frac{dA_1}{dz} = -\frac{1}{2} igA_2^* \qquad [3.5]$$

$$\frac{dA_2^*}{dz} = \frac{1}{2} igA_1 \qquad [3.6]$$

With boundary conditions a small signal field at z=0, $A_1(0)$, and $A_2(0)=0$ these differential equations may be solved to:

$$A_1(z) = A_1(0)\cosh\left(\frac{gz}{2}\right) \qquad [3.7]$$

$$A_2^*(z) = iA_1(0)\sinh\left(\frac{gz}{2}\right) \qquad [3.8]$$

For gz>0 a reasonable approximation is:

$$|A_1(z)|^2 = |A_2(z)|^2 \propto e^{gz} \qquad [3.9]$$

So both waves at frequencies ω_1 and ω_2 are found to grow with a *gain factor* g. It may be proven straightforwardly from the coupled amplitude equations (with the assumption that the $\alpha_i=0$) that:

$$-\frac{d}{dz} A_3 A_3^* = \frac{d}{dz} A_1 A_1^* = \frac{d}{dz} A_2 A_2^* \qquad [3.10]$$

Where $A_iA_i^*$ is the photon flux of a wave, the physical meaning of this relation is that for each photon taken away from the pump beam, two photons are created: one at the signal frequency ω_1 and one at the idler with ω_2. This may also be expressed as the Manley-Rowe relation:

$$-\Delta\left(\frac{P_3}{\omega_3}\right) = \Delta\left(\frac{P_1}{\omega_1}\right) = \Delta\left(\frac{P_2}{\omega_2}\right) \qquad [3.11]$$

3.2 *PARAMETRIC OSCILLATION*

In the preceding paragraph we have seen that a pump beam at frequency ω_3 can provide via a non-linear interaction in a phase-matched medium, simultaneous amplification of optical waves at the signal wave ω_1 and the idler wave ω_2; with the condition that $\omega_3=\omega_1+\omega_2$. In such a system there was found to be *parametric gain*. Parametric denotes here that the process depends on a parameter, namely the phase-matching condition $\Delta k=0$.

Placed inside an optical resonator the parametric gain will at some *threshold pumping* cause simultaneous *oscillation* at signal and idler waves. Similar to lasing operation in a resonator (where the gain is derived from a population inversion) the oscillation will start from *noise* photons. A device based on parametric gain in a resonator is called an *optical parametric oscillator* or in short OPO.

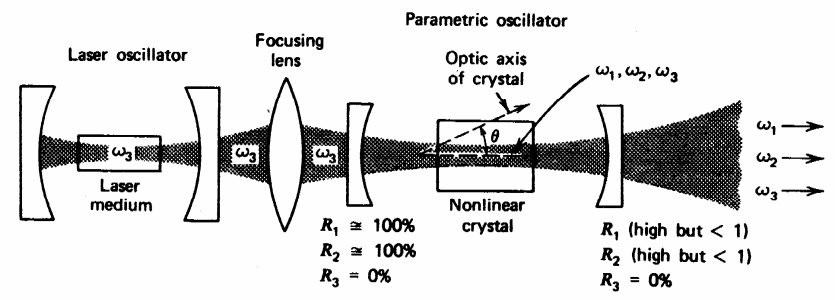

We will first look at a threshold for oscillation. Such a threshold will be reached when the parametric gain equals the losses in the resonator. Under those conditions the coupled amplitude equations will be in steady state:

$$\frac{dA_1}{dz} = \frac{dA_2}{dz} \qquad [3.12]$$

so in steady state, with α_i the absorption losses and g the parametric gain:

$$-\frac{1}{2}\alpha_1 A_1 - \frac{1}{2} igA_2^* = 0 \qquad [3.13]$$

$$\frac{1}{2} igA_1 - \frac{1}{2}\alpha_2 A_2^* = 0 \qquad [3.14]$$

This set of coupled linear equations has a nontrivial solution at this threshold if:

$$g^2 = \alpha_1\alpha_2 \qquad [3.15]$$

We may also conclude that above threshold oscillation will occur if:

$$g^2 > \alpha_1\alpha_2 \qquad [3.16]$$

3.3 *TUNING OF AN OPO*

Parametric amplification and oscillation may be viewed upon as an inverse sum-frequency process, for which the same phase-matching conditions will hold; it is these phase-matching conditions that determine which frequencies ω_1 and ω_2 will be generated at a certain setting of the angle of the crystal with respect to the wave vector $\mathbf{k}_3$ of the pump beam.

$$\Delta\mathbf{k} = 0 \qquad \rightarrow \qquad \mathbf{k}_3 = \mathbf{k}_1 + \mathbf{k}_2 \qquad [3.17]$$

for co-linear beams the following relation must hold in order to achieve phase-matching:

$$n_3\omega_3 = n_1\omega_1 + n_2\omega_2 \qquad [3.18]$$

Of course the conservation of energy is a strict condition for frequency conversion in an OPO:

$$\omega_3 = \omega_1 + \omega_2 \qquad [3.19]$$

Again, because of dispersion in any medium these relations can only be met under the special conditions of anisotropic crystals with a tunable index; and again we distinguish between Type I and II phase-matching conditions. For example:

ω_1 and ω_2 are *ordinary* waves with index, respectively n_1^o and n_2^o

ω_3 is an *extraordinary* wave with index $n_3^e(\theta)$

So Type I phase-matched oscillation is obtained at ω_1 and ω_2 at a specific angle $\theta=\theta_m$, with the condition:

$$n_3^e(\theta_m) = \frac{n_1\omega_1 + n_2\omega_2}{\omega_3} \qquad [3.20]$$

At each specific phase- match angle θ_m the OPO will produce a particular combination of two frequencies that obey the phase-matching condition.

Next we consider what will happen if we rotate the angle θ of the crystal for an amount $\Delta\theta$; so $\theta_m \rightarrow \theta_m+\Delta\theta$. As the pump frequency ω_3 is fixed at the phase-matched frequencies will change:

$$\omega_1 \rightarrow \omega_1 + \Delta\omega_1 \qquad [3.21]$$

$$\omega_2 \rightarrow \omega_2 + \Delta\omega_2 \qquad [3.22]$$

because of energy conservation: $\Delta\omega_1=-\Delta\omega_2$. All the indices of refraction will change:

$$\begin{aligned} n_1 &\rightarrow n_1 + \Delta n_1 \\ n_2 &\rightarrow n_2 + \Delta n_2 \\ n_3 &\rightarrow n_3 + \Delta n_3 \end{aligned} \qquad [3.23]$$

Note that the index at the pump frequency changes, because it is an extraordinary wave and the angle has been rotated; the index of the signal and idler wave change because of dispersion; so the changes in the indices are:

$$\Delta n_1 = \left|\frac{\partial n_1}{\partial \omega_1}\right|_{\omega 1} \Delta\omega_1 \qquad \text{frequency dependence} \qquad [3.24]$$

$$\Delta n_2 = \left|\frac{\partial n_2}{\partial \omega_2}\right|_{\omega 2} \Delta\omega_2 \qquad \text{frequency dependence} \qquad [3.25]$$

$$\Delta n_3 = \left|\frac{\partial n_3}{\partial \theta}\right|_{\theta m} \Delta\theta \qquad \text{angle dependence} \qquad [3.26]$$

With these relations a new phase-matching condition has to be satisfied, although at a different angle $\theta_m+\Delta\theta$:

$$(n_3+\Delta n_3)\omega_3 = (n_1+\Delta n_1)(\omega_1+\Delta\omega_1) + (n_2+\Delta n_2)(\omega_2+\Delta\omega_2) \qquad [3.27]$$

so:

$$\underline{n_3\omega_3}+\Delta n_3\omega_3 = \underline{n_1\omega_1}+\Delta n_1\omega_1+n_1\Delta\omega_1+\Delta n_1\Delta\omega_1+\underline{n_2\omega_2}+\omega_2\Delta n_2-n_2\Delta\omega_1-\Delta n_2\Delta\omega_1 \qquad [3.28]$$

Here $\Delta\omega_2=-\Delta\omega_1$ was used. With use of the original phase-matching relation at $\theta=\theta_m$ (underlined parts) and neglect of second order derivatives, such as $\Delta n_1\Delta\omega_1$, we solve for $\Delta\omega_1$:

$$\Delta\omega_1 = \frac{\omega_3\Delta n_3 - \omega_1\Delta n_1 - \omega_2\Delta n_2}{n_1 - n_2} \qquad [3.28]$$

Substituting the above relations in the equation for $\Delta\omega_1$ gives:

$$\Delta\omega_1 = \frac{\omega_3\left|\frac{\partial n_3}{\partial\theta}\right|\Delta\theta - \omega_1\left|\frac{\partial n_1}{\partial\omega_1}\right|\Delta\omega_1 + \omega_2\left|\frac{\partial n_2}{\partial\omega_2}\right|\Delta\omega_1}{n_1 - n_2} \qquad [3.29]$$

Solving $\Delta\omega_1$:

$$\frac{\Delta\omega_1}{\Delta\theta} = \frac{\partial\omega_1}{\partial\theta} = \frac{\omega_3\left|\frac{\partial n_3}{\partial\theta}\right|}{(n_1 - n_2) + \left[\omega_1\frac{\partial n_1}{\partial\omega_1} - \omega_2\frac{\partial n_2}{\partial\omega_2}\right]} \qquad [3.30]$$

In the paragraph on the opening angle for phase-matched second harmonic generation the derivative $dk/d\theta$ was determined at the phase matched angle θ_m. Also k was written in terms of the index of refraction of an extraordinary wave $n_e(\theta)$. Now we use this result for the derivative $\partial n_3/\partial\theta$:

$$\left|\frac{\partial n_3}{\partial\theta}\right|_{\theta m} = -\frac{1}{2}n_o^3\left[n_e^{-2}(\omega_3) - n_o^{-2}(\omega_3)\right]\sin 2\theta_m \qquad [3.31]$$

Finally we have obtained an equation for the angle dependence of the generated frequency of the signal wave as a function of the indices of refraction and their dispersion relations.

$$\frac{\partial\omega_1}{\partial\theta} = \frac{-\frac{1}{2}n_o^3(\omega_3)\omega_3\left[n_e^{-2}(\omega_3) - n_o^{-2}(\omega_3)\right]\sin 2\theta_m}{(n_1 - n_2) + \left[\omega_1\frac{\partial n_1}{\partial\omega_1} - \omega_2\frac{\partial n_2}{\partial\omega_2}\right]} \qquad [3.32]$$

In an experiment with an OPO, the parameters ω_3 and therewith $n_o(\omega_3)$, $n_e(\omega_3)$, are constant. If the indices of the medium are known, and their frequency dependence then the dependence of the frequency of the signal wave ω_1 as a function of the angle θ may be calculated numerically, using the above equation. Such an *angle tuning curve* for an OPO based on a BaB_2O_4 crystal (also called BBO) is shown in the following figure. The wavelength of both the signal and the corresponding idler (energy conservation) at the particular easily accessible pump wavelength of 354.7 nm is shown.

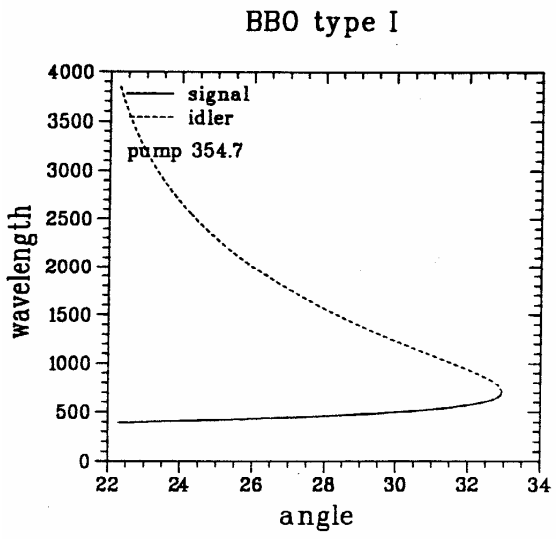

Thus we find that such a device, an OPO based on the material BBO, and pumped by the UV-output of a Nd-YAG laser, is a source for coherent radiation in the wavelength range 420-2500 nm, this means the *whole visible and near infrared part of the spectrum*. (Wavelengths longer than 2.5 mm are absorbed in the BBO-material). And the tuning of such a device may be simply arranged by rotating the crystal over an angle from 22 to 33 degrees.

3.4 *BANDWIDTH OF THE OPO*

As a consequence of the *opening angle* associated with a sum-frequency mixing process even under the conditions of a perfectly parallel pump beam at ω_3 with an infinitely narrow bandwidth $\Delta\omega_3$ the signal and idler waves will have certain widths $\Delta\omega_1$ and $\Delta\omega_2$ in the frequency domain. The opening angle corresponds to a wavelength range that may be determined from the analysis in the preceding paragraph. Particularly at the degeneracy point, i.e. where signal and idler waves have the same frequency, a small variation in the tuning angle corresponds to a large frequency spread; so the bandwidth will be very large here.

An additional broadening effect on the output of an OPO is caused by the pump beam divergence. Because of a spatial spread of k-vectors non-co-linear phase-matching also occurs. This will cause an increase of the opening angle and therewith an increase of bandwidth.

For the example of an OPO based on a BBO-crystal the linewidth for the signal has been calculated for two different beam divergencies of 0.1 mrad and 0.5 mrad and a pump wavelength of 354.7 nm. Note that the bandwidth of the pump laser is not taken into account.

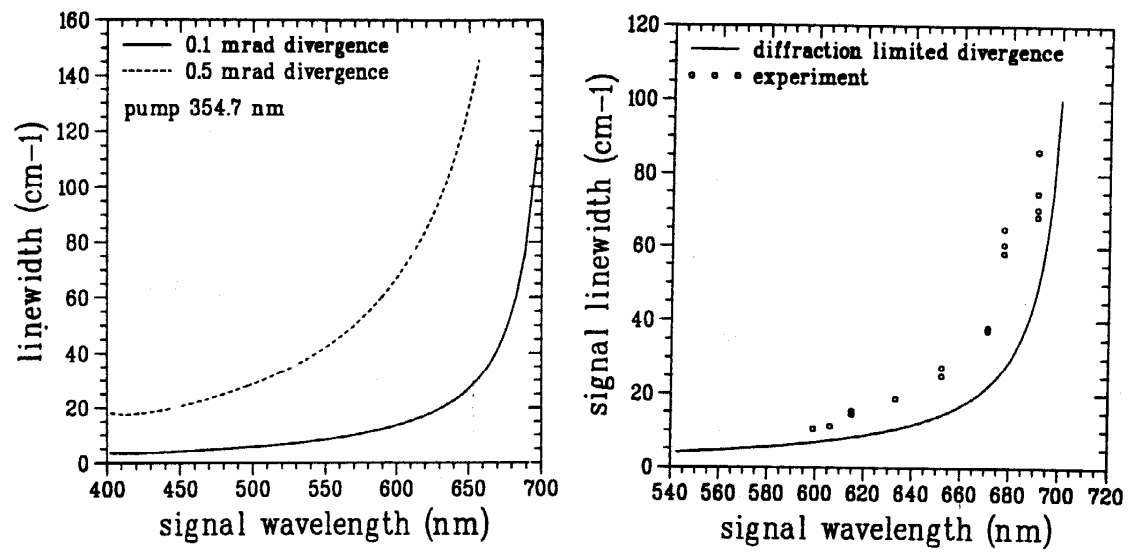

3.5 *PUBLIC DOMAIN SOFTWARE*

Calculations of phase-matching properties and effective non-linear coefficients, particularly in the case of bi-axial crystals are quite intricate. A large number of research papers on this topic have been published as well as several textbooks.

A sophisticated computer program to calculate all relevant nonlinear properties has been designed by A.V. Smith of Sandia National Laboratories, Albuquerque, New Mexico. The program "SNLO" has been made publicly available at:

http://www.sandia.gov/imrl/XWEB1128/xxtal.htm

and is regularly updated for new materials and new measurements of e.g. refractive indices. It is equipped with plotting routines to produce phase-matching curves for OPO's as well as effective non-linear coefficients d_{eff} for all processes and crystals. It also includes the use of periodically poled materials and the construction of resonators for intra-cavity frequency conversion.

A typical display for the calculation of phase-matching angles for an OPO pumped at 350 nm is shown for the CLBO crystal.

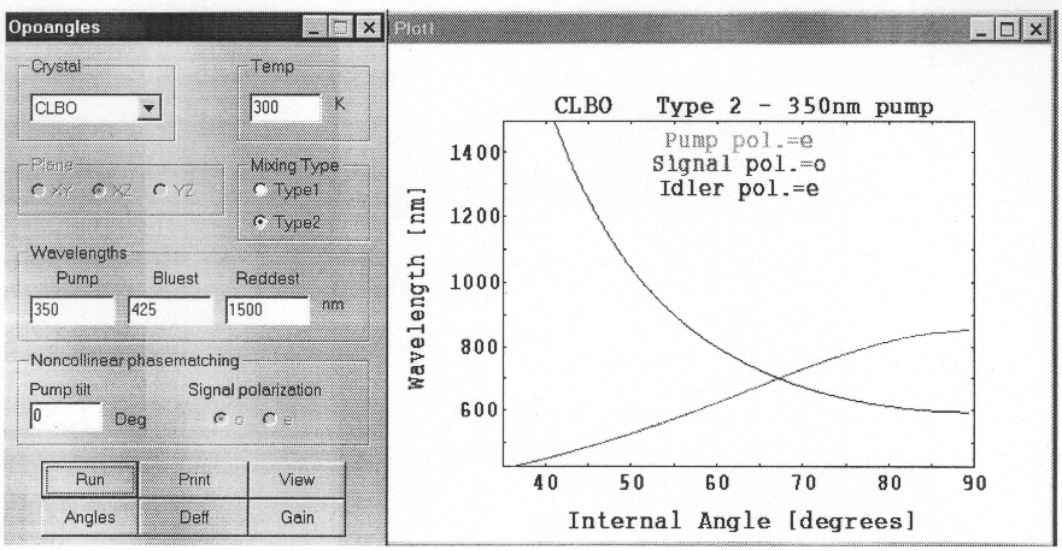
Opoangles
Crystal
CLBO
Temp
300
K
Plane
XY
XZ
YZ
Mixing Type
Type1
Type2
Wavelengths
Pump
Bluest
Reddest
350
425
1500
nm
Noncollinear phasematching
Pump tilt
0
Deg
Signal polarization
o
e
Run
Print
View
Angles
Deff
Gain
Plot1
CLBO Type 2 - 350nm pump
Pump pol.=e
Signal pol.=o
Idler pol.=e
Wavelength [nm]
1400
1200
1000
800
600
40
50
60
70
80
90
Internal Angle [degrees]

Chapter 4

Quantum theory of the nonlinear susceptibility

4.1 *SCHRöDINGER EQUATION; PERTURBATION THEORY*

Similar to Chapter 2 we adopt Schrödingers equation as a starting point for a derivation of nonlinear susceptibilities. Again this treatment, based on the properties of the atomic wave function will have a restricted validity. Particularly for the *relaxation processes* upon resonant excitation the outcome will lack validity and a more complex density matrix formalism may be used for a proper description. Note also that the present description is semi-classical; the electromagnetic field is not quantized. It is assumed that all properties of the atoms can be described in terms of the wave function, which is a solution to the time-dependent Schrödinger equation:

$$ih\frac{\partial\Psi}{\partial t} = \hat{H}\Psi \qquad [4.1]$$

where $\hat{H}$ is the Hamilton operator that may be written as:

$$\hat{H} = \hat{H}_0 + \hat{V}(t) \qquad [4.2]$$

$$\hat{V}(t) = -\hat{\mu}\cdot E(t) \qquad [4.3]$$

$$E(t) = \sum_n E(\omega_n)e^{-i\omega_n t} \qquad [4.4]$$

$\hat{H}_0$ represents the Hamiltonian for a free atom, $\hat{V}(t)$ the interaction of the atom with the external electromagnetic field E(t), which is written in an expansion of frequency components. In order to solve [4.1] in terms of a perturbation expansion the Hamiltonian is written:

$$\hat{H} = \hat{H}_0 + \lambda\hat{V}(t) \qquad [4.5]$$

where λ is a continuously varying parameter, and a solution of the wave function is seeked as a power series:

$$\Psi(\mathbf{r},t) = \Psi^{(0)}(\mathbf{r},t) + \lambda\Psi^{(1)}(\mathbf{r},t) + \lambda^2\Psi^{(2)}(\mathbf{r},t) + \qquad [4.6]$$

Now a solution is required for every value of λ and all terms in λ^N satisfy the equation separately. When the wave function [4.6] is inserted in [4.1] a set of equations is obtained:

$$ih\frac{\partial\Psi^{(0)}}{\partial t} = \hat{H}_0\Psi^{(0)}$$

$$ih\frac{\partial\Psi^{(N)}}{\partial t} = \hat{H}_0\Psi^{(N)} + \hat{V}\Psi^{(N-1)} \qquad , N=1,2,3, .. \qquad [4.7]$$

We assume that initially the atom is in its ground state |g>, represented by a solution of $\hat{H}_0$:

$$\Psi^{(0)}(\mathbf{r},t) = u_g(\mathbf{r})\exp\left[-\frac{iE_g t}{h}\right] \qquad [4.8]$$

The energy eigenfunctions for the free atom form a complete set, and this set is now used as a basis for the description of the higher order wave functions:

$$\Psi^{(N)}(\mathbf{r},t) = \sum a_p^{(N)}(t)\, u_g(\mathbf{r}) e^{-i\omega t} \qquad [4.9]$$

The amplitude $a_p^{(N)}(t)$ gives the probability that up to N-th order in the perturbation the atom is in the eigenstate |p> at time t. Inserting [4.9] into wave equation [4.7] a set of equations for the amplitudes is found:

$$ih\sum_p \frac{\partial}{\partial t} a_p^{(N)}\, u_p(\mathbf{r}) e^{-i\omega_p t} = \sum_p a_p^{(N-1)}\, \hat{V} u_p(\mathbf{r}) e^{-i\omega_p t} \qquad [4.10]$$

The left side of [4.10] is multiplied by u_m* and through the use of the ortho-normality relation:

$$\int u_m^* u_n d^3r = \delta_{mn} \qquad [4.11]$$

dynamical equations for the probability amplitudes, similar to [2.15] and [2.16] follow:

$$\frac{\partial a_m^{(N)}}{\partial t} = \frac{1}{ih}\sum_p a_p^{(N-1)} \hat{V}_{mp} e^{i\omega_{mp} t} \qquad [4.12]$$

where the definitions are used:

$$\hat{V}_{mp} = \left\langle u_m \middle| \hat{V} \middle| u_n \right\rangle = \int u_m^* \hat{V} u_n d^3r \qquad [4.13]$$

$$\omega_{mp} = \omega_m - \omega_p \qquad [4.14]$$

Note that the derivation is exactly the same as in Chapter 2, but now for a multi-level system. If the amplitude up to order N-1 is determined Eq. [4.12] can be used straightforward to calculate the amplitude of order N through integration:

$$a_m^{(N)} = \frac{1}{ih}\sum_p \int_{-\infty}^{t} dt' \hat{V}_{mp}(t') a_p^{(N-1)}(t') e^{i\omega_{mp} t'} \qquad [4.15]$$

4.2 *CALCULATION OF PROBABILITY AMPLITUDES*

Equation [4.15] in fact represents a set of dynamical equations, from which the probability amplitudes up to all orders may be derived. The resulting wave functions then govern the behavior of the atoms under influence of the radiation field. As a starting point we assume that the atom is initially in the ground state, so:

$$a_p^{(0)} = \delta_{pg} \qquad [4.16]$$

This delta function is now inserted in the integral equation [4.15]. Following the above definitions we set:

$$\hat{V}_{mp}(t') = -\sum_k u_{mp} \cdot E(\omega_k) e^{-i\omega_k t'} \qquad [4.17]$$

and the transition dipole moment:

$$u_{mp} = \int u_m^* \hat{\mu} u_p d^3 r \qquad [4.18]$$

Now the integral [4.15] is easily evaluated, and when it is assumed that at $t=-\infty$ there is no contribution the following result follows:

$$a_m^{(1)} = \frac{1}{h} \sum_k \frac{u_{mg} \cdot E(\omega_k)}{\omega_{mg} - \omega_k} e^{i(\omega_{mg} - \omega_k)t} \qquad [4.19]$$

Now when the first order perturbation amplitude is found the second order can be derived from integrating Eq. [4.15] once more:

$$a_n^{(2)} = \frac{1}{h} \sum_{kl} \sum_m \frac{[u_{nm} \cdot E(\omega_l)]}{(\omega_{ng} - \omega_k - \omega_l)} \frac{[u_{mg} \cdot E(\omega_k)]}{(\omega_{mg} - \omega_k)} e^{i(\omega_{ng} - \omega_k - \omega_l)t} \qquad [4.20]$$

The same procedure once more yields the third order amplitudes:

$$a_s^{(3)} = \frac{1}{h} \sum_{pqr} \sum_{mn} \frac{[u_{sn} \cdot E(\omega_r)]}{(\omega_{sg} - \omega_p - \omega_q - \omega_r)} \frac{[u_{nm} \cdot E(\omega_q)]}{(\omega_{ng} - \omega_p - \omega_q)} \frac{[u_{mg} \cdot E(\omega_p)]}{(\omega_{mg} - \omega_p)} \times e^{i(\omega_{sg} - \omega_p - \omega_q - \omega_r)t} \qquad [4.21]$$

With this derivation of the probability amplitudes we also have obtained the time-dependence of the wave functions under the influence of the external field, i.e. the response of the medium up to third order. The susceptibility functions representing this response will now be evaluated.

4.3 *FIRST ORDER SUSCEPTIBILITY*

In the preceding paragraph the wave function of the system is determined. In the perturbation expansion λ is set at 1, then Ψ follows through Eq. [4.6] and [4.9]. The expectation value of the electric dipole moment is given by:

$$\langle \hat{p} \rangle = \langle \Psi | \hat{\mu} | \Psi \rangle \qquad [4.22]$$

The lowest order contribution to this dipole moment, i.e. the one linear in the field amplitude is then:

$$\langle \hat{p}^{(1)} \rangle = \langle \Psi^{(0)} | \hat{\mu} | \Psi^{(1)} \rangle + \langle \Psi^{(1)} | \hat{\mu} | \Psi^{(0)} \rangle \qquad [4.23]$$

The wave function in 0-th order is given by [4.8] and in 1-st order by [4.9], after inserting the first order amplitude, calculated in [4.19]. Substituting these results then yields:

$$\langle \hat{p}^{(1)} \rangle = \frac{1}{h} \sum_p \sum_m \left(\frac{\mu_{gm} [\mu_{mg} \cdot E(\omega_p)]}{\omega_{mg} - \omega_p} e^{-i\omega_p t} + \frac{[\mu_{mg} \cdot E(\omega_p)]^* \mu_{mg}}{\omega_{mg}^* - \omega_p} e^{i\omega_p t} \right) \qquad [4.24]$$

This equation involves a summation over all positive and negative field frequencies. Moreover we have allowed the possibility of complex frequencies (see below). In the second term of [4.24] the field frequency is replaced by its negative counterpart, which is allowed because all possible frequency combinations appear in the summations. For negative frequencies replace ω_p by ω_{-p} and apply [4.19]. Then it is found:

$$\langle \hat{p}^{(1)} \rangle = \frac{1}{h} \sum_p \sum_m \left(\frac{\mu_{gm} [\mu_{mg} \cdot E(\omega_p)]}{\omega_{mg} - \omega_p} + \frac{[\mu_{mg} \cdot E(\omega_p)] \mu_{mg}}{\omega_{mg}^* + \omega_p} \right) e^{-i\omega_p t} \qquad [4.25]$$

This result can be used for the calculation of the linear susceptibility. The macroscopic susceptibility is:

$$\tilde{P}^{(1)} = N \langle \tilde{p}^{(1)} \rangle = \sum_p P^{(1)}(\omega_p) e^{-i\omega_p t} \qquad [4.26]$$

where the last part is an expansion of the polarization in Fourier components. Note that the polarizations as derived above have a vector character. Eq. [4.25] involves a dot product of the electric dipole moment and the electric field vector and the resulting scalar is then multiplied by the dipole moment, a vector. If the linear susceptibility is defined as follows:

$$P_i^{(1)} = \sum_j \chi_{ij}^{(1)} E_j(\omega_p) \qquad [4.27]$$

an expression for the linear susceptibility is found:

$$\chi_{ij}^{(1)}(\omega_p) = \frac{N}{h}\sum_m \left(\frac{\mu_{gm}^i \mu_{mg}^j}{\omega_{mg} - \omega_p} + \frac{\mu_{gm}^j \mu_{mg}^i}{\omega_{mg}^* + \omega_p} \right) \qquad [4.28]$$

The second term is called the anti-resonant contribution that is usually negligible. If g denotes the ground state it can never become resonant. In the figure below the contributions to the linear susceptibility are represented in a so-called energy diagram.

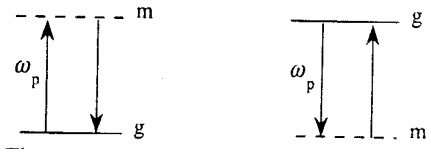

Fig.: The resonant and anti-resonant contributions to the linear susceptibility

The frequencies formally represent a complex quantity in above expressions. If the frequencies are written as:

$$\omega_{mg} = \omega_{mg}^0 - i\frac{\Gamma_m}{2} \qquad [4.29]$$

where ω^0 is a real transition frequency and Γ the population decay rate of the upper level |m>. This inclusion of damping only accounts for the phenomena that are related to population effects and not to dephasing processes that are not accompanied by transfer of population. In other terms: [4.29] only describes T_1 processes and not T_2 processes (in the language of NMR)

4.4 *SECOND ORDER SUSCEPTIBILITY*

Now that the wave function Ψ is known up to all orders of N, through the description in temrs of dynamical amplitudes [4.19-4.21] the higher order polarization terms can be gathered. Including all terms that contain a second order contribution in the applied electric field the second order polarization can be written:

$$\left\langle \hat{p}^{(2)} \right\rangle = \left\langle \Psi^{(0)} \middle| \hat{\mu} \middle| \Psi^{(2)} \right\rangle + \left\langle \Psi^{(1)} \middle| \hat{\mu} \middle| \Psi^{(1)} \right\rangle + \left\langle \Psi^{(2)} \middle| \hat{\mu} \middle| \Psi^{(0)} \right\rangle \qquad [4.30]$$

Inserting the wave function and amplitudes then gives an expression:

$$\left\langle \hat{p}^{(2)} \right\rangle = \frac{1}{h^2} \sum_{pqmn} \sum \left(\frac{\mu_{gn} \left[\mu_{nm} \cdot E(\omega_q) \right] \left[\mu_{mg} \cdot E(\omega_p) \right]}{(\omega_{ng} - \omega_p - \omega_q)(\omega_{mg} - \omega_p)} e^{-i(\omega_p + \omega_q)t} \right.$$

$$+\frac{\left[\mu_{ng}\cdot E(\omega_q)\right]^{*}\mu_{nm}\left[\mu_{mg}\cdot E(\omega_p)\right]}{(\omega_{ng}^{*}-\omega_q)(\omega_{mg}-\omega_p)}e^{-i(\omega_p-\omega_q)t}$$
$$+\frac{\left[\mu_{ng}\cdot E(\omega_q)\right]^{*}\left[\mu_{mn}\cdot E(\omega_p)\right]^{*}\mu_{mg}}{(\omega_{ng}^{*}-\omega_q)(\omega_{mg}^{*}-\omega_p-\omega_q)}e^{-i(\omega_p+\omega_q)t} \qquad [4.31]$$

Again by replacing $-\omega_q$ by ω_q in the second term, which is allowed because the summation over p and q are independent, the equation may be written as:

$$\left\langle\hat{p}^{(2)}\right\rangle=\frac{1}{h^2}\sum_{pq}\sum_{mn}\left\{\frac{\mu_{gn}\left[\mu_{nm}\cdot E(\omega_q)\right]\left[\mu_{mg}\cdot E(\omega_p)\right]}{(\omega_{ng}-\omega_p-\omega_q)(\omega_{mg}-\omega_p)}+\frac{\left[\mu_{gn}\cdot E(\omega_q)\right]\mu_{nm}\left[\mu_{mg}\cdot E(\omega_p)\right]}{(\omega_{ng}^{*}+\omega_q)(\omega_{mg}-\omega_p)}\right.$$
$$\left.+\frac{\left[\mu_{gn}\cdot E(\omega_q)\right]\left[\mu_{nm}\cdot E(\omega_p)\right]\mu_{mg}}{(\omega_{ng}^{*}+\omega_q)(\omega_{mg}^{*}+\omega_p+\omega_q)}\right\}e^{-i(\omega_p+\omega_q)t} \qquad [4.32]$$

If now, similar to Eq. [4.26] the second order polarization is defined and written in a Fourier series expansion:

$$\tilde{P}^{(2)}=N\left\langle\tilde{p}^{(2)}\right\rangle=\sum_p P^{(2)}(\omega_p)e^{-i\omega pt} \qquad [4.33]$$

Along the same lines as in [4.27] a second order susceptibility $\chi^{(2)}$ is defined through:

$$P_i^{(2)}=\sum_{jk}\sum_{(pq)}\chi_{ijk}^{(2)}(\omega_p+\omega_q,\omega_p,\omega_q)E_j(\omega_q)E_k(\omega_p) \qquad [4.34]$$

then an expression for this second order nonlinear susceptibility follows in a straightforward manner:

$$\chi_{ijk}^{(2)}(\omega_p+\omega_q,\omega_q,\omega_p)=\frac{N}{h^2}\Im_I\sum_{mn}\left\{\frac{\mu_{gn}^{i}\mu_{nm}^{j}\mu_{mg}^{k}}{(\omega_{ng}-\omega_p-\omega_q)(\omega_{mg}-\omega_p)}\right.$$
$$\left.+\frac{\mu_{gn}^{j}\mu_{nm}^{i}\mu_{mg}^{k}}{(\omega_{ng}^{*}+\omega_q)(\omega_{mg}-\omega_p)}+\frac{\mu_{gn}^{j}\mu_{nm}^{k}\mu_{mg}^{i}}{(\omega_{ng}^{*}+\omega_q)(\omega_{mg}^{*}+\omega_p+\omega_q)}\right\} \qquad [4.35]$$

Here the expression is somewhat simplified by the inclusion of the so-called intrinsic permutation operator $\Im_I$. Frequencies ω_p and ω_q are to be permuted and the contributions included in the expression for $\chi^{(2)}$. Cartesian indices i and j have to be permuted with these fields. Eq. [4.35] is written in this form to ensure that the resulting expression indeed obeys the condition of intrinsic permutation symmetry. Thus 6 terms appear in the expression for $\chi^{(2)}$; with the use of the permutation operator $\chi^{(2)}$ may be written as a sum of three terms that can each be expressed as an energy diagram.

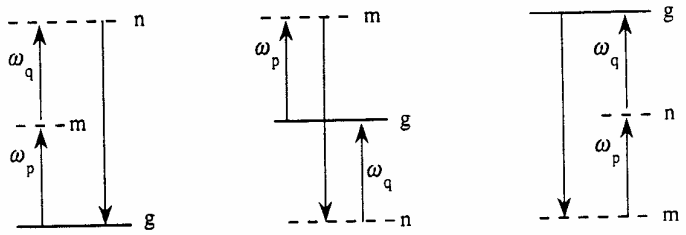

4.5 *THIRD ORDER NONLINEAR SUSCEPTIBILITY*

The procedure for the derivation of the third order nonlinear susceptibility is exactly similar to the derivation of the second order, shown above. First the polarization is defined:

$$\left\langle \hat{p}^{(3)} \right\rangle = \left\langle \Psi^{(0)} \middle| \hat{\mu} \middle| \Psi^{(3)} \right\rangle + \left\langle \Psi^{(1)} \middle| \hat{\mu} \middle| \Psi^{(2)} \right\rangle + \left\langle \Psi^{(2)} \middle| \hat{\mu} \middle| \Psi^{(1)} \right\rangle + \left\langle \Psi^{(3)} \middle| \hat{\mu} \middle| \Psi^{(0)} \right\rangle \qquad [4.36]$$

where terms up to the third order in the field are retained. Evaluation yields:

$$\left\langle \hat{p}^{(3)} \right\rangle = \frac{1}{h^3} \sum_{pqr} \sum_{mnv} \left\{ \frac{\mu_{gv}\left[\mu_{vn} \cdot E(\omega_r)\right]\left[\mu_{nm} \cdot E(\omega_q)\right]\left[\mu_{mg} \cdot E(\omega_p)\right]}{(\omega_{vg} - \omega_r - \omega_q - \omega_p)(\omega_{ng} - \omega_q - \omega_p)(\omega_{mg} - \omega_p)} \times e^{-i(\omega_p + \omega_q + \omega_r)t} \right.$$

$$+ \frac{\left[\mu_{vg} \cdot E(\omega_r)\right]^* \mu_{vn}\left[\mu_{nm} \cdot E(\omega_q)\right]\left[\mu_{mg} \cdot E(\omega_p)\right]}{(\omega^*_{vg} - \omega_r)(\omega_{ng} - \omega_q - \omega_p)(\omega_{mg} - \omega_p)} \times e^{-i(\omega_p + \omega_q - \omega_r)t}$$

$$+ \frac{\left[\mu_{vg} \cdot E(\omega_r)\right]^* \left[\mu_{nv} \cdot E(\omega_q)\right]^* \mu_{nm}\left[\mu_{mg} \cdot E(\omega_p)\right]}{(\omega^*_{vg} - \omega_r)(\omega^*_{ng} - \omega_r - \omega_q)(\omega_{mg} - \omega_p)} \times e^{-i(\omega_p - \omega_q - \omega_r)t}$$

$$\left. + \frac{\left[\mu_{vg} \cdot E(\omega_r)\right]^* \left[\mu_{nv} \cdot E(\omega_q)\right]^* \left[\mu_{mn} \cdot E(\omega_p)\right]^* \mu_{mg}}{(\omega^*_{vg} - \omega_r)(\omega^*_{ng} - \omega_r - \omega_q)(\omega^*_{mg} - \omega_r - \omega_q - \omega_p)} \times e^{-i(\omega_p + \omega_q + \omega_r)t} \right\} \qquad [4.37]$$

Replacing negative frequencies by their positive counterparts and making use of [4.40] yields:

$$\left\langle \hat{p}^{(3)} \right\rangle = \frac{1}{h^3} \sum_{pqr} \sum_{mnv} \left\{ \frac{\mu_{gv}\left[\mu_{vn} \cdot E(\omega_r)\right]\left[\mu_{nm} \cdot E(\omega_q)\right]\left[\mu_{mg} \cdot E(\omega_p)\right]}{(\omega_{vg} - \omega_r - \omega_q - \omega_p)(\omega_{ng} - \omega_q - \omega_p)(\omega_{mg} - \omega_p)} \right.$$

$$+ \frac{\left[\mu_{gv} \cdot E(\omega_r)\right]\mu_{vn}\left[\mu_{nm} \cdot E(\omega_q)\right]\left[\mu_{mg} \cdot E(\omega_p)\right]}{(\omega^*_{vg} + \omega_r)(\omega_{ng} - \omega_q - \omega_p)(\omega_{mg} - \omega_p)} + \frac{\left[\mu_{gv} \cdot E(\omega_r)\right]\left[\mu_{vn} \cdot E(\omega_q)\right]\mu_{nm}\left[\mu_{mg} \cdot E(\omega_p)\right]}{(\omega^*_{vg} + \omega_r)(\omega^*_{ng} + \omega_r + \omega_q)(\omega_{mg} - \omega_p)}$$

$$+\frac{\left[\mu_{g\nu}\cdot E(\omega_r)\right]\left[\mu_{\nu n}\cdot E(\omega_q)\right]\left[\mu_{nm}\cdot E(\omega_p)\right]\mu_{mg}}{(\omega^*_{\nu g}+\omega_r)(\omega^*_{ng}+\omega_r+\omega_q)(\omega^*_{mg}+\omega_r+\omega_q+\omega_p)}\Bigg\}\times e^{-i(\omega_p+\omega_q+\omega_r)t}\Bigg\} \qquad [4.38]$$

Again defining the macroscopic nonlinear polarization and expanding in Fourier components:

$$\tilde{P}^{(3)} = N\left\langle \tilde{p}^{(3)}\right\rangle = \sum_s P^{(2)}(\omega_s)e^{-i\omega_s t} \qquad [4.39]$$

Writing the nonlinear third order polarization as a function of a third order nonlinear susceptibility $\chi^{(3)}$:

$$P_k^{(3)}(\omega_p+\omega_q+\omega_r) = \sum_{hij}\sum_{(pqr)} \chi^{(3)}_{kjih}(\omega_\sigma,\omega_r,\omega_q,\omega_q)E_j(\omega_r)E_i(\omega_q)E_h(\omega_p) \qquad [4.40]$$

giving an expression for $\chi^{(3)}$:

$$\chi^{(3)}_{kjih}(\omega_\sigma,\omega_r,\omega_q,\omega_p) = \frac{N}{h^3}\Im_I \sum_{mn\nu}$$

$$\times\Bigg\{\frac{\mu^k_{g\nu}\mu^j_{\nu n}\mu^i_{nm}\mu^h_{mg}}{(\omega_{\nu g}-\omega_r-\omega_q-\omega_p)(\omega_{ng}-\omega_q-\omega_p)(\omega_{mg}-\omega_p)}$$
$$+\frac{\mu^j_{g\nu}\mu^k_{\nu n}\mu^i_{nm}\mu^h_{mg}}{(\omega^*_{\nu g}+\omega_r)(\omega_{ng}-\omega_q-\omega_p)(\omega_{mg}-\omega_p)} \qquad [4.41]$$
$$+\frac{\mu^j_{g\nu}\mu^i_{\nu n}\mu^k_{nm}\mu^h_{mg}}{(\omega^*_{\nu g}+\omega_r)(\omega^*_{ng}+\omega_r+\omega_q)(\omega_{mg}-\omega_p)}$$
$$+\frac{\mu^j_{g\nu}\mu^i_{\nu n}\mu^h_{nm}\mu^k_{mg}}{(\omega^*_{\nu g}+\omega_r)(\omega^*_{ng}+\omega_r+\omega_q)(\omega^*_{mg}+\omega_r+\omega_q+\omega_p)}\Bigg\}$$

where again the intrinsic permutation operator is used. Eq. [4.41] contains 4 terms but if the complete expression for $\chi^{(3)}$ is written by evaluating $\Im_I$ then it actually contains 24 terms. Eq.[4.41] can also be viewed in terms of energy diagrams as displayed in the figure.

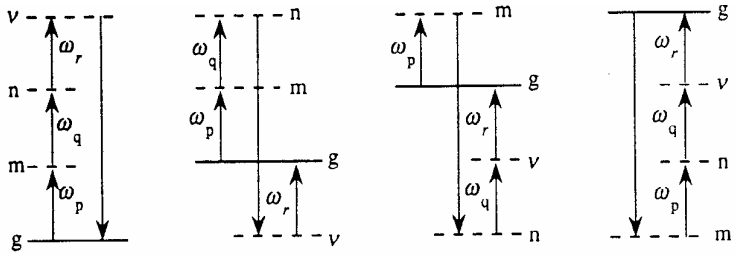

Fig.: Locations of the resonances of each term in the expression [4.41] for the third-order susceptibility.

The contents of this chapter are adapted from ref. [9]

[9] R.W. Boyd, *Nonlinear Optics*, Academic Press 1992

Chapter 5

Coherent Raman Scattering in Gases

5.1. *THIRD ORDER NONLINEAR SUSCEPTIBILITY*

In general, when no external fields are applied, the rule of inversion symmetry holds for gaseous media and thus all even order susceptibility tensors, as proven in Ch. 1, have zero elements:

$$\chi^{(2n)} = 0 \qquad [5.1]$$

and as a consequence all even orders of the non-linear polarization cancel:

$$\mathbf{P}^{(2n)} = 0 \qquad [5.2]$$

Thus the first term of importance, which rules the non-linear optical behavior of gases, is the one of third order (in SI units):

$$\mathbf{P}^{NL} = \varepsilon_0 \chi^{(3)} \mathbf{EEE} \qquad [5.2]$$

Here $\chi^{(3)}$ is a *material property* that governs the nonlinear response of a medium and all nonlinear processes occurring in that medium. It is therefore important to notice some aspects of $\chi^{(3)}$, even before starting a treatment of specific nonlinear processes.

1) A general expression of the third order nonlinear susceptibility was derived in Ch. 4. This expression consists of different terms, all having a different functional dependence on the *input frequencies*, the transition *dipole moments* describing the interaction matrix element for a single wave with quantum states of the medium, and the so-called *resonance denominators*. Perhaps most important are these resonance denominators that are the origin of resonance enhancement. Because the third order nonlinear processes are generally weak the resonance processes are usually dominant.

2) $\chi^{(3)}$ *is a fourth rank tensor*; so in the most general sense it contains 81 independent elements written as $\chi^{(3)}_{ijkl}$; for the specific case of an isotropic medium there are only 3 independent elements. In cases where all incident *electric field vectors* are chosen linear and parallel $\chi^{(3)}$ may be considered as a scalar function.

3) The generation of light by nonlinear optical processes is fully governed by the third order nonlinear susceptibility $\chi^{(3)}$. Of course this holds in the approximation that the higher order contributions, like the ones proportional to $\chi^{(5)}$, may be neglected. Furthermore the linear processes, governed by $\chi^{(1)}$, such as diffraction and absorption will play an important role in the propagation of input waves and the newly generated waves.

A distinction may be made between two ways in which the nonlinear susceptibility $\chi^{(3)}$ may be involved in the generation or amplification of waves. These are discussed in 5.1.1 and 5.1.2.

5.1.1 *NON-LINEAR GAIN PROCESSES*

Processes in which there occurs a direct coupling of waves, where one of the waves already present at the input is amplified with a certain *gain* factor. An example is the production of stimulated Stokes (Raman) radiation, where it is not even necessary that a strong light beam is present at the input; a source of Stokes noise-photons (always present of course) will do. Characteristic for these types of processes is that the intensity of the nonlinearly generated (or amplified) light beam is dependent on $\mathrm{Im}\chi^{(3)}$. In case this $\mathrm{Im}\chi^{(3)}$ is negative, there is effective gain in the medium. These processes will be called *nonlinear gain processes*.

5.1.2 *FOUR WAVE-MIXING PROCESSES*

b) Processes in which input waves of three different frequencies (in degenerate cases: only two or even one) effectively mix to generate a new wave at a different frequency. In that case the description is as follows. A polarization is generated at a new frequency ω_S:

$$\mathbf{P}^{NL} = \varepsilon_0 \chi^{(3)} \mathbf{E}_1 \mathbf{E}_2 \mathbf{E}_3 \qquad [5.4]$$

Inserting this polarization as a source terms into Maxwell's Wave Equation yields that a new wave at a certain modulation frequency is generated, proportional to this $\mathbf{P}^{NL}$:

$$\mathbf{E}_4 \propto \mathbf{P}^{NL} \qquad [5.5]$$

And we find that the intensity of this wave is proportional to:

$$I^{NL} = \left|\mathbf{E}_4\right|^2 \propto \left|\mathbf{P}^{NL}\right|^2 \propto \left|\chi^{(3)}\right|^2 \qquad [5.6]$$

These types of processes, that depend on the absolute square of the non-linear susceptibility are called *Four-Wave-Mixing* processes.

5.2 *SPONTANEOUS RAMAN SCATTERING*

Raman scattering is a two-photon linear *inelastic* light scattering process. The *elastic* counterpart is the well-known Rayleigh scattering process. In spontaneous Raman scattering the light is emitted in random directions (although for polarized light there may be preferred directions, depending also on the molecular mode). In Raman scattering an incoming photon with energy $h\omega_1$ is scattered by a molecule to an outgoing photon with energy $h\omega_2$, which is different from $h\omega_1$. In principle the incident frequency is not resonant with the medium. The difference in energy is absorbed or released by internal modes in the molecule, such as vibrational or rotational modes. The process in which energy is absorbed (red shifted photon produced) is called a Stokes process, whereas it is called Anti-Stokes in case of energy release (blue shifted photon produced).

For Raman processes in molecules specific selection rules are observed. First of all the parity of initial state and final state is the same, such as is always the case in a two-photon process. In

polyatomic molecules therefore only specific vibrational modes can be excited, that conserve the symmetry. In diatomic molecules there is no restriction on symmetry, as there is only a single symmetric vibration. Usually only modes Δv=1 are excited, although extremely weak overtone modes have been observed in spontaneous Raman scattering. For rotations the selection rules ΔJ=-2, ΔJ=0 and ΔJ=+2 apply. Purely rotational (then the ΔJ=0 transitions form the Rayleigh peak) and rovibrational excitations are possible. Below a schematic energy diagram is displayed for a purely rotational Raman spectrum, taken from ref [10].

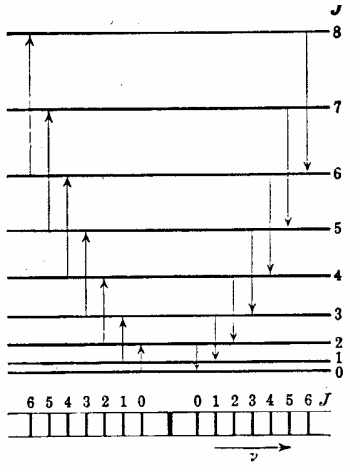

5.3 *STIMULATED RAMAN SCATTERING*

In spontaneous Raman scattering all Raman modes are excited at the same time and all frequencies are generated simultaneously. In stimulated Raman scattering one of these new fields is enhanced, similar as a particular mode in a laser is amplified. As a result a directional beam with high coherence is produced, with great similarities to a laser beam.

We go back to the Maxwell Wave equation that was derived in the general section on non-linear optics and we assume that the medium is nonconductive (σ=0) and non-magnetic (μ=1):

$$\nabla^2 E_i - \varepsilon_r \varepsilon_0 \mu_0 \frac{\partial^2}{\partial t^2} E_i = \mu_0 \frac{\partial^2}{\partial t^2} P_i^{NL} \qquad [5.7]$$

It is important to realize that this equation holds for a specific frequency ω, and in fact it should be considered for each frequency component of a Fourier decomposition of the frequency dependence of the waves; the index i refers to a specific frequency component. For each combination of three frequencies that add up to ω there is a corresponding term in the non-linear polarization. In fact the nonlinear polarization P^{NL} couples the waves of different frequencies, in this case the pump wave and the Stokes wave. The resonant terms (where two frequencies match with the Raman shift of the medium) are large, so all combinations of frequencies at resonance will be considered. Some simplifying approximations will be made now in order to find physical solutions:

a) one dimensional plane waves, for input and generated frequencies

[10] G. Herzberg, *Spectra of Diatomic Molecules*, Van Nostrand 1950

b) the concept of different orientations of the polarization vector is dropped
c) the slowly varying amplitude approximation is assumed again
d) the intensity of the pump is considered constant (no pump depletion)
e) the stationary limit or the steady state approximation

One of the frequency components will be written as:

$$\mathbf{E}(\mathbf{r},t,\omega) = \mathbf{A}(\mathbf{r},t)e^{i(\mathbf{k}\cdot\mathbf{r}-\omega t)} \qquad [5.8]$$

where **k** points in the direction of propagation of the wave (the wave vector). We then find:

$$\nabla^2\mathbf{E} = \left[\nabla^2\mathbf{A} + 2i(\mathbf{k}\cdot\nabla)\mathbf{A} - k^2\mathbf{A}\right]e^{i(\mathbf{k}\cdot\mathbf{r}-\omega t)} \qquad [5.9]$$

The energy transfer among waves is usually insignificant over distances of the order of their wavelengths and therefore we expect the variation of the amplitude to be small over one wavelength (slowly varying amplitude approximation):

$$\left|\nabla^2\mathbf{A}\right| << \left|(\mathbf{k}\cdot\nabla)\mathbf{A}\right| \qquad [5.10]$$

For the time derivative we find:

$$\frac{\partial^2}{\partial t^2}\mathbf{E} = \left[\frac{\partial^2}{\partial t^2}\mathbf{A} + 2i\omega\frac{\partial}{\partial t}\mathbf{A} - \omega^2\mathbf{A}\right]e^{i(\mathbf{k}\cdot\mathbf{r}-\omega t)} \qquad [5.11]$$

And we assume that the variation of the amplitude in time is slow compared to the frequency ω:

$$\left|\frac{\partial^2}{\partial t^2}\mathbf{A}\right| << \omega\left|\frac{\partial}{\partial t}\mathbf{A}\right| \qquad [5.12]$$

The non-linear polarization $\mathbf{P}^{NL}$ is a perturbation in the wave equation and it is a small quantity compared to $\varepsilon_r\varepsilon_0\mathbf{E}$, so not only the second but also the first time derivative of its amplitude can be ignored and only the term $-\omega^2\mathbf{P}^{NL}$ is retained.

Now we turn to the approximation of the stationary limit. On some *typical timescale* the stimulated Raman scattering process may be considered as a stationary process, even though the physical process is induced with pulsed lasers. The typical time scale is related to the relaxation time of the excitation, and this is again related to the characteristic linewidth for stimulated Raman scattering. For hydrogen these numbers are $\Delta\omega$=0.01 cm^{-1} and T_R=1.7 ns; verify that these numbers are related through the Fourier transform. So for pulsed lasers with time durations of 5 ns the steady state limit is still valid. So we neglect the term with $2i\omega\partial/\partial t$ **A**. Furthermore for ε_r we take the imaginary part ε''_r. Thus we obtain the coupled amplitude equation for stimulated Raman scattering;

$$2i(\mathbf{k}\cdot\nabla)\mathbf{A} + i\varepsilon_r''\varepsilon_0\mu_0\omega^2\mathbf{A} = -\mu_0\omega^2\mathbf{P}^{NL}e^{-i(\mathbf{k}\cdot\mathbf{r}-\omega t)} \qquad [5.13]$$

For wave propagation in one direction along a z-axis this reduces to:

$$\frac{d}{dr}\mathbf{A}_S(\mathbf{r}) + \alpha\mathbf{A}_S(\mathbf{r}) = i\beta\mathbf{P}_S^{NL}(\mathbf{r})e^{-i(\mathbf{k}_S\cdot\mathbf{r}-\omega_S t)} \qquad [5.14]$$

and with n_ω is the index of refraction at frequency ω:

$$\alpha = \frac{\varepsilon_r''\varepsilon_0\mu_0\omega^2}{2k} \qquad \text{and} \qquad \beta = \frac{\omega}{2\varepsilon_0 n_\omega c} \qquad [5.15]$$

5.4 FIRST STOKES GENERATION

It is necessary for a description to restrict the couplings to a few waves only. Consider the case where only the laser frequency and the so-called first Stokes are important. Assume the laser beam of constant intensity and propagating along the *z*-axis. Only Eq. [5.14] for the Stokes intensity remains to be solved. The growth of the Stokes beam depends on the attenuation constant α and the imaginary part of the nonlinear polarization. This nonlinear polarization consists of two terms:

$$\begin{aligned}&\varepsilon_0\chi_1^{(3)}(\omega_{S1};\omega_P,-\omega_P,\omega_{S1})|\mathbf{A}_P|^2\mathbf{A}_{S1}e^{i(k_P-k_P)z}e^{i\mathbf{k}_{S1}\cdot\mathbf{r}}e^{-i(\omega_P-\omega_P+\omega_{S1})}\\&\varepsilon_0\chi_2^{(3)}(\omega_{S1};\omega_{S1},-\omega_{S1},\omega_{S1})|\mathbf{A}_{S1}|^2\mathbf{A}_{S1}e^{i(\mathbf{k}_{S1}-\mathbf{k}_{S1}+\mathbf{k}_{S1})\mathbf{r}}e^{-i(\omega_{S1}-\omega_{S1}+\omega_{S1})}\end{aligned} \qquad [5.16]$$

where $|\mathbf{A}_P|^2$ and $|\mathbf{A}_{S1}|^2$ are the intensities of pump and first Stokes respectively. χ_1 is resonant at ω_{S1}-ω_P, while in χ_2 no combination of frequencies is in resonance. χ_2 is real and only modifies the refractive index. These nonlinear polarizations are inserted in the coupled equation [5.14] and then the phase factors all cancel giving:

$$\frac{d}{dz}\mathbf{A}_S(r) + \alpha\mathbf{A}_S(r) = i\varepsilon_0\beta\left[\chi_1^{(3)}|\mathbf{A}_P|^2\mathbf{A}_S + \chi_2^{(3)}|\mathbf{A}_S|^2\mathbf{A}_S\right] \qquad [5.17]$$

The solution to this equation depends on the input intensity at ω_{S1}:

$$\mathbf{A}_{S1}(\mathbf{r}) = \mathbf{A}_{S1}(0)e^{-\left[\varepsilon_0\beta|\mathbf{A}_P|^2\,\mathrm{Im}\,\chi_1^{(3)}+\alpha\right]}e^{i\varepsilon_0\beta\left[|\mathbf{A}_P|^2\,\mathrm{Re}\,\chi_1^{(3)}+\chi_2^{(3)}|\mathbf{A}_S|^2\right]} \qquad [5.18]$$

The real part of χ_1 and χ_2 only modify the refractive index, so a phase shift is introduced. A new wave at the Stokes frequency is built up if there is somehow some initial amplitude at the Stokes frequency and if the first exponential has a positive value. Then the imaginary part of χ_1 must be negative. Then a gain coefficient for stimulated Raman scattering may be defined as:

$$g = -\varepsilon_0\beta|\mathbf{A}_P|^2\,\mathrm{Im}\,\chi_1^{(3)} \qquad [5.19]$$

Of course the gain g must also be larger than the losses α, similar to the condition in a laser.
A very important point for the occurrence of Stimulated Raman scattering is the requirement that the imaginary part of the relevant term in $\chi^{(3)}$ is negative. In the figure the nonlinear Raman susceptibilities are displayed:

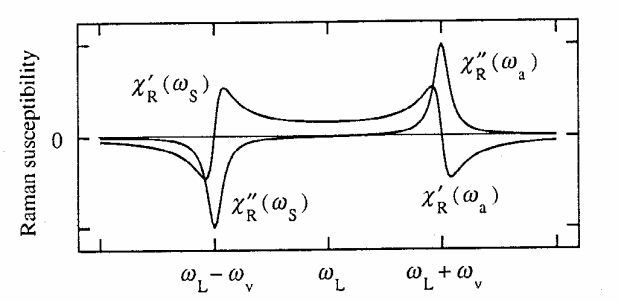

Note that at the Anti-stokes frequency the imaginary part of the $\chi^{(3)}$-term, which is negative for Stokes generation, is positive for Anti-Stokes generation. Therefore the term:

$$\chi^{(3)}(-\omega_{AS1};\omega_P;-\omega_P,\omega_{AS1}) \qquad [5.20]$$

cannot give rise to the generation of an Anti-Stokes beam in a similar way as it generates a Stokes beam. Stimulated Anti-Stokes can be produced through other nonlinear coupling mechanisms, for example through the term:

$$\chi^{(3)}(-\omega_{AS1};\omega_P;\omega_P,-\omega_{S1}) \qquad [5.21]$$

Via this and also other terms stimulated Anti-Stokes beams can be efficiently generated. Note however that in these processes *phase-matching* plays a role.

Verify that all exponentials containing frequencies have cancelled because of conservation of energy. Because the exponentials with the wave vectors have cancelled as well in the derivation there is in principal no preferential (or phase-matched) directionality for amplification of the first Stokes beam. But of course it will be amplified in the volume of the laser beam. The profile of the generated radiation will therefore resemble the profile of the incident pump beam. This process of First Stokes generation is a *non-phase-matched* or a *non-parametric* nonlinear optical process.

Rather high conversion efficiencies can be obtained for first Stokes generation. As soon as *S1* reaches high enough intensities it can act as a pump source to produce *S2* radiation and so on. In this way higher order Stokes beams resembling the spatial profile of the pump beam can be generated. These higher order Stokes-shifted frequencies correspond to:

$$\omega_{Sn} = \omega_{Sn} - n\omega_{Raman} \qquad [5.22]$$

where ω_{Raman} is the material excitation frequency of the medium. It should be noted that on the microscopic scale in higher order Stokes shifting different molecules are transferred into the first vibrationally excited state, and that vibrational overtones are *not* excited (i.e. excitation into v=2 or v=3). If this were the case anharmonicity shifts for the higher order Stokes frequencies would necessarily result, and these are *not* observed.

The figure below shows the efficiency curves for the production of the first, second and third Stokes frequencies of an input laser beam with characteristics: 20 mJ in 5 ns at λ=266 nm focused with f=50 cm. The horizontal axis shows the pressure (in atm) of H_2 in the Raman cell.

Note that at high pressures (6 Bar) the intensity of the first and even the second Stokes beam are higher than that of the fundamental input beam.

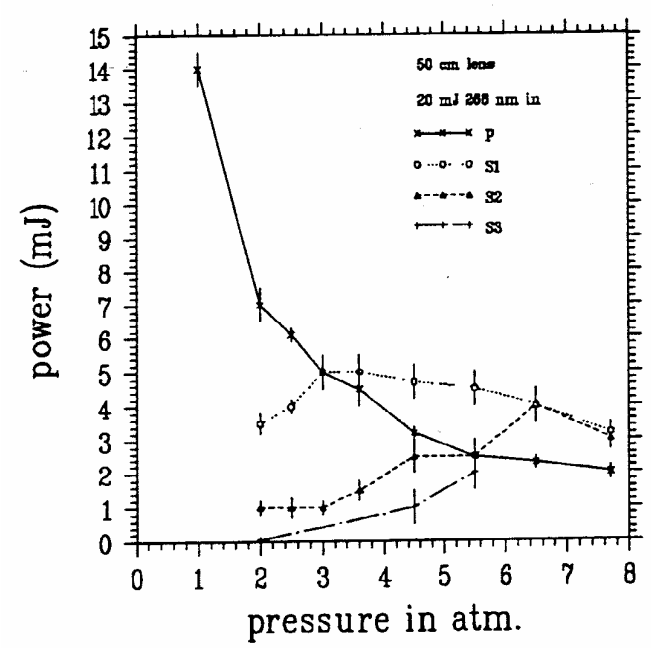

5.5. *RAMAN SHIFTING IN HYDROGEN*

In the above we have learned that the frequency of a pump laser may be efficiently Raman shifted towards the red (Stokes generation) or to the blue (Anti-Stokes generation). With the help of this technique wavelength regions, which are not easily accessible for tunable dye lasers may come into reach. We recall some important properties of H_2 as a Raman shifting medium:
- large Raman shift (4155.26 cm^{-1}), the largest of all molecules
- nearly all molecules in a single quantum state $|v=0, J=1>$
- a small relaxation width $\Gamma=0.01$ cm^{-1}, so shifted frequencies of narrow bandwidth are produced.

These properties make that H_2-gas, available at high pressures against low costs, is ultimately suitable as a Raman shifting medium. Starting out from a Nd-YAG pumped dye laser (with DCM-dye) the following regions can be covered using Stokes shifting:

pump	615 - 660 nm
1st Stokes	826 - 909 nm
2nd Stokes	1258 - 1461 nm
3rd Stokes	2635 - 3722 nm

Use of other dyes may cover the ranges in between. Anti-Stokes Raman shifting has been employed to generate radiation in the vacuum ultraviolet, though at low powers. Starting out from a XeCl-excimer laser pumping a DMQ-dye up to the 12th Anti-Stokes are observed with a (tunable) wavelength down to 129 nm.

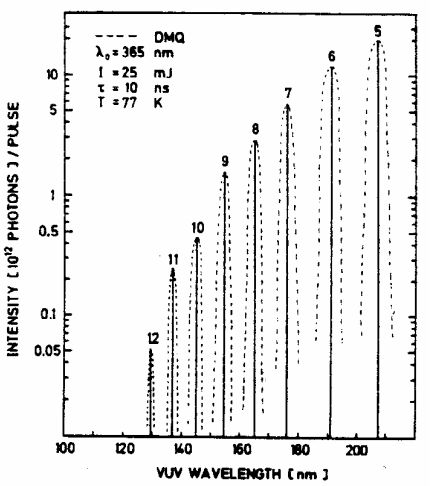

Fig.: From ref [11] .

5.6 *COHERENT ANTI-STOKES RAMAN SPECTROSCOPY (CARS)*

CARS is a Four-wave mixing process in which a new frequency $\omega_{as}=2\omega_1-\omega_2$ is generated. In the language of Raman spectroscopy this frequency is called the Anti-Stokes frequency, if there is a Raman resonance at $\omega_1-\omega_2$. The nonlinear polarization may be written as:

$$\mathbf{P}_{CARS}(\omega_S) = \chi^{(3)}(\omega_{as}=2\omega_1-\omega_2)\,\mathbf{E}(\omega_1)\mathbf{E}(\omega_1)\mathbf{E}(\omega_2)^* \qquad [5.23]$$

The generated intensity in a medium with length L is then:

$$I_{CARS} \propto \omega_{AS}^2 \left|\chi^{(3)}(\omega_{AS})\right|^2 I_1^2 I_2 \mathrm{sinc}\left[\frac{\Delta kL}{2}\right] \qquad [5.24]$$

The last factor in the equation determines the necessary conditions of phase matching, similar to the example of second harmonic generation or the OPO. However, if CARS is performed in a dilute gaseous medium there is almost no dispersion, so the value of the phase mismatch:

$$\mathbf{\Delta k} = \mathbf{k}_{as} - (2\mathbf{k}_1 - \mathbf{k}_2)$$

is small and nearly negligible even in the case of a co-linear beam geometry. In general the phase matching condition can also be fulfilled in non-co-linear geometries. In such a case a wave vector diagram may be constructed. From the direction and magnitude of the incoming wave vectors $\mathbf{k}_1$ and $\mathbf{k}_2$ the direction of the generated wave vector:

$$\mathbf{k}_{as} = 2\mathbf{k}_1 - \mathbf{k}_2$$

may be calculated. Also three dimensional phase matching diagrams may be applied. The technique of "BOXCARS" takes advantage of this: a beam is generated in a direction, where there is no input beam. The name originates in the box-like structure of the wave vector diagram.

[11] H. Wallmeier and H. Zacharias, Appl. Phys. B**45** (1988) 263

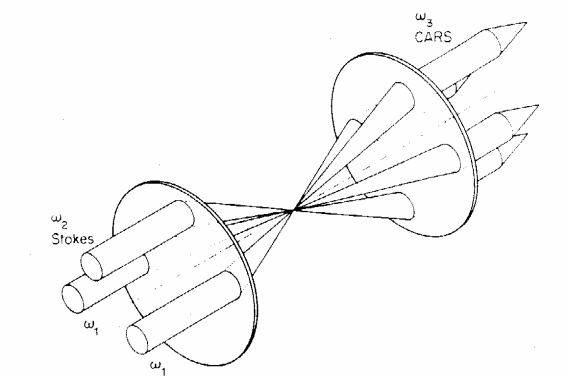

CARS is generally applied for the detection of molecular species, so the quantum structure of molecules needs to be considered in the evaluation of the nonlinear susceptibility $\chi^{(3)}$. In most relevant molecules there are no electronic transitions from the occupied ground states involving visible photons that are used in a CARS experiment. In a CARS energy level diagram:

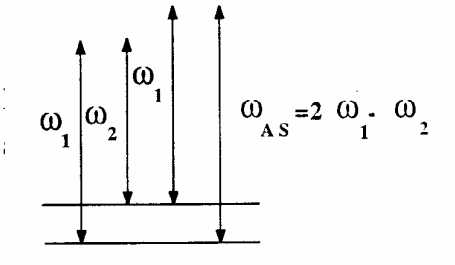

the quantum states at the one-photon electronic level are therefore represented by "virtual states". For CARS the different vibrational and rotational levels in molecules are important. In the sequence of the four photon interactions appearing in the non-linear susceptibility, states |1> and |3> are the virtual electronic states, denoted by |i>, whereas level |2> is a rovibrational state of the molecule, with the same electronic character. The expression for $\chi^{(3)}$ reduces to:

$$\chi^{(3)} = \sum N\rho_{gg} \frac{\mu_{gi}\mu_{iv}\mu_{vi}\mu_{ig}}{(\omega_1 \pm \omega_{i0})(\omega_1 - \omega_2 - \omega_{v0} - i\Gamma_{v0})(\omega \pm \omega_{i0})} \qquad [5.25]$$

where the ±-signs refer to the fact that different terms will appear in the expression with different combinations of signs.

In the Born-Oppenheimer approximation the transition moments, such as μ_{i0}, may be written in a product of independent electronic, vibrational and rotational parts. The electronic and vibrational parts then take the place of the Raman cross-section. Thus:

$$\chi^{(3)}_{CARS} \propto \left[\frac{d\sigma}{d\Omega}\right]_{Raman} \qquad [5.26]$$

Note that this implies that the CARS-signal is proportional to the square of the Raman cross section. Note also that in CARS signals are proportional to the density squared (N^2), in contrast to most spectroscopic techniques.

Similar to the spontaneous Raman effect, where only the vibrational transitions of $\Delta v=1$ occur, this holds also, and for the same reason in the coherent Raman effect, CARS. This implies also that the rotational selection rules will be the same for CARS as for spontaneous Raman scattering. For simple diatomic molecules such as N_2, H_2, and CO $\Delta J= -2, 0, 2$ rotational transitions are possible, denoted by O, Q and S-branches. Generally the equation for the CARS-susceptibility is then written as:

$$\chi^{(3)} \propto \frac{N_J S_{JJ}}{\left(\omega_1 - \omega_2 - \omega_{v0} - i\Gamma_{v0}\right)} + \chi_{NR} \qquad [5.27]$$

where N_J represents the population of a particular rotational state, $S_{JJ'}$ is the rotational linestrength factors (Placzek-Teller coefficients) and the summation is over all populated states with quantum number J. χ_{NR} is generally added for the contribution the to CARS signal of the non-resonant terms in the non-linear susceptibility.

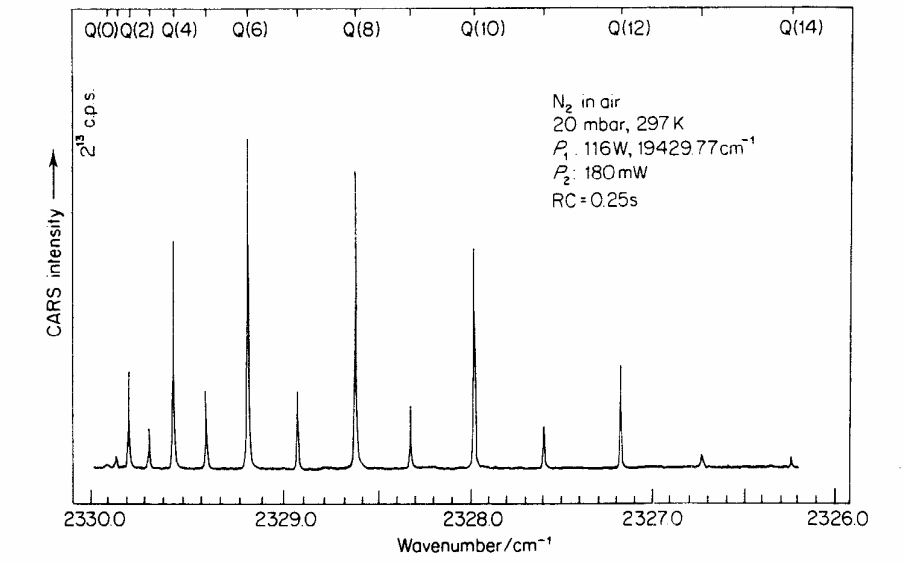

The resulting equation for the nonlinear susceptibility has important consequences for the CARS-*spectrum*. A spectral resonance is found whenever the denominator approaches a zero-value. This happens for:

$$\omega_1 - \omega_2 = \omega_{v0} \qquad [5.28]$$

A spectral line is found if the difference in energy (in fact frequency) of the two incoming waves equals a Raman resonance in the molecule; an important condition is that the transition ω_{v0} is Raman-allowed, i.e. fulfills the Raman selection rules. Because in the expression there is a summation over all initially populated rotational levels with quantum numbers J in the spectrum, and because of the appearance of 3 branches (O,Q and P) the spectrum will consist of 3 times J lines. These lines are centered at a Raman shift of ω_{v0}. Γ_{v0} represents a damping factor that is related to the time scale of relaxation of the vibrational excitation in the molecule; ultimately this damping factor will determine the linewidth to be observed in the spectrum. An example of a *vibrational* CARS-spectrum is given above.

Apart from the above described vibrational CARS processes, where a rotational structure is superimposed on the vibrational transition, also a *purely rotational* CARS spectrum may be observed. The energy difference ω_{v0} of a vibrational excitation is then to be replaced by the much smaller energy difference of a rotational excitation $\omega_{JJ'}$. In rotational CARS the quantum states J' probed by the energy difference ω_1-ω_2 may be populated initially. Therefore the expression for the susceptibility has to be replaced by:

$$\chi^{(3)} \propto \frac{(N_J - N_{J'})S_{JJ'}}{(\omega_1 - \omega_2 - \omega_{JJ'} - i\Gamma_{JJ'})} + \chi_{NR} \qquad [5.29]$$

Examples of purely rotational CARS spectra for N_2, O_2 and CO molecules are shown below. Note that the full spectrum covers less than 200 cm^{-1}; moreover the lowest J lines are shifted from the so-called pump-frequency ω_1 by only 20 cm^{-1}. For visible wavelengths of the commonly used Nd-YAG laser at 532 nm this corresponds to a shift of only 0.5 nm; in order to retrieve the CARS-signal from the background stray-light from the pump-laser BOXCARS configurations are helpful.

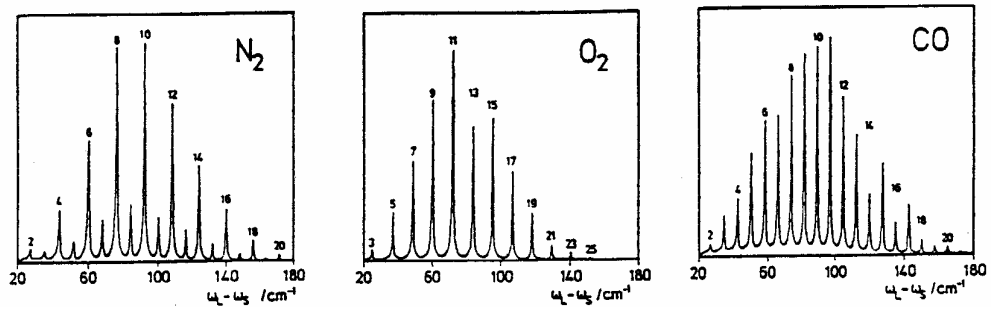

Fig.: Rotational CARS spectra of N_2, O_2 and CO recorded in the BOXCARS configuration, from ref. [12]

The population factors N_J and $N_{J'}$ are dependent of the temperature. In thermodynamic equilibrium these are equal to:

$$N_J \propto (2J+1)\exp\left[-\frac{B_{rot}J(J+1)}{k_B T}\right] \qquad [5.30]$$

where B_{rot} is the rotational constant of the probed molecule and k_B the Boltzmann constant. In the expression for the nonlinear susceptibility the rotational line-strengths $S_{JJ'}$ can be calculated and the expressions for N_J and $N_{J'}$ substituted. The observed line intensities of a spectrum may then be fitted to a temperature. As such this procedure is a *non-intrusive* temperature probe for a medium. An example of temperature dependent CARS spectra is shown below.

[12] B. Dick and A. Gierulski, Applied Physics B**40**, 1 (1986)

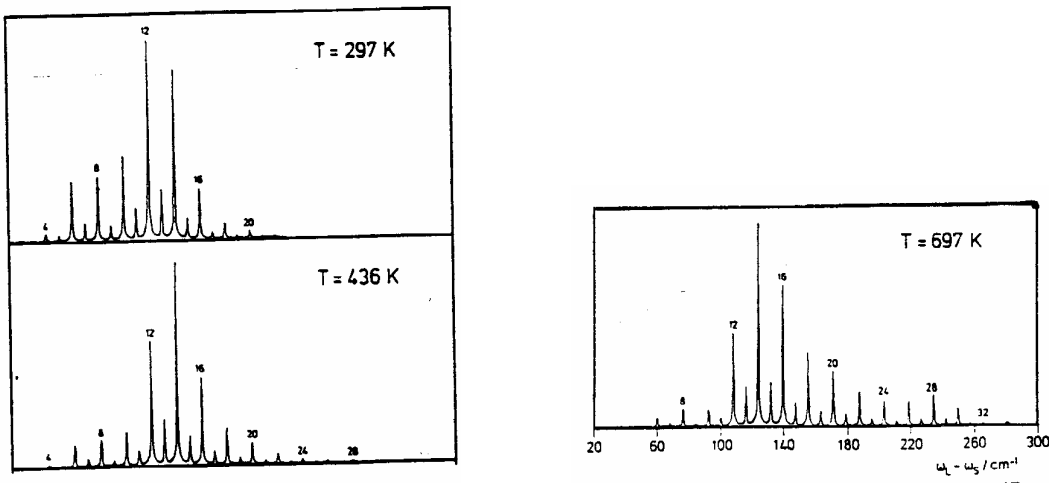

Fig: Temperature dependent CARS spectra, the non-intrusive thermometer. Also from ref [12]

Chapter 6

The production of vacuum ultraviolet radiation by FWM

6.1. *THIRD HARMONIC GENERATION*

A theoretical analysis of third harmonic generation (THG) was first given by Armstrong, Bloembergen, Ducuing and Pershan in their seminal paper in 1962[13]. Experiments in isotropic crystals (note that third harmonic generation can occur in media with inversion symmetry) were then performed by Maker *et al.*[14] THG in gaseous media was first reported by Ward and New[15]. Although metal atom vapors were shown to have large third order nonlinear susceptibilities by the group of Sorokin[16], noble gases are particularly suitable for use in the vacuum ultraviolet for reasons of transparency.

Starting equations for describing THG are again the coupled wave equations derived from Maxwell theory:

$$\frac{d}{dz}\mathbf{E}_q = i\frac{2\pi(q\omega)^2}{ck_q}\mathbf{P}_q^{NL} \qquad [6.1]$$

where $\mathbf{E}_q$ and $\mathbf{P}_q^{NL}$ are the Fourier components of the electric field and the nonlinear polarization at the frequency $q\omega$. [6.1] represents two coupled equations with q=1,3. The electric field is defined as:

$$\mathbf{E}_q = \hat{\mathbf{E}}_q(z,t)\exp[ik_q z] \qquad [6.2]$$

and the nonlinear polarization can be written as:

$$\mathbf{P}_3^{NL} = \frac{N}{4}\left[3\chi_T^{(3)}(3\omega)\mathbf{E}_1\mathbf{E}_1\mathbf{E}_1 + \chi_S^{(3)}(3\omega)\mathbf{E}_3|\mathbf{E}_3|^2 + \chi_S^{(3)}(\omega,3\omega)\mathbf{E}_3|\mathbf{E}_1|^2\right] \qquad [6.3]$$

where the term with $\chi_T^{(3)}$ is responsible for the actual THG and the other terms give rise to intensity dependent index of refraction. Also a similar equation for $\mathbf{P}_1^{NL}$ can be written, that couples the fields $\mathbf{E}_1$ and $\mathbf{E}_3$ nonlinearly to a polarization at frequency ω [17].

Before proceeding with theory it should be realized that THG depends on:

- phase matching, in combination with focused beams giving rise to the Gouy phase
- the nonlinear susceptibility involving transition dipole moments of the atoms
- the occurrence of resonances in the atomic level structure, also related to $\chi^{(3)}$

---

[13] J.A. Armstrong, N. Bloembergen, J. Ducuing, and P.S. Pershan, Phys. Rev. **127**, 1918 (1962).
[14] P.D. Maker, R.W. Terhune, and C.M. Savage, Proceedings of the Third International Conference on Quantum Electronics, Paris, 1963 (Columbia University Press 1964, p. 1559).
[15] G.H.C. New and J.F. Ward, Phys. Rev. Lett. **19**, 556 (1967); J.F. Ward and G.H.C. New, Phys. Rev. **185**, 57 (1969)
[16] R.T. Hodgson, P.P. Sorokin, and J.J. Wynne, Phys. Rev. Lett. **32**, 343 (1974).
[17] H.B. Puell and C.R. Vidal, IEEE J. Quant. Electr. **14**, 364 (1978).

6.2. *PHASE MATCHING UNDER FOCUSING CONDITIONS*

In this paragraph, which is based on ref [18], a comparison is made between three four-wave mixing processes:

$$\begin{aligned} &\omega_1+\omega_2+\omega_3\rightarrow\omega_4 && \text{I}\\ &\omega_1+\omega_2-\omega_3\rightarrow\omega_4 && \text{II}\\ &\omega_1-\omega_2-\omega_3\rightarrow\omega_4 && \text{III} \end{aligned} \qquad [6.4]$$

The fundamental electric field is written as:

$$\mathbf{E}(\mathbf{r},t)=\mathrm{Re}\left[\mathbf{E}_1(\mathbf{r})\exp(-i\omega_1 t)+\mathbf{E}_2(\mathbf{r})\exp(-i\omega_2 t)+\mathbf{E}_3(\mathbf{r})\exp(-i\omega_3 t)\right] \qquad [6.5]$$

The fundamental beams at ω_1, ω_2 and ω_3 are lowest order Gaussian and propagate along the *z*-axis:

$$\mathbf{E}_n(\mathbf{r})=\mathbf{E}_{n0}(\mathbf{r})\exp(ik_n z)\frac{1}{1+i\xi}\exp\left[\frac{-k_n\left(x^2+y^2\right)}{b(1+i\xi)}\right] \qquad [6.6]$$

with the confocal parameter defined as in [1.64]:

$$b=\frac{2\pi w_0^2}{\lambda}=\frac{2\pi w_0^2 n}{\lambda_0}=\frac{2\lambda_0}{n\theta^2}=kw_0^2 \qquad [6.7]$$

Here w_0 is the beam waist radius, *n* the index of refraction, λ_0 the vacuum wavelength, and θ the far-field diffraction half angle. ξ is a normalized coordinate along *z*, defined as:

$$\xi=\frac{2(z-f)}{b} \qquad [6.8]$$

where *f* is the position of the focus (beam waist) along the *z*-axis.

In the analysis the fundamental and generated beams are considered as linearly polarized (all along the same axis), so the vector nature of the fields and the tensor nature of the nonlinear susceptibility may be dropped. The polarization at the generated frequency ω_4 can be written as:

$$P_4(\mathbf{r},t)=\mathrm{Re}\left[P_4(\mathbf{r})\exp(-i\omega_4 t)\right] \qquad [6.9]$$

with:

$$\begin{aligned} P_4(\mathbf{r})&=\frac{3}{2}N\chi(-\omega_4;\omega_1,\omega_2,\omega_3)E_1(\mathbf{r})E_2(\mathbf{r})E_3(\mathbf{r})\\ P_4(\mathbf{r})&=\frac{3}{2}N\chi(-\omega_4;\omega_1,\omega_2,-\omega_3)E_1(\mathbf{r})E_2(\mathbf{r})E_3^*(\mathbf{r})\\ P_4(\mathbf{r})&=\frac{3}{2}N\chi(-\omega_4;\omega_1,-\omega_2,-\omega_3)E_1(\mathbf{r})E_2^*(\mathbf{r})E_3^*(\mathbf{r}) \end{aligned} \qquad [6.10]$$

[18] G.C. Bjorklund, IEEE J. Quant. Electr. **11**, 287 (1975)

with χ the nonlinear susceptibility per atom and N the number density of atoms in the nonlinear medium. When two or three of the input frequencies are degenerate, the factor of 3/2 must be changed to ¾ or ¼).

Now the polarization at ω_4 for process I becomes:

$$P_4(\mathbf{r}) = \frac{3}{2} N\chi(-\omega_4;\omega_1,\omega_2,\omega_3)E_{10}E_{20}E_{30}\exp(ik'z)\frac{1}{(1+i\xi)^3}\exp\left[\frac{-k'(x^2+y^2)}{b(1+i\xi)}\right]B(z) \quad [6.11]$$

with k' the wave vector for the generated field in process I, which is set equal to k'' for future use:

$$k' = k_1 + k_2 + k_3 = k'' \quad [6.12]$$

The factor *B(z)* defined as *B(z)*=0 for $z < 0$ and *B(z)*=1 for $z > 0$ signifies that the space at $z < 0$ is vacuum, while the nonlinear medium exists at $z>0$.
For the process II one finds similarly:

$$P_4(\mathbf{r}) = \frac{3}{2} N\chi(-\omega_4;\omega_1,\omega_2,-\omega_3)E_{10}E_{20}E_{30}\exp(ik'z)\frac{1}{(1+i\xi)^2(1-i\xi)} \exp\left[\frac{(-k''+i\xi k')(x^2+y^2)}{b(1+\xi^2)}\right]B(z) \quad [6.13]$$

where k'' is as before and k' is defined as $k' = k_1 + k_2 - k_3$:
Similarly for process III:

$$P_4(\mathbf{r}) = \frac{3}{2} N\chi(-\omega_4;\omega_1,-\omega_2,-\omega_3)E_{10}E_{20}E_{30}\exp(ik'z)\frac{1}{(1+i\xi)(1-i\xi)^2} \exp\left[\frac{(-k''+i\xi k')(x^2+y^2)}{b(1+\xi^2)}\right]B(z) \quad [6.14]$$

with $k' = k_1 - k_2 - k_3$
The next step is to perform a Fourier decomposition of $P_4(\mathbf{r})$ to determine the amplitudes of the plane wave components of the driving polarization. The amplitude with wave vector ***K*** is defined by:

$$P_4(\mathbf{K}) = (2\pi)^{-3}\int_{-\infty}^{\infty} dx'' \int_{-\infty}^{\infty} dy'' \int_{-\infty}^{\infty} dz'' P_4(\mathbf{r}'')\exp[-i\mathbf{K}\cdot\mathbf{r}''] \quad [6.15]$$

This frequency component can be inserted in Maxwell's equation:

$$\nabla\times\nabla\times E_{4(\mathbf{K})}(\mathbf{r}) - k_4^2 E_{4(\mathbf{K})}(\mathbf{r}) = 4\pi k_0^2 P_4(\mathbf{K})\exp[i\mathbf{K}\cdot\mathbf{r}] \quad [6.16]$$

where k_4 and k_0 are the wave vectors of the generated radiation in the medium and in vacuum respectively. It was shown that this equation can be solved under certain realistic conditions and with the wave vector mismatch:

$$\Delta k = k_4 - k' \qquad [6.17]$$

yielding for process I;

$$E_4(\mathbf{r}) = i\frac{3N}{2k_4}\pi k_0^2 b\chi(-\omega_4;\omega_1,\omega_2,\omega_3)E_{10}E_{20}E_{30}\exp(ik'z)\frac{1}{(1+i\xi)} \exp\left[\frac{-k'(x^2+y^2)}{b(1+i\xi)}\right]\int_{-\zeta}^{\xi}\frac{\exp[-(ib/2)\Delta k(\xi'-\xi)]}{(1+i\xi')^2}d\xi' \qquad [6.28]$$

with the integration boundary defined as $\zeta = 2f/b$.
For processes II a slightly different expression results:

$$E_4(\mathbf{r}) = i\frac{3N}{2k_4}\pi k_0^2 b\chi(-\omega_4;\omega_1,\omega_2,-\omega_3)E_{10}E_{20}E_{30}\exp(ik'z) \int_{-\zeta}^{\xi}\frac{\exp[-(ib/2)\Delta k(\xi'-\xi)]}{(1+i\xi')(k''-ik'\xi')H}\exp\left[\frac{-(x^2+y^2)}{bH}\right]d\xi' \qquad [6.29]$$

with the function *H* defined as:

$$H = H(\xi,\xi') = \frac{1+\xi'^2}{(k''-ik'\xi')} - i\frac{(\xi'-\xi)}{k'} \qquad [6.30]$$

For process III a similar expression can be retained.

The equations [6.28] and [6.29] are important results for harmonic conversion in a medium contained in a cell of length *L* with the entrance window at *z* = 0, the focus at *z* = *f* and parameters $\xi = 2(L-f)/b$ and $\zeta = 2f/b$. The expressions give the generated field at the position *z* = *L*. i.e. at the 'end' of the cell.

General conclusions can be drawn from these expressions.

1) If $k' = k''$ then the generated beam has a lowest order Gaussian mode. Inspection of the equations reveals that this holds for process I, but not for the processes II and III. The sum- and difference frequency mixing yield higher order transverse modes, even if the fundamentals are lowest order Gaussian. The mismatch may be represented by the ratio: k''/k'.
2) In all processes $E_4(\mathbf{r})$ is circularly symmetric around the *z*-axis. The total generated power at ω_4 is obtained by performing integrals (transverse in space) of the form:

$$\int_0^{\infty} 2\pi R|E_4(R)|^2 dR \qquad \text{with} \qquad R = \sqrt{x^2+y^2} \qquad \text{and} \qquad z = L \qquad [6.31]$$

Then dimensionless functions can be defined of the form:

$$F_j\left(b\Delta k,\frac{b}{L},\frac{f}{L},\frac{k''}{k'}\right)=\frac{8}{9}\frac{k_4^2k'}{\pi^3k_0^4}\frac{1}{b^3\chi^2\left|E_{10}E_{20}E_{30}\right|^2}\int_0^\infty 2\pi R\left|E_4(R)\right|^2dR \qquad [6.32]$$

where j refers to the specific process (I, II, III). The integrated intensity depends on dimensionless parameters $b\Delta k$, b/L, f/L and k''/k'.

It can be shown that with all wave vectors expressed in units of cm^{-1}, b in cm, N in atoms/cm^3, χ in ESU/atom and the powers P in Watts then the total generated power P_4 is expresses as:

$$P_4=\eta\frac{k_0^4k_1k_2k_3}{k_4^2k'}N^2\chi^2P_1P_2P_3F_j\left(b\Delta k,\frac{b}{L},\frac{f}{L},\frac{k''}{k'}\right) \qquad [6.33]$$

The efficiency factor is η = 6.318 x 10^{-4} for three different beams, η = 1.580 x 10^{-4} for two degenerate beams and η = 1.755 x 10^{-5} for three degenerate beams (so for THG).

For process I the *phase-matching integral* F_I is:

$$F_I\left(b\Delta k,\frac{b}{L},\frac{f}{L},\frac{k''}{k'}\right)=\left|\int_{-\zeta}^{\xi}\frac{\exp\left[-(ib/2)\Delta k\xi'\right]}{(1+i\xi')^2}d\xi'\right| \qquad [6.34]$$

In the so-called tight-focusing limit, where b is short compared to the cell ($b<<L$), the entire focal region is contained within the cell ($\xi\to\infty$ and $\zeta\to\infty$), and the focus put half-way into the cell (f/L = 0.5) the integral can be solved in closed form:

$$F_I(b\Delta k,0,0.5,1)=\begin{matrix}\pi^2(b\Delta k)^2e^{(b\Delta k/2)} & \text{for} & \Delta k<0\\ 0 & & \Delta k\geq 0\end{matrix} \qquad [6.34]$$

For the other two processes expressions can be found by integration if the deviation from a Gaussian is neglected (so $k'=k''$ is set):

$$F_{II}(b\Delta k,0,0.5,1)=\pi^2e^{(-b|\Delta k|)} \qquad [6.35]$$

$$F_{III}(b\Delta k,0,0.5,1)=\begin{matrix}0 & \text{for} & \Delta k<0\\ \pi^2(b\Delta k)^2e^{(b\Delta k/2)} & & \Delta k\geq 0\end{matrix} \qquad [6.36]$$

This leads us to another important general conclusion (holding for the case of tight focusing): THG is only possible for the condition $\Delta k<0$, so for the condition of negative phase mismatch. Process II is possible for all signs in the phase mismatch, while process III is only possible for $\Delta k\geq 0$.

6.3 *NUMERICAL APPROACH TO THE PHASE MATCHING INTEGRALS*

In this section the functions *Fj* will be inspected in case of non-exact tight-focusing conditions. For this purpose the integrals contained in *Fj* can be evaluated numerically. The first example is that of F_I for *b/L* = small shown in the figure:

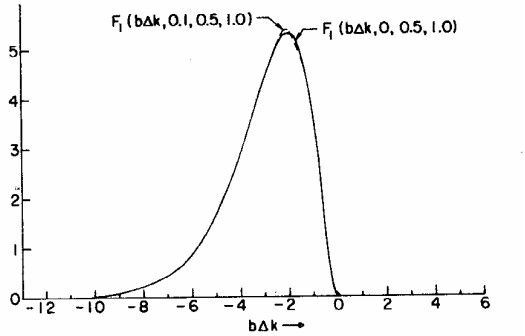

Fig: F_I versus $b\Delta k$ for b/L < 0.1and *f/L*=0.5

And for processes II and III:

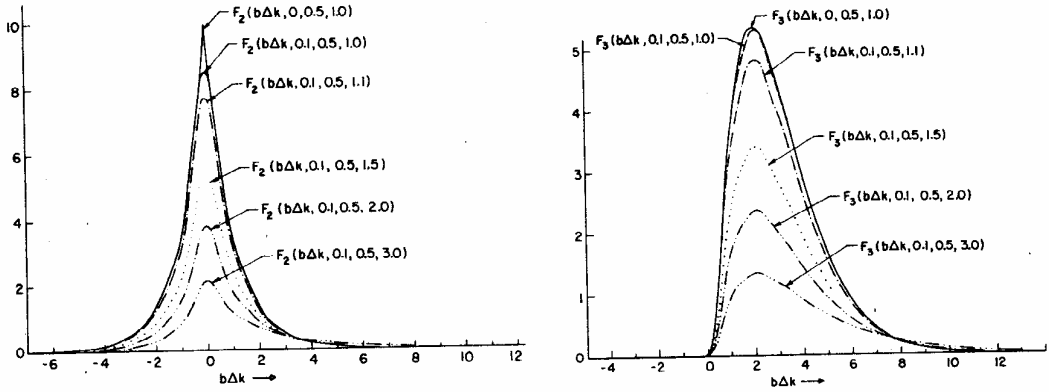

Fig: F_{II} (left) and F_{III} (right) versus $b\Delta k$ for b/L < 0.1and *f/L*=0.5 and varying values for k"/k'

These figures show that slight variations of the exact tight-focusing condition (*b/L* is small) does not affect the outcome of the integrals. The effect of deviation from Gaussian profiles in the generated beam is more profound as is shown in the lower figures for *k"/k'* up to 3. The decrease in generated power reflects the lack of overlap of the beams of differing transverse profiles.
For process II the optimum conversion is at Δk=0, while for processes I and III this optimum is at a nonzero value of $b\Delta k$, for process I at negative phase mismatch and for process III at positive phase mismatch.

Opposite to the case of *tight-focusing* is that of the *plane-wave limit*. This is the condition at which *b/L* >> 0. Then the result is found[19]:

[19] R.B. Miles and S.E. Harris, IEEE J. Quant. Electr. **9**, 470 (1973).

$$\lim_{b/L\to\infty} F_I\left(b\Delta k, \frac{b}{L}, 0.5, \frac{k''}{k'}\right) = \frac{4L^2}{b^2}\,\mathrm{sinc}^2\left(\frac{\Delta kL}{2}\right) \qquad [6.37]$$

The value of *k''/k'* does not influence the values of *Fj* in the plane wave limit. The evolution of the integral F_I when proceeding from the tight-focusing to the plane-wave limit with intermediate cases can be evaluated numerically as shown in the figure:

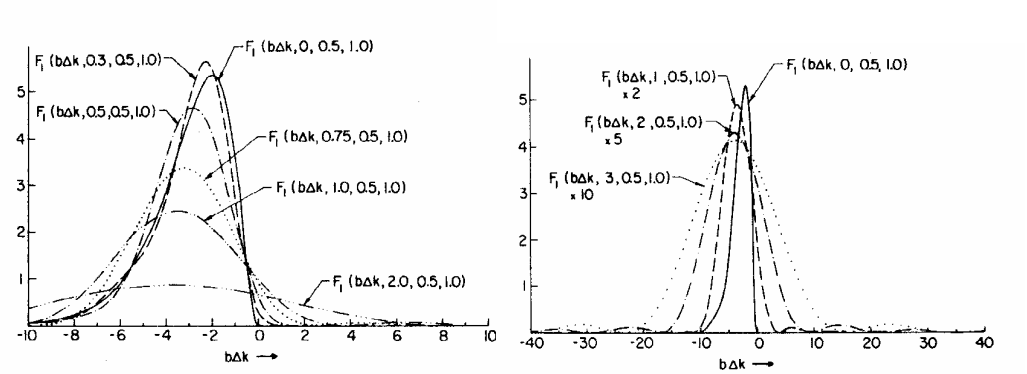

Fig: F_I versus $b\Delta k$ for f/L=0.5 and various b/L (left b/L = 0 – 2.0; right b/L = 0 – 3); Note the varying vertical scale on the right.

This shows that at b/L = 3 the peak has shifted already toward Δk = 0. Note also that the peak of the integral has decreased by an order of magnitude in the plane-wave limit. This results in another important conclusion of the algebra: tight focusing is more efficient in generating harmonics.

Now also the effect of positioning the focus in the cell can be studied by evaluating the phase-matching integrals. First for the near tight-focusing condition b/L = 0.1 the focal position is shifted from f/L = 0.5 to 1.5; results are shown in the figure:

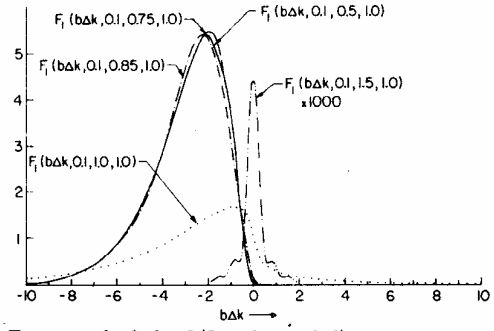

Fig: F_I versus $b\Delta k$ for b/L=0.1 and various f/L 0.5 to 1.5)

It shows that as long as the focus is contained in the cell no serious changes occur; only when the focus shifts outside the cell region the intensity reduces drastically. In fact, when f/L = 1.5 the focus is outside the cell and the condition is like in the plane-wave limit.

A similar evaluation can be performed for the true plane-wave limit, when b/L = 10. The values for the integral remains relatively unchanged as long as the cell is located close to the beam waist location. For f/L = 20 the focus is twice the distance of the confocal parameter b/L = 10.

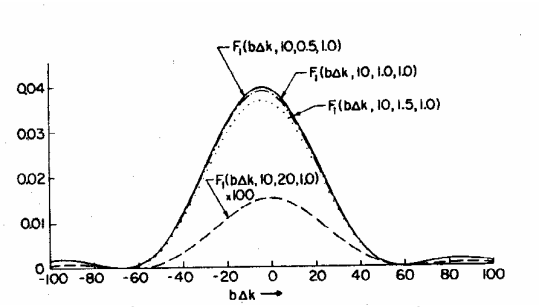

Fig: F_I versus $b\Delta k$ for b/L=10 and various f/L 0.5 to 20)

Similar calculations can be performed in the intermediate cases for the integrals F_{II} and F_{III}. In these cases the effect of non-overlapping spatial beams plays a role, an effect of $k''/k' \neq 1$. By numerically evaluating the field distribution $|E_4(R)|^2$ as a function of the transverse coordinate R, and then for each value of $b\Delta k$ this phenomenon can be investigated. A typical evolution of this far-field pattern is shown for process II with k''/k' =3.

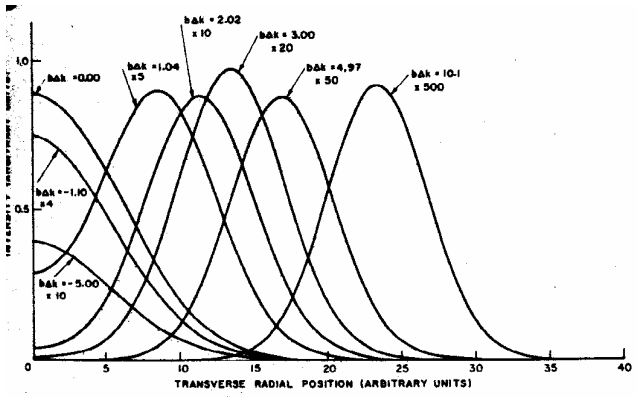

Fig: Far-field intensity distribution versus $b\Delta k$ for f/L=0.5, b/L =0.1 and k''/k'=3.0

Note that for small values of $b\Delta k$ a nearly Gaussian transverse beam profile is found and that for high values of $b\Delta k$ a ring-like structure is obtained.

6.4 *PHYSICAL INTERPRETATION OF PHASE MATCHING INTEGRALS*

It is found that the amplitude of the driving polarization strongly peaks in the region of the fundamental beam waists. This is very well understandable: harmonic conversion occurs at the focus where the intensity is high. In the case of tight-focusing the boundaries of the generating region are located at $\xi = -2$ and $\xi = 2$ (or $z = f-b$ and $z = f+b$). In the case of loose focusing the boundaries are located at the input and output windows. From the definition of the Gaussian beam [6.6] it can be seen:

$$\frac{1}{1+i\xi} = \frac{1}{\sqrt{(1+\xi^2)}} e^{-i\arctan\xi} \qquad [6.38]$$

that a focused lowest order Gaussian beam undergoes a shift in phase by arctanξ as it propagates through the waist region (the Gouy phase). The driving polarization then experiences phase shifts of: 3arctanξ for process I, arctanξ for process II, and -arctanξ for process III.

It is assumed that the optimum conversion efficiency occurs when the generated radiation is in phase with the driving field. The generated beam may be considered to experience a phase shift of arctanξ. Thus a slip of phase between the driving polarization and the generated region occurs of 2arctanξ for process I, -2arctanξ for process III, while process II remains in phase. The slip in phases causes destructive interference in different portions of the generating region.

These phase slips are compensated to some degree by the dispersion effects in the medium, i.e. the wave vector mismatch Δk. The optimum value of Δk, Δk_{opt} is the value at which cancellation occurs. For the case of tight focusing this is at;

$$\Delta k_{opt} \cong \begin{matrix} -2.2/b \\ 0 \\ 2.2/b \end{matrix} \quad \text{for} \quad \begin{matrix} \text{I} \\ \text{II} \\ \text{III} \end{matrix} \qquad [6.39]$$

For the analysis in the plane wave limit the factors 2.2 are to be replaced by 4.

6.5 *OPTIMIZING DENSITY IN THE NONLINEAR MEDIUM*

It was derived that the total power generated obeys the proportionality relation:

$$P_4 \propto P_1 P_2 P_3 N^2 \chi^2 F_j\left(b\Delta k, \frac{b}{L}, \frac{f}{L}, \frac{k''}{k'}\right) \qquad [6.40]$$

The parameters P_1, P_2, P_3, χ and k''/k' are considered to be constant and thus an optimization procedure aims at maximizing the quantity $N^2 F_j$ by varying the parameters N, $b\Delta k$, b/L and f/L.

When N is a parameter independent of the other ones the density may be increase for optimization. Then the parameter $b\Delta k$ should be set at Δk_{opt} as defined in [6.39]. The value for $b\Delta k$ may be altered by changing b or Δk. But in the tight focusing approximation b/L should remain within 0.1, so the focal condition cannot be varied at will. In order to make Δk a parameter independent of N, another medium with a specific dispersion can be mixed.

When N is a parameter dependent on $b\Delta k$ optimization can proceed differently. One important case is when Δk is constrained proportional to N, b is constrained to be constant and N is a free parameter. Then the quantity $\Delta k^2 F_j\left(b\Delta k, b/L, f/L, k''/k'\right)$ should be optimized; this quantity is not dimensionless and depends on b. Hence a dimensionless quantity is defined:

$$G_j\left(b\Delta k, \frac{b}{L}, \frac{f}{L}, \frac{k''}{k'}\right) = \left(b\Delta k\right)^2 F_j\left(b\Delta k, \frac{b}{L}, \frac{f}{L}, \frac{k''}{k'}\right) \qquad [6.41]$$

and the quantity to be optimized is $(1/b)^2 G_j\left(b\Delta k, b/L, f/L, k''/k'\right)$. The function G_I is plotted below as a function of $b\Delta k$ for certain f/L parameters:

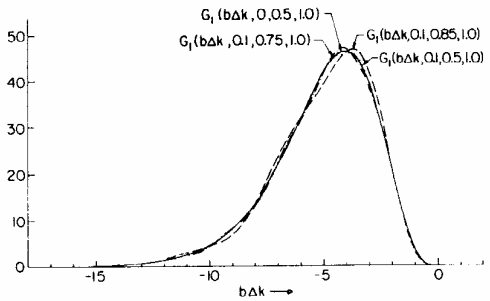

Fig: G_I versus $b\Delta k$, b/L =0.1(tight focus) and f/L=0.5, 0.75 and 0.85

So for tight focusing the specific value of f (focal position) does not matter, as long as the entire waist is contained in the cell.

Since N is the only free parameter, the optimization procedure is to adjust $b\Delta k$ to maximize G_j by adjusting N. Let $(b\Delta k)_{opt}$ the value of $b\Delta k$ which corresponds to the peak of G_j. Define the constant of proportionality:

$$\Delta k = \alpha N \qquad [6.42]$$

Then the optimization procedure reduces to adjusting N to the value $N_{opt} = (b\Delta k)_{opt} / \alpha b$. The total generated power is then:

$$P_4 = \eta \frac{k_0^4 k_1 k_2 k_3}{k_4^2 k'} \frac{\chi^2 P_1 P_2 P_3 G_j}{\alpha b} \qquad [6.43]$$

where the factor η is defined above G_j is at the peak of the function as displayed e.g. in the figures above (G_I) or below (G_{II}):

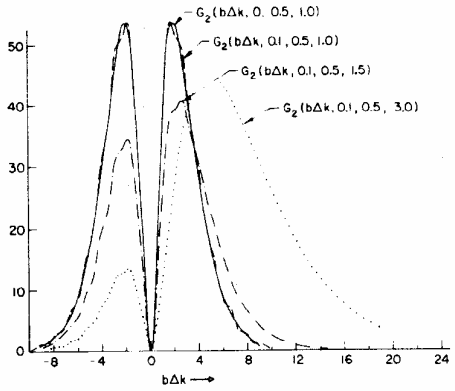

Fig: G_{II} versus $b\Delta k$, b/L =0.1(tight focus), f/L=0.5and k''/k'=1.0, 1.5, 3.0.

Again it may be noted that α must be negative for process I and that for process II α may both have positive and negative values.

6.6 *DISPERSION CHARACTERISTICS OF THE NOBLE GASES*

In the above the phase matching properties for the *tight-focusing* and the *plane-wave* limit were derived, as well as numerical procedures for intermediate cases. The generated third harmonic power produced by a beam at the center of a cell of length L can be expressed as:

$$P_{THG} = \frac{\eta}{(3\lambda)^4} N^2 \left[\chi^{(3)}(\lambda)\right]^2 P_1^3 F_j\left(b\Delta k, \frac{b}{L}, 0.5, 1\right) \qquad [6.44]$$

with η = 8.215 x 10^{-2}, P in Watts, $\chi^{(3)}$ in esu, λ (wavelength of generated beam) in cm.

In the *tight focusing* limit ($b<<L$) this results in [6.34]:

$$F_I(b\Delta k, 0, 0.5, 1) = \begin{cases} \pi^2 (b\Delta k)^2 e^{(b\Delta k/2)} & \text{for} \quad \Delta k < 0 \\ 0 & \Delta k \geq 0 \end{cases} \qquad [6.45]$$

with a maximum of F_I of 5.343 at $b\Delta k$ =-2.

In the *plane-wave* limit ($b>>L$) a result is obtained [6.37]:

$$F_I(b\Delta k, \infty, 0.5, 1) = \frac{4L^2}{b^2} \mathrm{sinc}^2\left(\frac{\Delta k L}{2}\right) \qquad [6.46]$$

with a maximum of $4L^2 / b^2$ at Δk =0.

A requirement for a rather tightly focused beam is that the medium should be negatively disperse. In the example of section *6.5* a value for Δk was obtained in a fit; it is also possible to calculate the dispersion a medium.

First it should be considered that through THG usually short wavelengths are generated, thus reaching the region of dense level structure in the atoms constituting the medium. For the following analysis we refer to ref [20].

In the region of the bound states the refractive index is given by:

$$(n-1)_{lines} = \frac{N r_e}{2\pi} \sum_i \frac{f_i}{\lambda_i^{-2} - \lambda} \qquad [6.47]$$

where r_e = 2.8181 x 10^{-13} cm is the classical electron radius, f_i the oscillator strength of the i^{th} transition, and λ_i the wavelength of this transition.

For the region of the continuum the transitions into the continuum are considered, that usually are broadened:

$$(n-1)_{continuum} = \frac{N}{2\pi} \int \frac{\sigma}{\bar{\nu}_i^2 - \bar{\nu}^2} d\bar{\nu}_i \qquad [6.48]$$

with σ(cm^2) the photo-ionization cross section and σ (cm^{-1})= λ^{-1}.

By taking the cross sections and oscillator strength from the literature (a large number of papers, listed in [20]) the k vector mismatch per atom, defined as C, can be calculated:

---

[20] R. Mahon, T.J. McIlrath, V.P. Myerscough, D.W. Koopman, IEEE J. Quant. Electr. **15**, 444 (1979).

$$\Delta k = CN = \frac{2\pi(n_1 - n_3)}{\lambda} \qquad [6.49]$$

where λ is the vacuum wavelength of the generated harmonic.

In the figures the calculated values for *C* are plotted for three noble gas atoms. Negative signs are represented by the gray shaded regions:

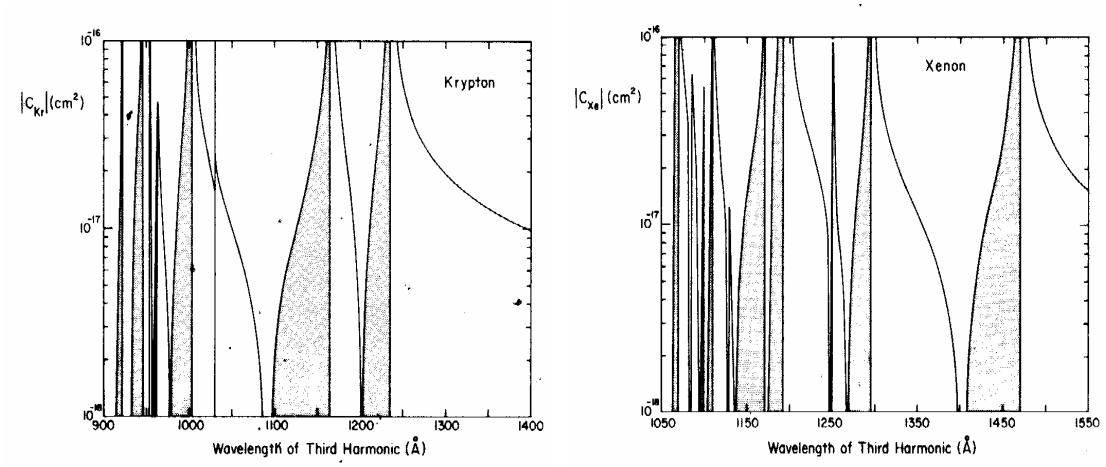

So in the gray shaded wavelength regions efficient third harmonic generation can be obtained. In some regions of wavelength there the refractive index strongly varies with wavelength. This gives rise to strong oscillations in THG yield and may even produce bandwidth filtering[20].

6.7 *THIRD HARMONIC GENERATION IN XENON*

The theories on the phase-matching were tested in an experiment on third harmonic generation in Xenon, in the case of tight focusing near the center of the cell (so $f/L = 0.5$) with $\lambda_1 = 354.7$ nm and $\lambda_3 = 118.2$ nm. b/L was adjusted to 0.025. The pressure dependent harmonic yield, plotted in the figure, was compared with the theory as established here. In fact the function $G_1(b\Delta k,0,0.5,1)$ was fitted to the data resulting in a value:
$\Delta k = (-5.99 \times 10^{-17}) N_{Xe}$ (cgs units).

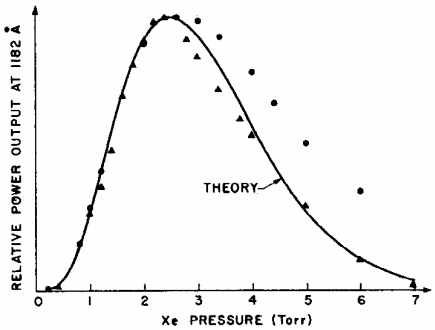

Fig: Relative power output at 118.2 nm for THG in Xenon

The yield of THG in Xenon gas can be measured and compared with calculation of a phase-matching integral. Results of ref [21] are reproduced in the figure. It should be noted that the experiment was performed in a gas jet with a limited interaction length of only a few times *b*.

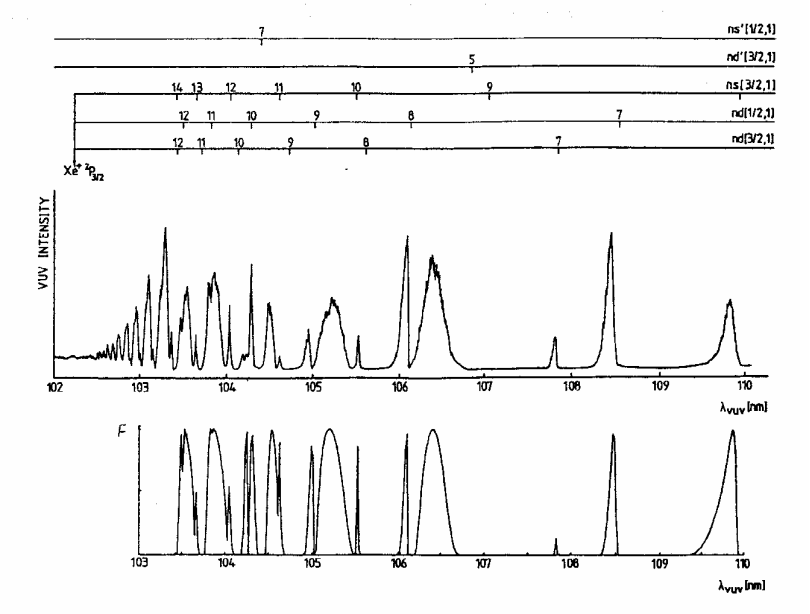

Fig: THG in Xenon as a function of wavelength in the range102-110 nm;
Upper curve: measured THG yield; Lower curve: calculated F_1 for b = 0.3 mm and 30 torr in a gas jet

Important conclusions on THG can be drawn from this figure:

1) The main features in the wavelength dependent THG can be explained by the phase-matching integral.
2) Resonances in the THG yield occur in many cases "at the blue" side of the *ns* and *nd* atomic one-photon resonances.

6.8 *RESONANCE ENHANCED VUV-PRODUCTION*

The nonlinear susceptibility can generally be written as:

$$\chi^{(3)} \propto \sum_{gijk} \sum_{terms} \frac{\langle g|\mathbf{r}|i\rangle\langle i|\mathbf{r}|j\rangle\langle j|\mathbf{r}|k\rangle\langle k|\mathbf{r}|g\rangle}{(\omega_{gi} \pm \omega)(\omega_{gj} \pm 2\omega)(\omega_{gk} \pm 3\omega)} \qquad [6.50]$$

It is an obvious result that the non-linear susceptibility blows up if one of the denominators is in resonance. This may occur if one of the applied electric fields has a frequency that matches the spacing between level energies in the medium. This may happen at the one, two or three photon level. A resonance at the one-photon level has the disadvantage that the incident field is strongly absorbed in the medium, therewith giving rise to many unwanted effects. Absorption at the three photon level implies that the generated field is (re)absorbed in the medium, also an unwanted effect. Resonances at the two-photon level do not have these disadvantages. In such case the nonlinear susceptibility becomes:

[21] A. Lago, PhD Thesis, University of Bielefeld, 1986

$$\chi^{(3)} \propto \sum_{ik} \sum_{terms} \frac{\langle g|\mathbf{r}|i\rangle\langle i|\mathbf{r}|J'\rangle\langle J'|\mathbf{r}|k\rangle\langle k|\mathbf{r}|g\rangle}{(\omega_{gi} \pm \omega)(\omega_{gj} - 2\omega - i\Gamma)(\omega_{gk} \pm 3\omega)} \qquad [6.51]$$

where the summation over *j* states is dropped in favor of the one selected two-photon resonant state $|J'\rangle$; the summation over $|g\rangle$ is also dropped, since only one ground state plays a role in the noble gases considered here. The resonance denominator has been given a phenomenological damping term to prevent $\chi^{(3)}$ of growing to infinity, which is unphysical.

Two two-photon resonance-enhanced processes are feasible: sum and difference frequency mixing, as shown in the figure.

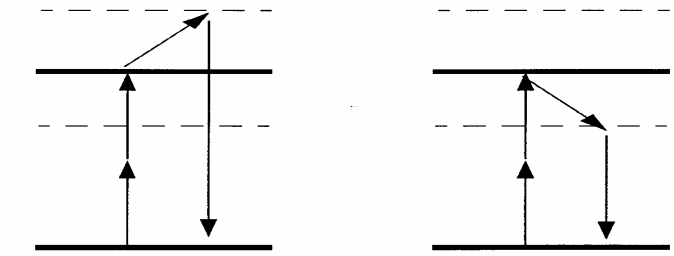

Fig: Energy level scheme in an atom; left two-photon resonant sum-frequency mixing; right: difference frequency mixing. Dashed lines are virtual levels; solid lines are real energy levels.

The level structure of the noble gases is particularly suitable to take advantage of resonance enhancement. Many levels are available for two-photon excitation in the ultraviolet: 200-250 nm, as shown in the list, adapted from ref [22]. These wavelengths can nowadays be produced with tunable pulsed lasers, particularly with BBO-crystals for frequency doubling. Recently two-photon resonance-enhanced sum-frequency mixing was demonstrated in Argon, using wavelengths $\lambda < 200$ nm [23].

	Two-photon resonance	excitation energy (cm^{-1})	resonance wavelength (nm)	relative efficiency[a]
Xe	5p - 6p' $[3/2]_2$	89162.9	224.3	40
	$[1/2]_0$	89860.5	222.6	187
	7p $[5/2]_2$	88352.2	226.4	4
	$[3/2]_2$	88687.0	225.5	9
	$[1/2]_0$	88842.8	225.1	26
	8p $[5/2]_2$	92221.9	216.9	9
	$[3/2]_2$	92371.4	216.5	5
	$[1/2]_0$	92555.7	216.1	119
Kr	4p - 5p $[5/2]_2$	92308.2	216.7	167
	$[3/2]_2$	93124.1	214.8	56
	$[1/2]_0$	94093.7	212.6	1000

[a] Fundamental power is 20 kW.

Note the important difference between the two processes described here. Sum-frequency mixing is a process I and must obey the F_1 phase integral with optimum at negative dispersion, while

[22] K. Miyazaki, H. Sakai, and T. Sato, Appl. Opt. **28**, 699 (1989).
[23] H. Palm and F. Merkt, Appl. Phys. Lett. **73**, 157 (1998).

the difference frequency mixing is a process II and must obey the F_{II} phase integral with optimum near $\Delta k = 0$.

6.9 *POLARIZATION PROPERTIES*

In the previous sections the polarization properties in the harmonic conversion processes are neglected. Polarization is associated with the vector character of the electromagnetic fields, coupled by susceptibilities that have a tensor nature. The third order nonlinear polarization can be written as:

$$\mathbf{P}_\sigma\left(\omega_r;\omega_i,\omega_j,\omega_k\right)\propto \chi^{(3)}_{\sigma\alpha\beta\gamma}\mathbf{E}^i_\alpha\mathbf{E}^j_\beta\mathbf{E}^k_\gamma \qquad [6.52]$$

where the indices *i,j,k,r* refer to the frequencies and σ,α,β,γ, to the spatial coordinates of the vectors. Hence $\chi^{(3)}$ is a tensor of rank 3 with 81 elements that represents the response of a medium induced by polarizations of the input fields. Here $\chi^{(3)}$ is written as a single term; in fact there are many (see Chapter 4) with differing frequency dependences. The nonlinear susceptibility can be written:

$$\chi^{(3)}\propto\sum_{gijk}\sum_{terms}\frac{\langle g|\mathbf{r}|i\rangle\langle i|\mathbf{r}|j\rangle\langle j|\mathbf{r}|k\rangle\langle k|\mathbf{r}|g\rangle}{(\omega_{gi}-\omega)(\omega_{gj}-2\omega)(\omega_{gk}-3\omega)} \qquad [6.53]$$

where a general summation over "terms" is taken, each having a different frequency dependence. Here the term is written that is generally the most resonant for THG. The matrix elements $\langle a|\mathbf{r}|b\rangle$ contain the electronic transition dipole moments that have an explicit vector character.

In four-wave mixing it is of importance to note that it is a coherent "cycling" process. Four waves interact in such a way that no population transfer occurs. Hence $|g\rangle$ and $\langle g|$ at the beginning and end of the loop. This is of importance for the derivation of polarization dependence. The summation over populated ground states $|g\rangle$ can be dropped in the case of atoms where only a singly populated ground state exists (particularly for noble gases). The states can be written in terms of quantum numbers and their projections; the angular momentum quantum number is of importance here: $|i\rangle = |J_i M_i\rangle$ with neglect of the electronic character and fine structure. Using methods from atomic physics (the Wigner-Eckart theorem) a transition dipole moment can be decomposed as:

$$\langle g|\mathbf{r}|i\rangle = \langle J_g M_g|\mathbf{r}^{(1)}_q|J_i M_i\rangle = (-)^{J_i-M_i}\begin{pmatrix} J_i & 1 & J_g \\ -M_i & q & M_g\end{pmatrix}\langle J_g\|\mathbf{r}^{(1)}\|J_i\rangle \qquad [6.54]$$

where the superscript (1) denotes a first rank tensor and the Wigner-*6j* symbols are introduced. The angular momentum characteristics associated with the non-linear susceptibility is then:

$$\chi^{(3)}\propto\begin{pmatrix} J_i & 1 & J_g \\ -M_i & q_1 & M_g\end{pmatrix}\begin{pmatrix} J_j & 1 & J_i \\ -M_j & q_2 & M_i\end{pmatrix}\begin{pmatrix} J_k & 1 & J_j \\ -M_k & q_3 & M_j\end{pmatrix}\begin{pmatrix} J_g & 1 & J_k \\ -M_g & q_4 & M_k\end{pmatrix} \qquad [6.55]$$

Polarization selection rules in four-wave mixing arise from this expression. Only specific combinations of the q_j lead to a non-zero angular part. In fact the q_j are the projections of the dipole moment on a basis of spherical harmonics: q = 0 linear polarization, q= 1 and q= -1 right and left-handed circular polarization.

1) For the case of all polarizations linear along the same axis: $q_1 = q_2 = q_3 = 0$. This is possible and yields also $q_4 = 0$. So the third harmonic is polarized along the input beam.
2) Third harmonic generation with circularly polarized light: $q_1 = q_2 = q_3 = 1$ is <u>not</u> possible.
3) In case of two-photon resonant sum- or difference frequency mixing there is a real level in the atom with a specific quantum number J_j. It follows that J_j = 1 is <u>not</u> possible. If the intermediate level has either J_j = 0 or J_j = 2 there are solutions, hat also determine the polarization of the generated light. The table gives the options with calculated polarization factors deriving from the sequence of Wigner-6*j* symbols.

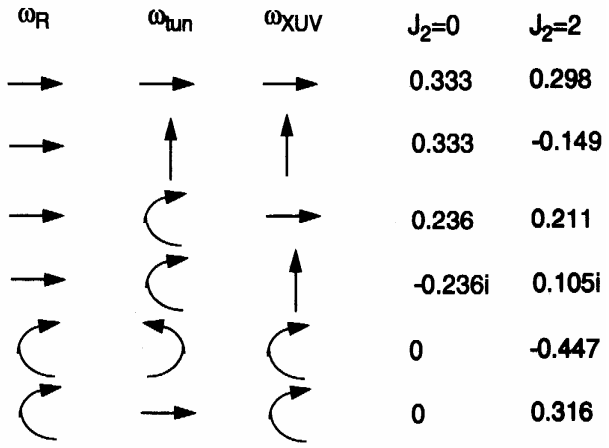

6.10 *PULSED JETS*

From a practical perspective it should be realized that below the so-called LiF-cutoff at 105 nm there are no window materials available for experiments; the region below 105 nm is usually called the extreme ultraviolet (XUV). So no exit windows can be employed to close off the cell. A pulsed jet, first employed by Kung[24], can deliver the gaseous non-linear medium; in the figure below such a setup is shown, although still with a LiF exit window. This window can be replaced by a narrow orifice; differential pumping techniques can sustain vacuum conditions at the detector side, such that wavelengths $\lambda < 105$ nm can also propagate. Note that under these conditions the interaction length L can no longer be freely chosen.

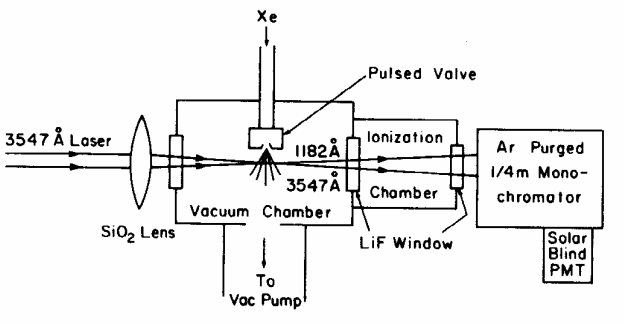

Fig: Experimental setup as used in ref[24]

[24] A.H. Kung, Opt. Lett. **8**, 24 (1983).